INFORMATION TO USERS

This manuscript has been reproduced from the microfilm master. UMI films the text directly from the original or copy submitted. Thus, some thesis and dissertation copies are in typewriter face, while others may be from any type of computer printer.

The quality of this reproduction is dependent upon the quality of the copy submitted. Broken or indistinct print, colored or poor quality illustrations and photographs, print bleedthrough, substandard margins, and improper alignment can adversely affect reproduction.

In the unlikely event that the author did not send UMI a complete manuscript and there are missing pages, these will be noted. Also, if unauthorized copyright material had to be removed, a note will indicate the deletion.

Oversize materials (e.g., maps, drawings, charts) are reproduced by sectioning the original, beginning at the upper left-hand corner and continuing from left to right in equal sections with small overlaps.

ProQuest Information and Learning
300 North Zeeb Road, Ann Arbor, MI 48106-1346 USA
800-521-0600

THE PHOTOLYSIS OF HYDROGEN IODIDE IN PRESENCE OF NITRIC OXIDE

by

EMBAR VENKATACHARI SUNDARAM

A thesis submitted in partial fulfillment

of the requirements for the degree of

Doctor of Philosophy

in the

Department of Chemistry

University of Ottawa

Ottawa, Canada

J. D. Holmes
Associate Professor of Chemistry
Research Supervisor

E. V. Sundaram
Ph. D. Candidate

PREFACE

The thesis is divided into four chapters. The first chapter deals with a general introduction to photochemistry. The second chapter deals with the photolysis of hydrogen iodide and reactions of HNO. The third chapter is about the photolysis of hydrogen iodide in the presence of nitric oxide at 45° and 25°C, and the last chapter describes the extension of this work to lower temperatures, 6° and -20°C

Nitric oxide has been widely used to inhibit gas phase reactions which proceed by free radical chain mechanisms. The basis for the inhibition is the reaction of nitric oxide with free radicals, the initial step being presumably the formation of a nitroso compound. These nitroso compounds were found to undergo further reactions with excess nitric oxide to form N_2 and NO_2 among other products. The analogous entity HNO was also postulated as one of the intermediates in the inhibited reactions of hydrocarbons.

The reactions of HNO were found to be different in different systems. In flow systems, the products are only H_2 and NO, whereas in static systems, mostly in photosensitized reactions, the products are N_2, N_2O and other

oxides of nitrogen. In view of the importance of HNO as a reactive intermediate in inhibited reactions, the present work was undertaken to study the reactions of HNO in a photolytic system. The photolysis of HI in the presence of NO was carried out using radiation 3130 Å, so that there would be very little hot atom effect. The photolysis of HI would produce H atoms which on reacting with NO will yield HNO. Thus it should be possible to study the reactions of HNO in this system. The effect of other inert gases on the photolysis of HI was also studied to gain more information about the hot atom effect.

ACKNOWLEDGMENT

I wish to extend my sincere thanks to my research supervisor, Professor J. L. Holmes, for his willingness to discuss any and every problem and for the critical approach he brings to these problems. His enthusiasm and originality have been the source and mainstay of this work.

I would like to thank the Canadian Commonwealth Scholarship and Fellowship Committee for their financial assistance over the last three years and for making this visit to Canada possible. With gratitude the author wishes to remember Dr. Margaret Back for many useful and constructive criticisms during the course of this work. Finally, it is the author's special pleasure to record the assistance rendered, by Dr. and Mrs. M. R. Bridge, in technical preparation of this thesis.

TABLE OF CONTENTS

LIST OF TABLES

LIST OF FIGURES

ABSTRACT

The photolysis of hydrogen iodide in the presence of nitric oxide has been studied in the temperature range 45° to -20°C, using a Hg arc, with radiation above 3000 Å. It was found that the addition of nitric oxide at 45° and 25°C reduces the quantum yield of hydrogen production. This reduction in quantum yield was dependent both on I_2 and HI concentration and also the NO/HI ratio. However, after a certain ratio of NO/HI was reached, the quantum yield remained constant. There was no consumption of nitric oxide. Mechanisms involving HNO as a reactive intermediate have been proposed to explain the behaviour. From the derived rate equations, the rate constant ratio for $HNO + HI \longrightarrow H_2 + NOI$ and $HNO + I_2 \longrightarrow HI + NOI$, has been derived as 79.9 at 25°C and 38.1 at 45°C. From the pressure dependence of the rate constant for the reaction $H + NO + M \text{ —— } HNO + M$, the life time of HNO* has been calculated as $\geq 10^{-10}$ sec. The change from third order to second order for the above reaction occurs when M is greater than 0.5 atmospheres at 25°C. At 45°C, the formation of NH_4I was found to be larger than at 25°C and prevented detailed study.

At 6°C and -20°C, the behaviour is similar to that

at high temperature, except that nitrogen is now an important product. Two different mechanisms for nitrogen production have been discussed. It was found that the rate of nitrogen production was second order at low pressures and first order at high pressures in nitric oxide. From intensity measurements it was also shown that the rate of nitrogen production was first order in HNO. From the rate of hydrogen and nitrogen production, the activation energies for the reactions $HNO + HI \longrightarrow H_2 + NOI$; $HNO + I_2 \longrightarrow HI + NOI$ and $HNO + 2NO \longrightarrow N_2 + HNO_3$ have been calculated as 3.0, 0.5 and -0.5 k.cal. $mole^{-1}$ respectively.

The effect of inert gases, like H_2, He and N_2 as well as carbon monoxide, on the photolysis of HI was studied, using the full mercury arc and also at wavelengths above 3100 $\mathring{A}$. The rate constant ratio for $H + I_2 \longrightarrow HI + I$ and $H + HI \longrightarrow H_2 + I$ was determined at 70° and 110°C.

INTRODUCTION

A photochemical reaction begins with the act of absorption of radiation. By the Stark - Einstein law of photochemical equivalence (1) this is a quantum process involving one photon per absorbing molecule. The number of molecules absorbing is therefore equal to the number of photons absorbed. Generally, these reactions are complex in nature, and the actual measured change is rarely that directly produced by the light. It is necessary, therefore to distinguish between the 'primary' effect of the light and the 'secondary' thermal reactions which follow. If there were only primary processes then the quantum yield, ϕ, which is defined as the number of molecules reacting per quantum absorbed, should be unity. In most cases, owing to secondary processes taking place, the quantum yield is greater or less than one. Thus according to Bodenstein (2) who measured the quantum yield of a large number of reactions, the values of ϕ range from 0.002 for the decolouration reactions of certain dyes to 10^6 for the reaction of chlorine with hydrogen.

Absorption of Light:

The interaction of light with matter is governed by quantum mechanical laws. The light is quantised into photons of energy $h\upsilon$ where 'h' is the Planck's constant and 'υ' is the frequency of light; whether or not a molecule will absorb a

quantum of energy $h\nu$ depends on whether there is an energy difference between two energy levels in the molecule equal to $h\nu$ and whether a transition between these two states is allowed by symmetry and momentum conservation rules.

The energy in a molecule can be divided into translational, vibrational and rotational and electronic contributions; electronic transitions require the greatest energies. Changes in electronic energy are of the order of 100 k.cal $mole^{-1}$, giving a spectrum in the visible or ultraviolet region. The associated vibrational energy changes are about 5 k.cal $mole^{-1}$ and the rotational changes about 0.02 k.cal $mole^{-1}$ and they produce the coarse 'vibrational' and the finer 'rotational' structure of the electronic spectral band. In comparison with the above energy values it may be noted that the average translational kinetic energy of a molecule at the ordinary temperature is 3/2 RT or about 1 k.cal $mole^{-1}$, and since the probability of a molecule possessing energy $\geq E$ is proportional to $\exp(-E/RT)$, it is evident that high temperatures are necessary to produce electronic transitions by heat alone, and that at ordinary temperatures all but a few molecules will be in their lowest vibrational level, but most of the molecules will have several quanta of rotational energy.

The immediate product of absorption of a photon is, an excited state of the absorbing molecule, with energy in

excess of the normal state equal to the energy of the photon which it absorbed. The excited molecule may then react with another, since its reactivity is greatly increased, or it might possibly dissociate or cause another molecule to dissociate into radicals, which subsequently reacts in diverse ways. It is because photons in this range are capable of rupturing the molecule, that visible and ultra-violet light are of chemical importance.

Apart from dissociation of molecules into neutral particles, one of which may be excited, Terenin and Popov (3) observed cases of photoionisation consisting of the decomposition of a molecule into oppositely charged ions. This type of photoionisation was detected during the exposure of halide salts of univalent thallium which decomposes as

$$TlX + h\nu = Tl^+ + X^-$$

The absorption at very low wavelengths may lead entirely to the ionisation of a molecule. Photons may ionise a molecule much more readily than dissociate it, even if its ionisation potential is higher than its dissociation energy. The process may be represented as

$$M + h\nu = M^+ + e^-$$

This is a particular case of photoelectric effect, but in ordinary photochemical reactions, it apparently does not play a particularly important part since the ionisation potential

is usually 10eV and higher which corresponds to a wavelength ($\lambda \leq 1200$ Å) in the vacuum region of the spectrum. A number of experimental procedures have been described to determine ionisation potentials in the vacuum ultra-violet using more or less conventional photolysis technique, with windows of LiF (4), artificial sapphire or very thin quartz separating the lamp from the photolysis vessel. Below 1000 Å, the transparency of the window materials becomes extremely poor and hence windowless apparatus have been designed (5) which utilises the principle of a fast-flow separation system. By these methods, ionisation potentials have been measured for a number of compounds (6). These ionisation potentials are very useful parameters for correlating many physicochemical properties, like electronegativity, heterolytic bond dissociation energy, strain in cyclic ring, etc.

It can be shown that the energy corresponding to a particular wavelength is given by

$$E \text{ (k.cal mole}^{-1}) = \frac{28.635 \times 10^4}{\lambda \text{ (in Å)}} \qquad [1]$$

The amount of energy absorbed by a mole of compound at any particular wavelength corresponds to the Avogadro's number of photons, and this energy, in k.cal, has been called an einstein.

For a photochemical reaction to occur, the energy

of the quantum absorbed must be equal to or greater than the energy required to produce activation or dissociation. It does not necessarily follow, however, that such dissociation will occur merely because sufficient energy has been provided.

Nature of photochemical reactions:

Photochemical reactions may be classified as direct or sensitized . In a direct photochemical reaction one or more of the substances undergoing reaction absorb the light. In a sensitized reaction some substance absorbs light and induces a reaction in which it does not participate. Many compounds like hydrogen, nitric oxide and hydrocarbons, absorb light in the far ultra-violet region which is difficult to study, though recently McNesby and co-workers,(7) with improved experimental techniques, have studied the photolysis of hydrocarbons in the far ultra-violet. However, mixing with a foreign substance - a sensitizer - which absorbs light in a more accessible spectral region, and using the possibility of transfer of excitation energy of the sensitizer to reactant molecules, makes it possible to carry out photochemical reactions of compounds which do not absorb in this spectral region. Photosensitization by mercury, cadmium and zinc has received considerable attention in recent years (8). It is not proposed to go into the details of these reactions.

The study of photochemical reactions may be divided into two main parts: (A) a study of the immediate effect of the light on the absorbing molecule which is the primary process; and (B) a study of the reactions of the molecules, atoms or radicals produced by the primary process.

Photochemical primary processes:

Noyes et al (9) defined the primary process as "one which comprises the series of events beginning with the absorption of a photon by a molecule and ending with the disappearance of that molecule or with its conversion into a state such that its reactivity is statistically no greater than that of similar molecules in thermal equilibrium with their surroundings."

In the primary photochemical process there are usually a variety of paths for degradation of electronic energy of excitation. Chemical paths include intramolecular rearrangements (10)(11)(12) or the formation of free radicals and excited molecules which may react in secondary processes to form new products of chemical interest. However, also usually included in the overall photochemical reactions are radiative and non-radiative photophysical processes which do not lead to a net chemical change, yet are alternate paths for the loss of the absorbed energy. Such processes involving electronically excited states are of great interest to the spectroscopist and and photochemist alike. Thus, as Noyes et al (9) point out,

"The complete elucidation of a primary photochemical process must include an understanding of all that transpires, whether or not a chemical reaction occurs."

The majority of the unexcited molecules will be in the ground electronic and vibrational states and during an electronic transition the nuclei of the molecule can be considered to be stationary, since the transition occurs within about 10^{-15} sec. Thus a transition on an energy level diagram is approximately vertical. This statement due to Frank and elaborated by Condon (13) is known as the Frank-Condon principle. The nature of photoexcitation is determined by this principle, by the energy of incident radiation and by the relative positions of the potential energy surfaces (14). Electronic transitions in a molecule are also subject to spin conservation rules first postulated by Wigner (15) according to which, transitions involving change in multiplicity are forbidden. This rule is well obeyed by small molecules, but in the case of large molecules, perturbation of the energy levels leads to a partial breakdown of this selection rule and the transition can occur.

When a molecule in the ground singlet state absorbs a photon the resulting excited molecule will also be in a singlet state and may do one of the following things:
(a) Fluoresce: The vibrational quanta possessed by the electronically excited molecules will be quickly degraded imto

thermal energy through intermolecular collisions. Since the undisturbed life time of the excited state is of the order of 10^{-8} sec., it being assumed that the transition back to the ground state is allowed, emission of the absorbed quantum as fluorescence will occur from the lowest vibrational level of the upper state to upper levels of the ground state, or to put it alternatively, the fluorescence emission spectrum will be of longer wavelengths than the absorption spectrum and will bear an approximately "mirror-image" relationship to the absorption.

(b) Undergo internal conversion: In many cases, the electronically excited state of the molecule, although potentially fluorescent, is deactivated before it can emit its energy as fluorescence. This can occur, amongst other ways, when there is crossing of potential energy surfaces of the excited and the ground electronic states. A radiationless transition can then occur from the excited state to high vibrational levels in the ground state. The vibrational energy is then quickly degraded into thermal energy through molecular collisions. Usually the term internal conversion refers to a non-radiative transition between states of the same multiplicity and inter-system cross-over refers to a non-radiative transition between states of different multiplicity (16).

(c) Undergo intersystem cross-over to a triplet state: These are schematically illustrated in Figure 1. Figure 2 indicates more clearly these primary processes on a potential energy diagram.

(d) Undergo energy transfer through collision: Here two kinds of collision can be visualised, "elastic" collision in which there is no transfer of energy from the excited to the unexcited molecule, and "inelastic" collision in which there is an energy transfer. These collisions are sometimes called "collisions of the second kind". The most likely conditions for an energy transfer are obtained when there is resonance between the corresponding energy levels which may be either electronic, vibrational or rotational. The smaller the amount of energy which appears as kinetic energy in a transfer, the more likely it is that the transfer will occur. Electronic energy transfer may lead to the phenomenon of sensitized fluorescence, as well as the possibility of dissociation of the acceptor molecule.

(e) Undergo dissociation: As was mentioned earlier, the absorption of a photon of visible or ultra-violet light by a molecule can, in some instances, lead to its rupture. This can occur either through the excited molecules being in a repulsive state as in the case of HI (17) at longer wavelength or through its having sufficient vibrational energy in either

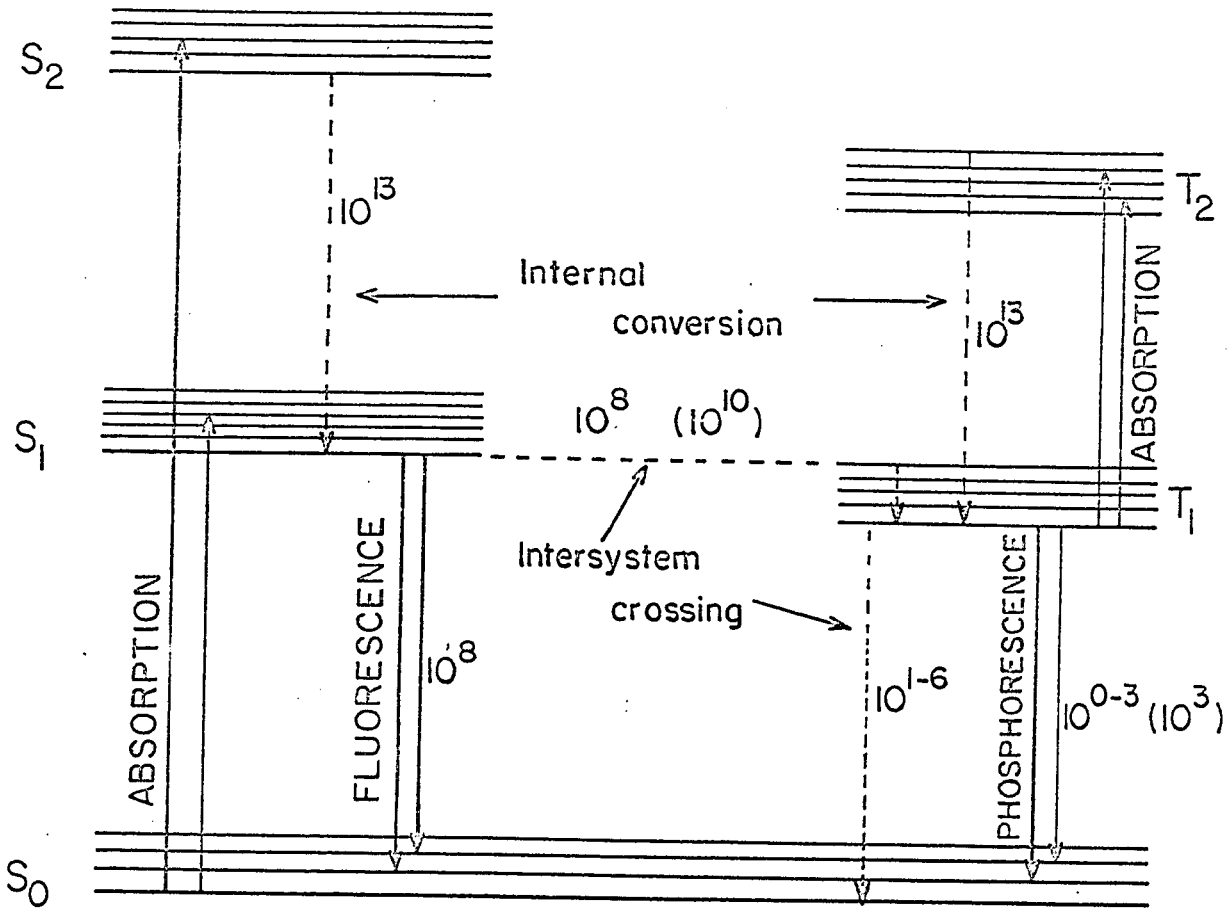

Figure 1. Electronic energy state diagram showing typical unimolecular rate constants in sec.$^{-1}$ for radiative and non-radiative transitions (continuous and broken lines respectively) for organic molecules with lower π^* — π states (values in brackets refer to molecules with low π^* — n states).

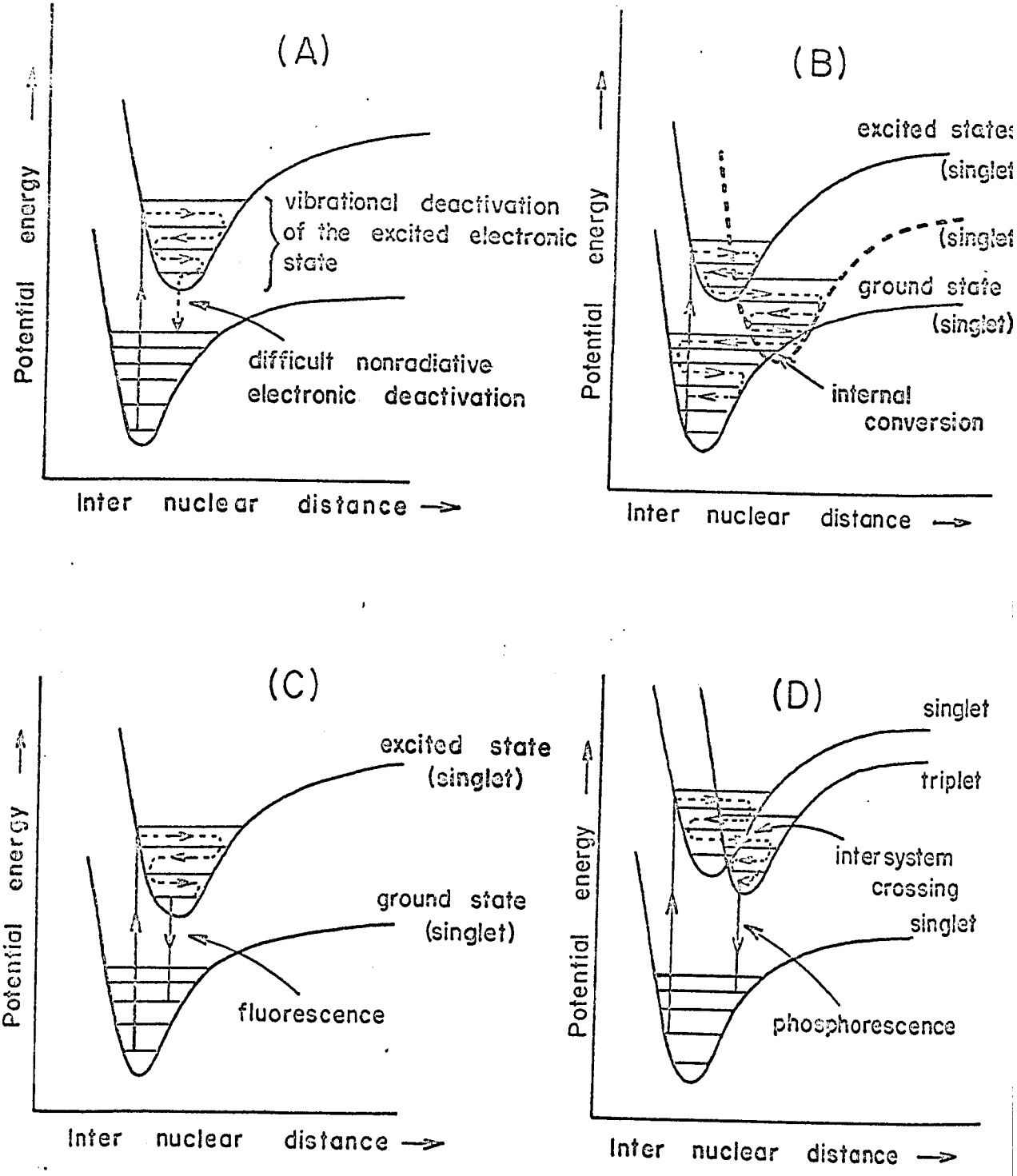

Figure 2. Potential energy diagrams showing radiative and non-radiative transitions (continuous and broken lines, respectively).

A vibrational deactivation
B internal conversion
C fluorescence
D intersystem crossing and phosphorescence

its upper or lower state to cause it to dissociate. Generally the bond broken is the same one as is responsible for light absorption (disulphides, azo compounds etc.). Sometimes, however, when the bond energies in the chromophoric group are greater than that of the absorbed quantum, this energy may find its way to another weaker bond in the molecule through resonance energy transfer, and this bond is broken. For example, the irradiation of acetone leads to the production of a methyl and an acetyl radical, although the light is absorbed by the carbonyl group. This process can be thought of as an internal energy transfer.

(f) Chemical quenching: The excited state can lose its energy, not only through a physical energy transfer on collision, but also through chemical reaction with the quencher molecule. In many cases self-quenching of the excited state may occur, either as a physical effect analogous to solvent quenching or else through dimerisation.

Quenching of fluorescence consists of the weakening of the intensity of fluorescence in the presence of foreign admixtures or during increase in pressure (or concentration) of the fluorescent substance itself. The method of measuring the absolute quenching efficiencies of gases are fully set out by Mitchell and Zemansky (18) and are not elaborated here.

Much work has been done on the quenching of fluorescence of Hg (6^3P_1). When Hg (6^3P_1) atoms interact with molecules of a foreign gas, a transfer of energy may occur with the return of the Hg atoms to the ground state (6^1S_0) by means of a non-radiative transition. The (6^3P_1) $\longrightarrow$ (6^1S_0) fluorescence is thus quenched. Absolute values of quenching cross sections which are a measure of the probability of quenching processes have been reported (14)(19). The simplest kinetic system of this type may be represented by the following scheme.

(a) $A + h\nu \longrightarrow A^*$

(b) $A^* + A \longrightarrow$ } Production of unexcited A

(c) $A^* + M \longrightarrow$ }

(d) $A^* \longrightarrow A + h\nu$

Here A denotes the atom or molecule which is excited electronically to A* by the absorption of radiation (reaction a) and M is a substance which can quench by reaction (c). In addition there is self-quenching by A (reaction b). The kinetic equations for this system were worked out by Stern and Volmer (20) whose results are given in the following equation,

$$\frac{I}{I_o} = \frac{1}{1 + k_b \tau [A] + k_c \tau [M]} \qquad [2]$$

where I is the intensity of emitted radiation in einsteins per

second, I_o is the intensity of emitted radiation in the absence of foreign gas M and τ ($= 1/k_d$) is the mean radiative life of A*. Since τ can be obtained from spectroscopic data, k_b and k_c can be found from the effect on the ratio I/I_o of varying the concentrations of A and M. However, it has been shown recently (21) that for the Stern - Volmer formula to be valid both the pressure of the fluorescent substance and the pressure of the quenching gas must be sufficiently small.

Measurement of light emission may be used to determine the extent of fluorescence. A detailed study of the kinetics of the system will in principle provide information about the extent of dissociation. Unless there exists some way of determining the amount of triplet state molecules formed, there is no way to distinguish clearly between internal conversion and intersystem cross-over (22). Evidence for internal conversion in most polyatomic molecules is far from conclusive. In principle such conversions might occur as either kinetically first order or as second order processes. Under most experimental conditions, ground state molecules with very large amounts of vibrational energy which might be formed by internal conversion would be hard to detect. Fortunately, internal conversions seem to be of negligible importance (23)(24).

There are several methods to determine the presence of triplet state molecules. These may be summarised briefly as follows: (a) Character of the emission, that is, the emission must be demonstrated clearly to be characteristic of the triplet state either by analysis of the spectrum or by determination of the mean life time of the emission (25). In this connection it may be pointed out, that an excited singlet state can be converted to a triplet state, through a radiationless inter-system cross-over as shown in Figure 2. Emission can then take place from triplet to ground state, which is a spin-forbidden transition, of a longer mean life than that from the corresponding singlet state. This is often called phosphorescence. (b) by energy transfer to other molecules on collision, thus leading to a preferential emission or reaction from the triplet state of the colliding partner (22)(26). There are indirect and much less reliable methods available in some instances. For example, triplet states are at lower energies than the corresponding singlet states. This means frequently that dissociation from such states will require more activation energy than from corresponding singlet states.

The triplet state molecules may go back to the excited singlet state by intersystem cross-over, which may then lead to emission. This is known as 'delayed fluorescence' and is

similar to ordinary fluorescence but the emission occurs only after a certain interval of time.

The Nature of photochemical processes in organic compounds:

When a molecule absorbs ultra-violet or visible light of frequency ν , an electron undergoes a transition from a lower to a higher energy level. In general non-bonding lone pairs of electrons are the least strongly bound in a molecule, and in the bonding levels π -electrons have higher energies than corresponding σ electrons, whilst in the antibonding levels that order is reversed. This is shown in Figure 3. Thus in the spectra of simple molecules, the bands due to $\pi^* \leftarrow n$ transitions generally lie at longer wavelengths than those arising from $\pi^* \leftarrow \pi$ transitions, whilst $\sigma^* \leftarrow \sigma$ absorptions usually lie in the far ultra-violet region. This type of notation was introduced by Kasha (27) to specify different molecular states. Mulliken (28) introduced another type of classification. In this classification states are represented by different capital letters N,Q,V,T,R,etc., where N (normal) stands for the ground state and V (valence), for example, stands for an excited state having large ionic character. Thus the absorption of hydrogen at 1100 Å

$H_2 + h\nu \longrightarrow H^+ H^-$ is a $V \longleftarrow N$ transition. Such transitions have high intensities and in organic molecules are often

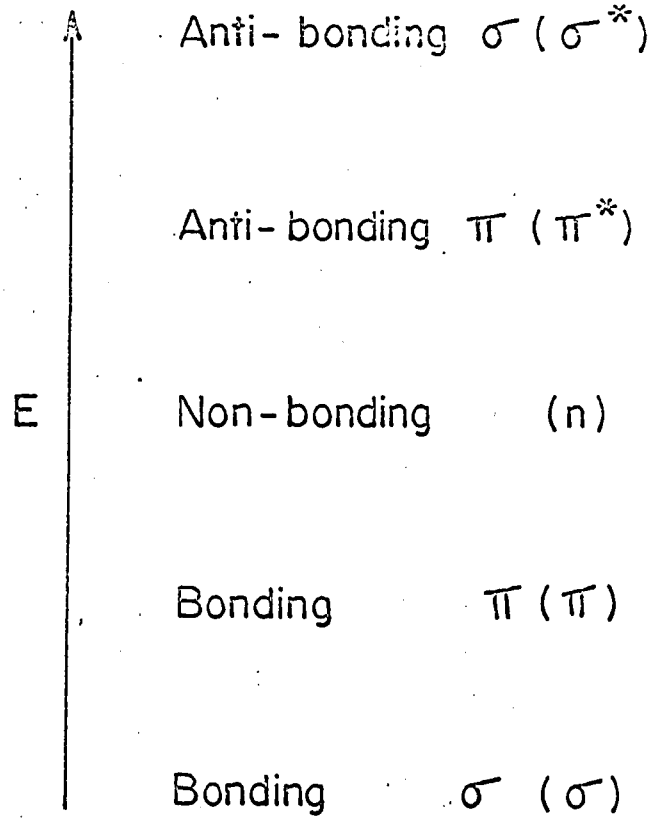

Figure 3. Energy level diagram for bonding and non-bonding orbitals.

designated as $\pi^* \leftarrow \pi$ transition. Transitions in which the transition moment is at right angles to the internuclear axis are $Q \leftarrow N$ and the bands typically have low intensities. This can also be designated as $\pi^* \leftarrow n$ transition. Examples of such transitions are numerous and only a few will be stated here. In formaldehyde, which has both n and π electrons, two types of transitions are observed. The $\pi^* \leftarrow \pi$ transition occurs around 1850 Å and has a high intensity, while $\pi^* \leftarrow n$ transition, with a low intensity is observed at 2700 Å. All organic iodides have absorption bands in the ultra-violet region. Methyl, ethyl and propyl iodides in water have maxima round 2500 Å and the bands have been interpreted as arising from $\sigma^* \leftarrow n$ transition, in which one of the lone-pair electrons on iodine is promoted into the antibonding orbital.

The intensities in these electronic transitions are expressed in terms of molar absorption coefficient ϵ, which can be obtained from the experimentally measured value of absorbance. The relation between the two is given by Lambert - Beer's law which can be mathematically represented as

$$A = \log\left[\frac{I_o}{I}\right] = \epsilon C d \qquad [3]$$

where 'A' is the absorbance measured spectrophotometrically 'C' is the concentration in moles liter^{-1}, and d is the cell

lenth in cms. The units of the molar absorption coefficient ϵ are liters $mole^{-1}$ cm^{-1}. This is related to the oscillator strength f, a theoretically derived quantity obtained from the transition moment and often used to express the intensity of transition (24), by the relation

$$f = 4.32 \times 10^{-9} \int \epsilon \, d\nu \qquad [4]$$

The integration is done graphically by plotting the extinction coefficient as a function of ν the frequency. The area under the curve gives the value of integral from which f can be calculated. This can be compared with the value of f obtained from the transition moment.

The transition moment is a wave mechanical quantity which is proportional to the square root of the intensity of a transition and is given by the integral

$$\sqrt{I} \propto \sqrt{D} = \int \Phi_i M \Phi_f \, d\tau \qquad [5]$$

where Φ_i and Φ_f are the total wave functions of the initial and final states respectively, $d\tau$ represents the product of volume elements in the co-ordinates of all the nuclei and electrons, D is the dipole strength and M is the so called dipole moment vector. The dipole moment vector M is given by

$$M = \sum er \qquad [6]$$

where e is the electronic charge and r is the radius vector from the centre of gravity of the positive charge to the electron. M is also known as dipole moment operator.

The above equation permits the evaluation of the intensity, provided the total wave function Φ_i and Φ_f are known. This is, however, never the case, and a long series of approximations are required. First, it is assumed that rotational and vibrational wave functions can be factorised out and the above equation reduces to

$$\sqrt{D} = \int \Psi_i M \Psi_f \, d\tau \qquad [7]$$

where Ψ_i and Ψ_f are the total electronic wave functions of the initial and final states respectively and $d\tau$ is the product of the volume elements in terms of co-ordinates of all the electrons. Integrals of the form of equation [7] can be evaluated and the calculations have been performed for a series of simple molecules (28). The relation between the transition moment and the oscillator strength f is given by

$$f = 1.08 \times 10^{11} \nu \; D \qquad [8]$$

where ν is the frequency of emission and 'D' is the square of the transition moment. Mulliken (28) has, in a series of papers, compared the theoretical values of f calculated from transition moment and 'f' calculated from extinction coefficients for a number of compounds and they seem to agree fairly well.

The most useful property of integrals of the type of equation [7] is that they frequently vanish identically; that is, the integral is equal to zero. If this is the case the transition is called forbidden, and should, according to the approximate theory, not occur at all. Actually, forbidden transitions do occur because calculation by more refined theories give small but non-vanishing values for the intensities. Observed intensities of forbidden transitions are generally quite small, much smaller than those of allowed transitions (for which equation (7) gives non-vanishing intensities).

Fortunately, it is usually possible to tell, from the symmetry properties of the wave functions, whether or not equation [7] will vanish. Relatively simple rules can be established which predict the vanishing or non-vanishing of the intensity integral; these rules are referred to as selection rules.

The first selection rule is concerned only with molecules which have a centre of symmetry. All wave functions (orbitals) are either symmetric or antisymmetric with respect to the centre [that is either gerade (g) or ungerade (u)], and all components of vector M are of necessity ungerade. The product of two functions is ungerade only if one is gerade and

the other ungerade. Hence the integrand of equation [7] can be gerade only if M is multiplied by an ungerade quantity, which can happen only if Ψ_i , the ground state wave function (orbital) and Ψ_f the excited state wave function, are of unequal parity. Hence the selection rule $g \longrightarrow u$ or $u \longrightarrow g$; but $g \not\longrightarrow g$ and $u \not\longrightarrow u$. The crossed arrows indicate the transitions are forbidden.

The integrals of the above equation vanish if there is change in electron spin on excitation and hence transitions involving change in multiplicity are forbidden. Transitions involving no change in parity are also forbidden. A rotational level is called positive or negative depending on whether the total eigenfunction remains unchanged or changes sign for such a reflection. The property positive or negative is also called parity. According to the above selection rule, positive levels combine only with negative and vice versa. Transitions between two positive levels or between two negative levels are forbidden. This selection rule may be written symbolically:

$$+ \longrightarrow - \ , \quad - \longrightarrow + \ , \quad + \not\longrightarrow + \ , \quad - \not\longrightarrow -$$

Other examples involving special cases are outlined by Herzberg (29). The importance of the selection rule lies in the fact that from a knowledge of allowed transitions, the symmetry of the molecule can be ascertained, which in turn leads to the geometry of the molecule.

Secondary reactions: In the great majority of photochemical reactions which have been studied in detail, it has been found that the primary process consists of a dissociation of the absorbing molecule into free radicals or atoms. The free radicals or atoms then take part in secondary reactions. These reactions may lead to stable molecules which, in turn, take part in still other reactions. The secondary reactions are thermal and are independent of the means by which the reactants concerned are produced. However, if the radicals or atoms so produced have excess of thermal energy, then they react at a different rate from that of normal atoms. Such examples have been reported in literature (30)(31), and are known as 'hot atom' reactions. The energy distributed in the fragments are given by

$$E_1 \left(1 + \frac{m_1}{m_2} \right) = E_{(\upsilon)} - D \qquad [9]$$

where E_1 is the energy present in the radical or atom of mass m_1, m_2 is the second fragment, $E_{(\upsilon)}$ is the energy of a photon and D is the bond dissociation energy of the bond being broken. These reactions were found to proceed with no activation energy. The excited species must carry this excess energy, if they are atoms, as electronic and translational, or if they are not atoms, as rotational and vibrational energies as well. In all these cases there are restrictions on the type of energy and

the way in which it can be divided between the two products of reaction.

The restrictions are (1) conservation of the momentum of the product fragments, which determines the partition of translational energy, that is, in the inverse ratio of the masses, $E_1/E_2 = m_2/m_1$. (2) conservation of spin, although this rule seems of questionable validity for any species containing atoms of atomic number in excess of ten. If the excess of energy is electronic, there is a chance that it may be emitted within a time of 10^{-6} to 10^{-8} sec. as radiation if the transition is possible. Otherwise such electronic energy must be degraded by inelastic collisions to other forms of energy, usually vibrational. Generally it is found that the electronic states produced in chemical reactions are metastable, so that one may expect electronically excited species to follow the path of collisional deexcitation. The rare cases of allowed transitions result in what are referred to as chemiluminescent reactions.

For excess energy distributed in other degrees of freedom, namely rotation, vibration and translation, only collisional degradation is possible. However it is known that degradation of vibrational energy is a slow process and so a considerable fraction of vibrationally excited species thus formed may be expected to persist for some time. Evidence

has been presented for the presence of vibrationally excited species in the new bond that is formed by such collisions (32). On the other hand rotational and translational energy appear to be exchanged very readily on collision, so that the species thus excited may be expected to be thermalised very rapidly.

The transfer of energy to translational motion during molecular collisions without change in the form of energy takes place in accordance with the laws governing the collisions of elastic spheres. It follows from these laws that in the simplest case of an oblique impact of a rapidly moving particle of mass m_1 on a stationary particle of mass m_2, the average fraction $\overline{\Delta E}/E$ of energy transferred to the stationary particle on impact is given by

$$\frac{\overline{\Delta E}}{E} = \frac{2m_1 m_2}{(m_1+m_2)^2} \qquad [10]$$

Thus the amount of energy transferred depends on the masses of the colliding particles, and the most favourable case for energy transfer occurs when the masses of both particles are the same. Therefore the addition of inert gas, to a system containing hot radicals or atoms, should remove the excess energy by collisions. The atoms or radicals thus thermalised react at a different rate and were found to be temperature dependent (30). If the radicals or atoms produced in a

primary photochemical act are thermalised atoms or radicals, then the secondary reactions that follow are the usual thermal or dark reactions which are common to any kinetic system.

Sources of light:

To study a photochemical reaction, a lamp which emits light in the particular region is required. Of all the sources of light employed in photochemical work, the mercury lamp is most extensively used. Its advantages are numerous. If operated under properly controlled conditions its output is fairly constant; it emits, if made of quartz, a number of intense lines from 1849 Å to the two yellow lines at 5683 Å and 5688 Å, which may be separated satisfactorily for most purposes by simple filters. Ordinary glass is opaque below 3300 Å and quartz below 2000 Å. Thin films of glass (10 μ) are transparent above 2500 Å and fused quartz above 1500 Å. Owing to absorption by oxygen below 2000 Å, a vacuum technique must be used for the far ultra-violet region.

The number of designs of mercury lamps described in the literature and manufactured by commercial undertakings is so large that no attempt can be made here to describe them in detail. Roughly, however, three types may be distinguished viz (a) Low-pressure lamps; (b) medium and (c) high pressure arcs. In the first class the mercury vapour pressure is kept

as low as practicable, with the result that the intrinsic brilliance is small. This type, however, has one advantage that much of the energy lies in the first resonance line of the mercury spectrum at 2537 Å and secondly, the line is unreversed. The difference between reversed and unreversed radiation may be explained as follows: A reversed radiation is obtained from a medium pressure arc. In these lamps due to the increase in pressure of mercury vapour, "pressure broadening" occurs, with the result that the emission line (2537 Å) with the radiation in the middle of "line" is virtually absent because of self-absorption near the walls. In case of low pressure lamps there is no pressure broadening and hence the line 2537 Å is a single, intense line. This is known as unreversed line. Such lamps are suitable where a particularly strong source of resonance light is required, as in mercury photensitized reactions: usually the amperage is never allowed to go higher than 180 m.A. The lamp has another advantage that it may be inserted in a furnace for photochemical experiments at high temperatures, thus permitting the intense radiation of reaction vessels. Lossing et al (33) has designed an assembly for mass spectometric study using this type of lamp. It may be noted that the output intensity of mercury resonance lamp is practically independent of temperature up to 600°C.

Medium pressure arcs: As the pressure in the lamp is raised, the intensity of light weakens in the far ultra-violet and becomes greater in the visible and in the near ultra-violet regions. Such lamps usually work at a pressure of the order of 100 mm. to 10 atmospheres and they carry currents of 1 to 5 A. An inconvenient feature of these lamps is the heat generated, several hundred watts being dissipated. One way out of this difficulty is to enclose the lamp in a water jacketed enclosure. Medium pressure arcs give several lines of mercury spectrumbut 2537 Å, 3130 Å and 3660 Å are the most intense lines. Even amongst these three, 2537 Å is four times more intense than 3660 Å which is of the same strength as 3130 Å, and these can be isolated by using different filters.

High pressure arcs: High pressure mercury arcs operate at pressures of a few, up to almost 300 atmospheres. At the higher pressures air or water cooling must be employed. In the event that water is used as a coolant, its purity may be of some significance when the lamp is to be used at wavelengths below 2800 Å. On the other hand, water cooled lamps possess the advantage that a good deal of infra-red radiation is absorbed by the water. These lamps must be so enclosed as to protect from possible explosion. The life time of these arcs is lower than that for medium pressure arcs, and their use for kinetic studies is usually in conjunction with filters or a

monochromator.

Vacuum ultra-violet sources: Among the more restrictive features of vacuum ultra-violet photochemistry is the material through which the photon must be propagated and behind which is contained the gas to be photolysed. Both lamp and reaction vessel usually require such a window. Ideally, the window should be transparent in the wavelength region where the gas absorbs, and should be capable of being affixed to a reaction vessel to make a vacuum-tight seal that can be subjected to extremes of temperature. LiF windows can transmit above 1050 Å, CaF_2 can transmit above 1200 Å and a sapphire window will allow radiation greater than 1450 Å. These are the commonly used window materials.

A major requirement in a photochemical light source is high intensity and it should be monochromatic. A continuum such as obtained in a hydrogen discharge (34) or the rare gas discharges (35) can be useful when used in conjunction with a vacuum monochromator. However, monochromator efficiencies are uniformly poor in the vacuum ultra-violet and hence this arrangement has not been widely employed. Of much more use are the rare gas resonance lamps, which have the twin virtues of high intensity and chromatic purity.

The development of the rare gas resonance lamp began with electrode lamps (36) and evolved recently into the

electrodeless lamp powered by microwave energy (37). The great advantage of the microwave powered lamp is simplicity of construction. If one uses a krypton resonance lamp, the wavelengths 1236 Å and 1165 Å are obtained, their intensities being in the ratio of 1 : 0.28. On the other hand xenon resonance lamp gives a powerful line at 1470 Å and a less intense line at 1295 Å. The most intense krypton resonance lamp was achieved by using 1 mm. of a mixture of 10% Kr and 90% He as the filling gas. It was found (37) that 10% H_2 in argon at a total pressure of 1 mm. gave an intense, almost pure Lyman α emission (1216 Å). These lamps have been used for studying photoionisation.

Filters and Monochromators:

In any photochemical work, it is always desirable to restrict the range of frequencies, so that one can observe the effect of wavelength on photolysis. To facilitate this, monochromators or filters are usually used. Filters are the cheapest and the most convenient means for restricting the radiation to a narrow range of frequencies. With them it is possible to isolate many of the mercury lines for photochemical investigation. Although the filters absorb a considerable amount of the desired light, they absorb much more of the light in other parts of the spectrum. The transmission curves for typical Corning glass filters are given in their catalogue (38).

These filters are ground to a given thickness and polished in standard sizes, 5 cm. square and larger. Many of the glasses have sharp cut-offs. Filter CS-9-53 cuts off light below 2700 Å while CS-9-54 cuts off below 2200 Å.

Several solutions and pure liquids have been used for isolating various regions of the spectrum. A complete description of types of solution that can be used to isolate certain wavelengths are given by Bowen (39).

Monochromators: In general, the undesired wavelengths can be refracted to one side with a prism more effectively than they can be absorbed in a filter. A spectrometer system which is arranged to supply radiation of a narrow range of frequencies is called a monochromator.

If a continuous light source is used, there may be overlapping of adjacent regions and for this reason a discontinuous spectrum, such as that of a mercury arc, is particularly advantageous for use with a monochromator. The handicap of low intensity can be offset in part by long exposures, by using larger prisms and lens and by using capillary arcs of greater intensity. Forbes and others (40) have given a good experimental description of setting up a monochromator in conjunction with a lamp and these monochromators are available commercially.

Measurement of light intensity:

The most distinguishing property of a photochemical reaction is the fact that it is produced by light. Similarly the most characteristic quantity which may be associated with that reaction is the relation between the number of molecules changed and the number of light quanta absorbed, or the quantum yield. The ratio ordinarily observed in the study of a photochemical reaction is the overall quantum yield, which may be defined as

$$\phi = \frac{\text{number of molecules finally decomposed or formed}}{\text{number of quanta absorbed}}$$

It can be shown that the determination of quantum yield will give an indication as to the nature of the most important process or processes in the reaction mechanism. If ϕ is large, a chain reaction is indicated; if it is small, either deactivation or recombination is suggested, although the possibilities of isomerisation, regeneration or an inner filter effect must not be overlooked. A ϕ equal to some small whole number and independent of changing experimental conditions, especially if accompanied by continuous absorption, indicates a rapid and complete dissociation either into stable molecules or radicals which react further by a non-chain process. An example of this is the photolysis of hydrogen iodide with a quantum yield of 2.

Thus to determine the quantum yield, a knowledge of the number of quanta absorbed by the reacting system and hence, measurement of the incident light intensity is essential. The number of molecules formed or decomposed can be ascertained by any standard analytical technique.

The fundamental method for measurement of radiation is by use of a thermopile; this instrument is calibrated against a true "black body" which radiates according to Stefan's law. In practice this is rarely done because of the difficulty of setting up a truly black body and when thermopiles are used, they are usually standardised against standard lamps whose energy output is exactly known. If the response of the thermopile is directly proportional to lamp intensity, this is a reasonably good indication that the thermopile response is independent of wavelength, as it must be. An excellent, brief outline of the construction and use of thermopiles is given by Strong (41). The more commonly used methods for measurement of light intensity involve the use of (a) photoelectric cells and (b) a photochemical reaction, the quantum yield for which has been established, in other words a chemical actinometer. The two most commonly used chemical actinometers are uranyl oxalate (42) and ferric oxalate (43). Use and applications of photoelectric cells are described by Melville and Gowenlock (44).

Chemical actinometry: Chemical actinometry possess considerable advantages for light intensity measurements, particularly

when the source does not involve the use of a monochromator. A chemical actinometer gives the average dose over a given period of time and over a given area. By carrying out actinometry in the reaction vessel itself, one may also eliminate complications resulting from the geometry of the experimental system.

(a) Uranyl oxalate actinometer: This is still the most widely used chemical actinometer, the reaction utilised being the uranyl ion photosensitized decomposition of oxalic acid. It decomposes as

$$H_2C_2O_4 \longrightarrow H_2O + CO + CO_2$$

A detailed description of the uranyl oxalate actinometer is given by Noyes and Leighton (45) and by Masson (46) for those cases where actinometry is applied to a light beam emerging from the reacting system. The quantum yield of this photolysis has been determined with great care over the region 5000 - 2000 Å (42), the value being 0.62 at 2537 Å, 0.49 at 3660 Å and 0.56 at 3130 Å. The amount of reaction is determined by titration of oxalic acid against standard permanganate solution. Several attempts have been made recently to improve the analytical technique for determining the amount of reaction. Zill (47) followed the reaction manometrically by measuring the amount of carbon monoxide and carbon dioxide liberated

during the decomposition of oxalic acid. For studies of photochemical reactions in aqueous solutions using volumes in the range of 1 to 10 μ l, Porter and Volman (48) developed a simplified method of uranyl oxalate actinometry. The actinometry is based on the determination of CO by flame-ionisation gas chromatography after catalytic hydrogenation to methane (49). This method is more sensitive than any other method or than any other chemical actinometer. However, this method can be useful only on a microscale. The uranyl oxalate actinometer has the advantage that the quantum yield does not vary much with changing wavelength and also has a small temperature coefficient, the coefficient being 1.03 per 10° at $20^{\circ}C$. Since the quantum yield does not vary much with changing wavelength, it is especially useful if the source of radiation is rendered monochromatic by employing filters instead of a monochromator. The percent decomposition of oxalic acid varies linearly with time provided the decomposition is kept below 20%. Hence knowing the amount of oxalic acid decomposed and its quantum yield, the number of quanta absorbed by the system can be calculated (46).

(b) Potassium Ferrioxalate actinometer: This actinometer has been developed by Parker (43)(50) and fulfils the requirements of constant quantum efficiency and high absorption factor over a wide range of operating conditions. The sensitivity is

about one thousand times greater than that of the normal uranyl oxalate actinometer. The concentrations used in this actinometer are .006 M or 0.150 M of $K_3Fe(C_2O_4)_3.3H_2O$ and exposure to light produces ferrous iron, which is estimated by measuring the optical density of the 1:10 phenanthroline complex at 510 mμ . The recommended procedure is given by Hatchard and Parker (50) and the quantum yields at two different wavelengths are $\phi_{2537} = 1.25$ and $\phi_{3660} = 1.21$. Recently Lee and Seliger (51) measured the quantum yield of this actinometer at 3660 Å relative to a calibrated thermopile and their value was essentially the same as determined by Hatchard and Parker (50). Gaseous actinometers: A number of gaseous actinometers are available for use either at near ultra-violet or far ultra-violet regions. Some of them are used as internal actinometers. Acetone (52) and diethyl ketone (53) have been studied in detail, and were found to have a quantum yield of unity, for ketone decomposition or carbon monoxide formation, at temperatures above 100°C. Carbon monoxide formed can be measured manometrically after condensing the hydrocarbon products. The photolysis of HI is another reliable gaseous actinometer with $\phi_{HI} = 2$ over a wide range of experimental conditions. The hydrogen bromide decomposition is less suitable, since, because of a back reaction, the yield decreases with the amount of decomposition.

For work in the Schumann region the ozone synthesis may be used (54) where $\phi_{O_3} = 2.0$. In the far ultra-violet region a N_2O gaseous actinometer which has a well established quantum yield for N_2 production of 1.44 at 1849 Å, is often employed (55).

CHAPTER II

PHOTOLYSIS OF HYDROGEN IODIDE AND REACTIONS OF HNO

In 1936, Goodeve and Taylor (17) investigated the absorption spectrum of hydrogen iodide in the ultra-violet region down to 2000 Å. They found a continuum which extends from above 3600 Å and which reaches a maximum at about 2200 Å. Earlier, Rollefson and Booher (56) also observed the spectrum up to 4000 Å, but above 3000 Å the absorption was weak and they had to use a long gas column. Since the dissociation of HI to give a ground state H atom and an excited I ($^2P_{\frac{1}{2}}$) atom requires 92 k.cal mole^{-1} corresponding to about 3100 Å, the relatively weak absorption above 3100 Å must be due to a transition to a repulsive state producing ground state atoms.

Later in 1948, Romand (57) studied the absorption spectrum of HI and his results are shown in Figure 4(a),curve 1. He analysed this experimental curve and postulated two theoretical curves (curves 2 and 3) corresponding to two transitions, one with a maximum around 2500 Å and the other, about three times more intense, with a maximum around 2100 Å. Curve 3 he ascribes to the $^3Q_1 \longleftarrow N$ transition (Refer Figure 4(b).

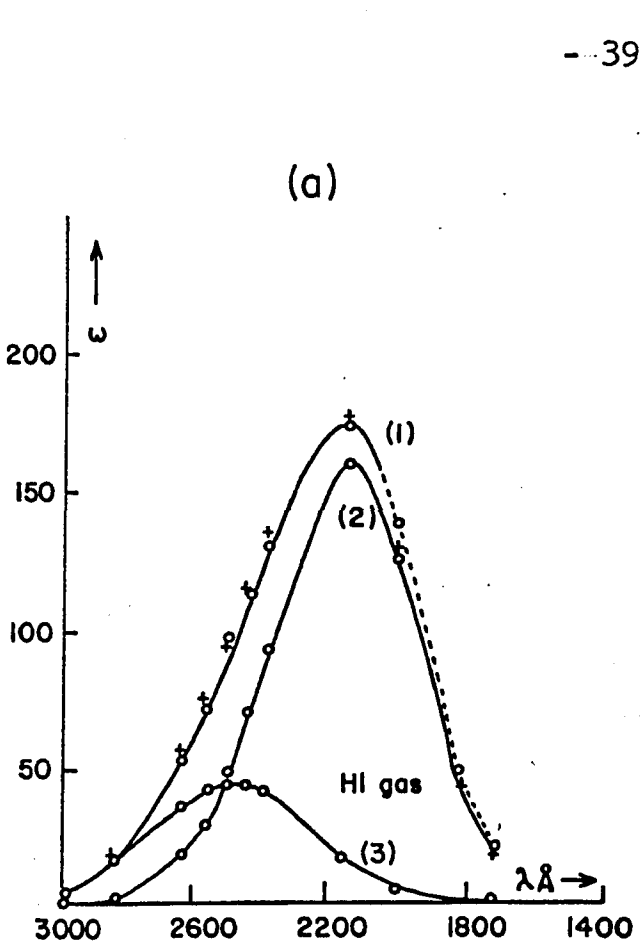

Figure 4.

HI absorption curves from the work of Romand (57). Solid portion of curve (1) is the experimental absorption curve, the dotted portion is the postulated continuum curve at lower wavelength. (2) and (3) are the calculated component curves corresponding to two different electronic transitions.

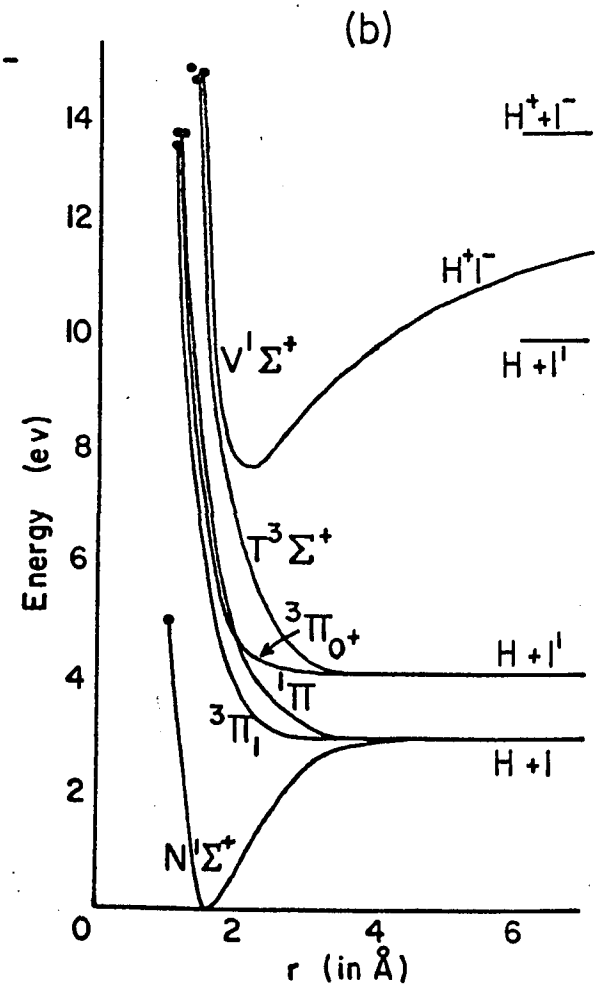

Potential energy curves for the lowest electronic states of HI from paper of Mulliken (58).

$^3Q_1$, ^1Q and Q_o according to Mulliken's terminology corresponds to $^3\Pi_1$, $^1\Pi$ and $^3\Pi_{o^+}$ states) yielding a ground state $^2P_{3/2}$ I atom, and curve 2 to the $Q_o \longleftarrow N$ transition yielding an excited $^2P_{1/2}$ I atom. Since the ^1Q potential energy curve lies above that of Q_o which in turn is above that of $^3Q_1$ on the vertical from the minimum in the ground state, the absorption curve maxima should be found in the order $^3Q_1$, Q_o, ^1Q according to the Frank - Condon principle, with the ^1Q transition peak at the lowest wavelength. Thus the production of ground state I atoms should be important at the extremes of the continuum while the production of excited iodine atoms is important in the centre. It is clear from the above discussion that photolysis of HI using a wavelength 2537 Å will yield both excited and unexcited iodine atoms, as is the case with 3130 Å. However, photolysis of HI using a wavelength of 3660 Å should yield unexcited iodine atoms.

The photolysis of hydrogen iodide was studied by Warburg (59) in 1918 at room temperature and at various pressures. The wavelengths used were 2070, 2530 and 2820 Å. Under all these experimental conditions it was found that the quantum yield of HI decomposition was two. Moreover, Bodenstein and Lieneweg (60) have shown that the quantum yield is independent of temperature up to 175°C. In 1931, Rollefson and Booher (56) while examining the absorption spectra of HI at longer

wavelengths, found the quantum yield of HI decomposition to be two even at a wavelength of 3660 Å. Thus it seems, the mechanism of photochemical decomposition is essentially the same for all effective wavelengths, except for the nature of the iodine atom.

Much work has been done on the photolysis of HI by 2537 Å radiation recently, by Ogg and co-workers (61)(62). It seems fairly certain that the initial act of absorption is followed by production of a normal H atom and an I atom which may be in the excited or unexcited state. These atoms then participate in the following sequence to give a quantum yield of two:

$$HI + h\nu \xrightarrow{I_a} H + I \qquad \phi = 1$$

$$[2] \qquad H + HI \longrightarrow H_2 + I$$

$$[7] \qquad I + I + M \longrightarrow I_2 + M$$

with an inhibitory reaction

$$[3] \qquad H + I_2 \longrightarrow HI + I$$

The reaction [7] is assumed to proceed rapidly enough, in comparison with other possible reactions of iodine atoms, so that the concentration of molecular iodine is equal to the concentration of molecular hydrogen. By the use of the "steady state" treatment, the following differential rate equation is obtained:

$$\frac{dH_2}{dt} = \frac{I_{abs}}{1 + k_3[I_2]/k_2[HI]} = \frac{dI_2}{dt} \qquad [11]$$

where I_{abs} is the concentration of photons absorbed per second. Considering k_3/k_2 as constant, integration of equation [11] leads to

$$I_{abs} \times t - [I_2]_f = \frac{k_3}{k_2}\left[\frac{[HI]_i}{4} \ln \frac{[HI]_i}{[HI]_i - 2[I_2]_f} - \frac{[I_2]_f}{2}\right] \qquad [12]$$

where $[I_2]_f$ is the final concentration of iodine, $[HI]_i$ is the initial concentration of hydrogen iodide and $I_{abs} \times t$ is the total quantity of light absorbed, measured actinometrically.

The results of Williams and Ogg (61) indicated that k_3/k_2 is experimentally constant at a value of 3.8 ± 0.3 over a range of iodine concentrations. They studied in the temperature range 102 - 189°C using wavelength 2537 Å. Later, Schwarz (30) obtained a value of 4.2 ± 0.2 for this ratio from experiments covering the range 12 - 30% photolysis. It was also found that this ratio was independent of temperature, which would imply that reactions [3] and [2] have the same activation energy but that iodine is 3.8 times more

efficient in reacting with H atoms than is hydrogen iodide. However, when inert diluents such as He, Ar, H_2 (30) or cyclohexane (61) were added to the reaction, it was found that the quantum yield of hydrogen production decreases or alternatively, the ratio k_3/k_2 seems to increase, reaching a limiting value at large inert gas pressure. Furthermore, this limiting ratio of rate constants was independent of the nature of the inert gas and was temperature dependent. At a given inert gas pressure no dependence of k_3/k_2 on $[I_2]/[HI]$ was observed. Schwarz (30) explained this on the basis of a 'hot atom' mechanism.

The 2537 Å radiation corresponds to 112.8 k.cal. $mole^{-1}$ while the bond strength of HI is 70.5 k.cal. $mole^{-1}$ and the electronic excitation energy of a $^2P_{\frac{1}{2}}$ iodine atom is 21.8 k.cal. $mole^{-1}$. To conserve momentum essentially all of the energy from the primary process in excess of that used in bond rupture and electronic excitation must appear as translational energy of the H atom, so that a 42 k.cal. $mole^{-1}$ H atom will be produced with a ground state I atom and a 20 k.cal. $mole^{-1}$ H atom will be produced with an excited ($^2P_{\frac{1}{2}}$) I atom. Since the hot H atoms have energy greater than the activation energy of reaction [2], it seems probable that this reaction will take place on almost every collision, and will be temperature independent. However, when inert diluents are added, the H

atom loses its excess energy by collision with inert gas molecules to become thermalised. It can be shown by the use of equation [10] that on an average, six collisions with helium are required to moderate hydrogen atoms from 42 to 4 k.cal. Similarly for moderation by hydrogen, it requires five collisions and fifty collisions are required with argon atoms before they can thermalise the hot H atoms. Thus, when a large inert gas pressure is added, all the hydrogen atoms which are hot will be thermalised before they can react with HI or I_2 according to reactions [2] and [3]. So the limiting ratio of the rate constants $(k_3/k_2)_\infty$ is the rate constants ratio for normal H atoms reacting with HI and I_2. Schwarz et al (30) found the ratio of rate constants $(k_3/k_2)_\infty$ at infinite gas pressure is independent of the nature of inert gas whether it is H_2, He or Ar. From the $(k_3/k_2)_\infty$ values at different temperatures $E_2 - E_3$ was calculated as 4.5 k.cal. $mole^{-1}$. Since E_3 is zero, they concluded E_2 is about 4 k.cal. $mole^{-1}$.

Sullivan (63)(64) while studying the synthesis of HI from H_2 and I_2 in the temperature range 666 - 799^{0}K calculated the ratio of rate constants k_3/k_2 for normal or thermal H atoms. His results indicate k_3/k_2 for normal H atoms is 13.0 and is independent of temperature. From this he concluded E_3 = 0 k.cal. $mole^{-1}$ and E_2 = 0 k.cal. $mole^{-1}$.

This seems at variance with the work of Schwarz (30).

From thermodynamic considerations, Sullivan (63) has calculated the rate constant and the activation energy for the above two reactions, which are given as follows

$$\log_{10}(k_2/T^{\frac{1}{2}}) = (12.2 \pm 0.2) - \frac{480 \pm 350}{4.575T} \qquad [13]$$

$$\log_{10}(k_3/T^{\frac{1}{2}}) = (13.0 \pm 0.2) - \frac{0 \pm 500}{4.575T} \qquad [14]$$

From this, the ratio of (k_3/k_2) at room temperature can be calculated as 14.0. This low value of 14 seems to be compatible with the quantum yield of two obtained during the photolysis of HI with radiation 3660 Å, wherein there will be little hot atom effect. Although, the 'hot atom' hypothesis explains the result at 2537 Å, the values obtained by Schwarz et al (30) for the ratio of rate constants seem to be in some doubt, because if $(k_3/k_2)_\infty$ values which they obtained at 114°, 154° and 198°C are extrapolated to 25°C a value of 100 is obtained for this ratio at room temperature. This high value if substituted in equation [11] should show a drastic reduction in the quantum yield of hydrogen production, which is not observed.

There is no mention in the literature of any kinetic study between HI and NO except for a thermal reaction. In the thermal reaction (65) it was observed that HI and NO react to form NH_4I, I_2 and H_2O as the main products in the temperature

range 90 - 300°C. The overall stoichiometry of the reaction was stated as:

$$6HI + NO = NH_4I + H_2O + 5/2\ I_2$$

HNO was postulated as an intermediate leading to the formation of NH_4I. From the energy of activation the bond strength of H-NO was calculated as 48.0 k.cal. $mole^{-1}$, which agreed well with the spectroscopic value of 48.6 k.cal. $mole^{-1}$ obtained by Clement and Ramsay (66).

Although the presence of HNO as a reactive intermediate has been postulated in the past (67), the question of its existence and structure has been satisfactorily settled only recently (68)(69)(70)(71).

Dalby (68) observed the absorption spectrum of HNO in the region 6500 Å - 7000 Å while studying the flash photolysis of nitromethane, nitroethane and nitric oxide - ammonia mixture. Later Clement and Ramsay (66) photographed the emission spectrum of HNO obtained from the reaction of H atoms with NO. Cashion and Polanyi (69) observed infra red chemiluminescence from the gaseous reaction of atomic H with NO, which they attributed as due to emission from HNO. Brown and Pimentel (70) found HNO in the products of photolysis of nitromethane in an argon matrix at 20°K and it was identified by its infra-red spectrum. From the vibrational frequencies

(1570 and 1110 cm.$^{-1}$) and the bending force constant, it was concluded that HNO is a bent molecule. They also pointed out that nitroxyl has a structure H-NO rather than HON, from their calculations. Ramsay from detailed analysis of spectroscopic data (71) obtained the bond lengths and the bond angles of HNO

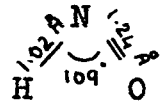

In 1944, Taylor and Tanford (72) found N_2 and H_2O as the products in the mercury photosensitized reaction of H_2 with NO. They proposed the following mechanism involving HNO to explain the formation of N_2 and H_2O.

4(a)	$H + NO$	$\longrightarrow HNO$
[8]	$HNO + HNO$	$\longrightarrow (HNO)_2$
[9]	$(HNO)_2$	$\longrightarrow H_2O + N_2O$
[10]	$N_2O + H$	$\longrightarrow N_2 + OH$
[11]	$OH + H_2$	$\longrightarrow H_2O + H$

Since they could not detect any N_2O it was concluded that this product was reduced as fast as it was formed, despite evidence (73) that reaction [10] has an activation energy of 15-20 k.cal. mole^{-1} and hence should be a slow step. The source of N_2 in the reaction therefore remained obscure. Dimerisation of HNO is based on an observation made by Harteck (74) who found that when H atoms are allowed to react with NO a yellow explosive solid is produced at liquid

air temperature, which decomposes at higher temperatures to N_2O and H_2O. However, when NO is allowed to react with H atoms from a discharge tube no N_2 was produced. This was similar to the observation made by Smallwood (75) in 1929, who found that NO merely catalyses the recombination of H atoms to form H_2. In the photosensitized reaction considerable amounts of N_2 and H_2O are formed. This can be explained as due to difference in experimental conditions, one being dynamic and the other being a static system. In a static system H atoms are continuously produced as is the case in a photosensitized reaction, while in discharge tube reactions the system is dynamic. If only a small fraction of HNO is decomposed into N_2O and H_2O and most of it reacted with H atoms, the decomposition would be negligible in a flow system but cumulative in the static system.

Recently Clyne and Thrush (76) studied, in a very elegant way, the reaction between H and NO in a fast flow system using H atoms obtained from an electric discharge. The rate of removal of H atoms in the presence of NO was determined by the rate of decay of HNO emission. They measured the intensity measurements from the principal emission band at 7525 Å. The total pressure in the system varied from 1 - 4 mm. of Hg and no N_2, N_2O or H_2O was found as a product.

The third order rate constant for the reaction

[4] $H + NO + M \longrightarrow HNO + M$

was obtained, which was found to be dependent on the nature of M, the third body. From an Arrhenius plot, the negative activation energy for the above reaction was obtained as 0.7 ± 0.3 k.cal. $mole^{-1}$.

In 1964, Strausz and Gunning (77) studied the reaction between H atoms and NO at room temperature, the source of H atoms being (a) Photosensitized decomposition of H_2 and (b) photolysis of CH_2O. The products were N_2, N_2O, H_2O and higher oxides of nitrogen; the latter reacted with the mercury present to form a white solid which was identified as predominantly $Hg(NO_2)_2$ and hence they concluded HNO_3 is also a product of this reaction. From the combined results of the sensitized and photolysis studies they proposed a mechanism capable of accounting for the following experimental findings: (a) both N_2 and N_2O are primary products of the reaction and arise from competing reactions: (b) the rate of N_2 production depends on a lower power of the HNO than that of the N_2O producing step: (c) the rate of the N_2 forming step is proportional to the first or higher power of NO concentration: (d) the N_2 and N_2O forming reactions are both of a non-chain character. The proposed mechanism was

[4] $H + NO + M \longrightarrow HNO + M$

[12] $H + HNO \longrightarrow H_2 + NO$

[8] $2HNO \rightleftharpoons (HNO)_2$

[9] $(HNO)_2 + M \longrightarrow H_2O + N_2O + M$

[13] $HNO + NO \rightleftharpoons HNO.NO$

[14] $HNO.NO + NO \longrightarrow N_2 + HNO_3$

Since the calculated apparent third order rate constant for N_2 production was pressure dependent they prefered a two stage step for N_2 production, to a direct termolecular reaction.

Srinivasan (78), while studying the photolysis of ^{15}N-ammonia in the presence of NO, found that the N_2 product consisted not only of $^{15}N^{14}N$ as expected but also of $^{14}N_2$. The source of this N_2 could be the reaction of NO with either HNO or a nitroso compound formed by the amino radical.

The reactions of HNO seem to be similar to the reactions of RNO, alkyl nitroso compounds, which have been investigated in detail by Christie and co-workers (79)(80)(81). They studied the disproportionation of nitric oxide by alkyl nitroso compounds which were obtained by the photolysis of alkyl iodides, CH_3I, C_2H_5I, $n\text{-}C_3H_7I$, $i\text{-}C_3H_7I$ and $t\text{-}C_4H_9I$, in the presence of NO. The photolysis of iodides gave the corresponding alkyl radicals which on reacting with NO gave RNO. The nitrosoalkane monomer can dimerise or isomerise to an oxime. Dimerisation is the predominant reaction at room temperature (82); isomerisation is more important at higher temperatures (83). However, in the presence of excess NO, it

was observed that N_2 and NO_2 were the products. They followed the reaction by studying the rate of NO_2 formation spectrophotometrically. The mechanism suggested was

$[1']$ $\quad R + NO \longrightarrow RNO$

$[2']$ $\quad RNO + 2NO \longrightarrow R\cdot + \cdot NO_3 + N_2$

$[3']$ $\quad \cdot NO_3 + NO \longrightarrow 2NO_2$

and when the nitric oxide pressure is not high monomeric nitroso alkanes tend to dimerise, setting up the equilibrium

$[4'][-4']$ $\quad 2RNO \rightleftharpoons (R.NO)_2$

The rate of NO_2 production was proportional to the first power of nitrosoalkane concentration and to the square of the NO concentration. For each nitrosoalkane studied the third order rate constant k_2', for N_2 production, decreased with increasing temperature, yielding a negative activation energy and in the homologous series

$$E_{t\text{-}Bu} < E_{Pr} < E_{Et} < E_{Me}$$

They also calculated the ratio of rate constants $R = k_{R+I_2}/k_{R+NO}$ for the above alkyl radicals and found

$$R_{i\text{-}Pr} > R_{Pr} > R_{Et} > R_{Me}$$

The negative activation energies for N_2 production imply that an equilibrium such as (5'), with (6') the rate determining step, is involved in the overall reaction

$[5'][-5']$ $\quad R.NO + NO \rightleftharpoons R(NO)_2$

$[6']$ $\quad R(NO)_2 + NO \longrightarrow R(NO)_3 \longrightarrow R. + N_2 + \cdot NO_3$

The temperature dependence of $k_{2'}$ will be negative provided that

$$E_{-5'} > E_{6'} + E_{5'}$$

In their experiments they were using a small ratio of NO/RI so that step 6' was rate determining, which will lead to second order in nitric oxide. At very high NO/RI ratios there may be a change in order with respect to NO.

In spite of similarities between HNO and RNO, one observation seems to be very pertinent, namely HNO is not a very efficient species for the disproportionation of NO (79) (84), compared with RNO.

Nitric oxide is widely used to inhibit gas-phase reactions which proceed by a free radical chain mechanism. In the inhibited reactions of hydrocarbons, aldehydes and ethers it has been postulated that HNO (85) and RNO (86) are intermediates in these reactions.

The effect of NO on pyrolytic reactions was first observed by Hinshelwood and Staveley (87), who found that the addition of NO causes a reduction in the rate of decomposition of diethyl ether and other organic compounds. A similar effect was also observed by Rice and Polly (88) with the addition of propylene to the reaction system. The fact that in many cases the inhibitors lead to a constant limiting rate and that the same limiting rates are given by different

inhibitors led Hinshelwood and co-workers (89) to believe that the residual reactions are molecular in nature. On the other hand there are certain characteristics of the fully inhibited reactions that seem to be incompatible with the view that a purely molecular mechanism is involved. These are (i) Rice and co-workers (90) found that hydrogen-deuterium mixing reactions take place as rapidly in certain fully inhibited reactions as they do in the uninhibited reactions. (ii) fully inhibited reactions exhibit a well defined induction period (91) and (iii) the fully inhibited rates are sometimes decreased by increasing the surface to volume ratio. It would seem to be quite impossible to reconcile these facts with the hypothesis of a simple molecular mechanism and hence mechanisms of the free radical type were developed by Laidler and Wojciechowski (92) and Norrish and Pratt (86).

The former authors suggested that in the case of nitric oxide inhibition, initiation is considered to be by the abstraction of a hydrogen by NO, while termination involves reaction between the most plentiful chain carrier and either HNO or NO, depending on whether or not H is a chain carrier. Mechanisms were proposed for decomposition of paraffins, ethers and aldehydes, when inhibited by NO and the resulting rate equations were shown to be consistent with the behaviour observed experimentally.

Since it was found by previous workers (91)(93) that there is very little consumption of nitric oxide in these inhibited reactions, mechanisms were proposed (94)(95)(96) involving equilibria of the type

$$H + NO \rightleftharpoons HNO \quad \text{or} \quad R + NO \rightleftharpoons RNO$$

In spite of the fact that the mechanism proposed by Laidler and Wojciechowski (92) explains in a simple way the experimental behaviour, both in the maximally inhibited and induced reaction, it fails to take into consideration the reactions of nitroso compounds, which are formed from alkyl or H atoms reacting with NO. These have been shown recently (79) to proceed to considerable extent.

Norrish and Pratt (86) proposed an alternative mechanism for the inhibited reaction by NO, which involves reactions of nitroso compounds. The main drawback of this treatment is the complicated rate equation that is obtained by the steady state treatment, involving many unknown rate constants, which have to be assumed to obtain any meaningful result. Secondly, they assume certain radicals are 'large radical' and 'small radical', and to distinguish them in all the systems may not be easy and lastly it does not seem to be applicable to all systems.

Thus, it may be concluded that although a large amount of work has been done on pyrolysis of hydrocarbons in the presence of nitric oxide, the mechanism of the inhibited

reaction is not yet clear. Possibly, the reactions of RNO and HNO may play an important role and the consumption, or otherwise, of NO in these systems may throw some light on this complicated problem.

With this in view we studied the photolysis of HI in the presence of NO using light above 3000 Å. The hydrogen atoms so produced will react with NO to form HNO and this may give further insight into the reactions of HNO. Our results, in general, show the same trend as was observed by Christie and co-workers with RNO.

CHAPTER III

EXPERIMENTAL

Apparatus

The apparatus and experimental procedure were very similar for the different temperatures and various inert gases employed, so the general description given here applies to chapters III and IV.

A typical static vacuum system was employed which is shown schematically in Figure 5.

The entire system could be evacuated to less than 10^{-5}mm. Hg by means of a "three stage" mercury diffusion pump (P_1) which was backed by a single stage Welch rotary pump (P_2). A single manifold connected all parts of the apparatus. Gases used in the experiments were stored in bulbs V_1, V_2, and V_3, each having freezing nipples for purification of the gases. Storage bulb V_1 was of 2 liter capacity and was used to store purified hydrogen iodide. The bulb was painted black to prevent photolytic decomposition. After several unsuccessful trial runs, it was found that Apiezon T stopcock grease was best for greasing the stopcocks in frequent contact with hydrogen iodide. This stopcock grease proved to be resistant to attack by HI after some initial colouration. The bulb V_2 also of 2 liter capacity was used

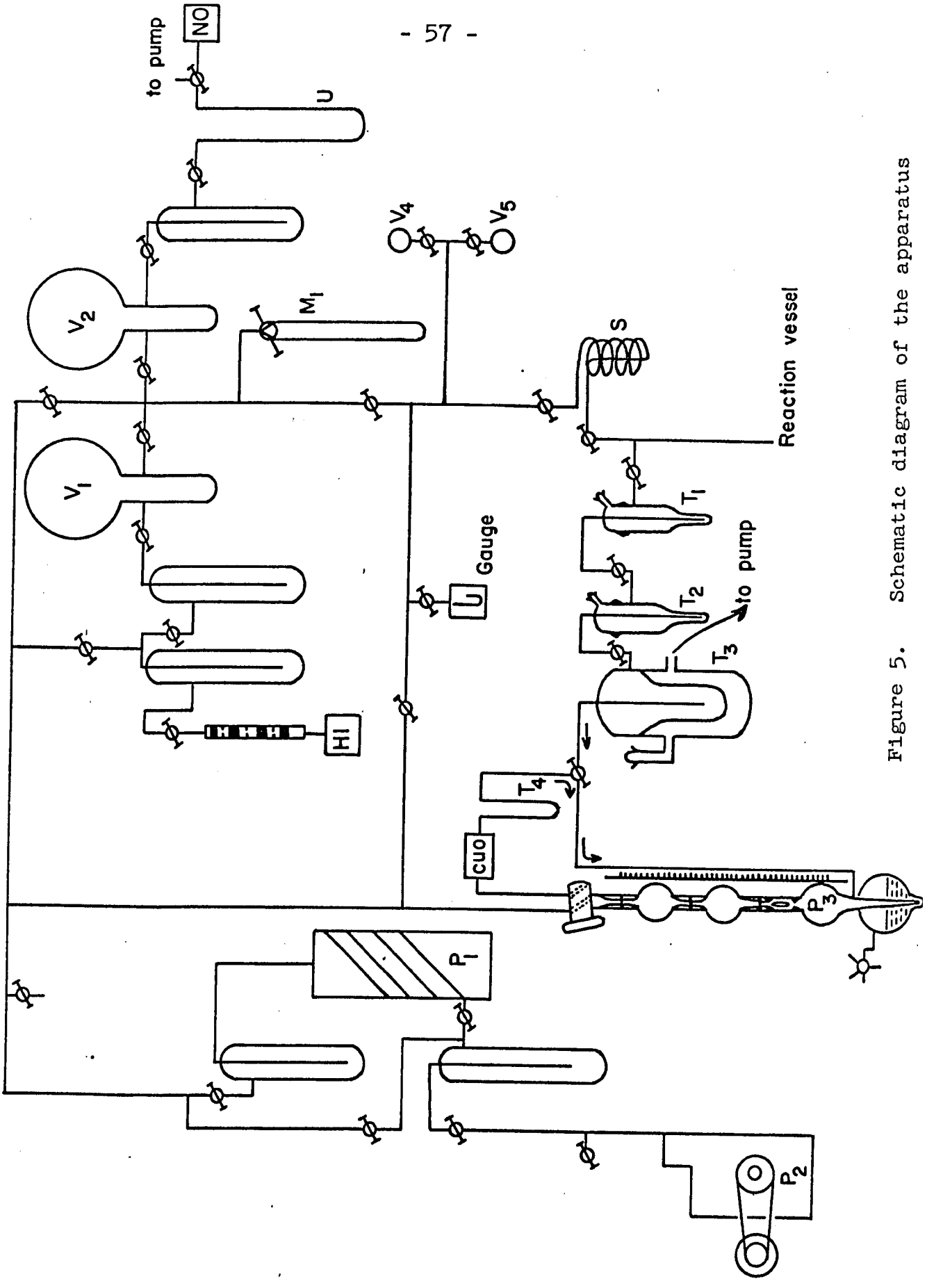

Figure 5. Schematic diagram of the apparatus

to store pure NO and bulb V_3 was for pure inert gases. V_4 and V_5 were small calibrated vessels whose volume was determined by weighing several times with distilled water. The standard volumes of these bulbs were taken as the mean average of several readings. V_4 had a volume of 157.0 ml. and V_5 was 25.5 ml. Pressures in these bulbs were measured with a mercury manometer M_1, which had a three way stopcock connected to the main manifold. One arm was always used for measuring hydrogen iodide pressures, while the other arm was used for measuring nitric oxide pressures. The reason for using separate arms for HI and NO, was, hydrogen iodide slowly attacks mercury thereby contaminating it with iodides of mercury. The inlet to each bulb V_1 and V_2 was attached to a purification unit which in turn was attached to the cylinders of the research grade gases or to the hydrogen iodide generating unit as the case may be. A U-trap (U), approximately one metre long and one cm. diameter, containing high activity silica gel for the purification of nitric oxide, was connected to the inlet side of bulb V_2. A trap was also connected between the U-trap and the inlet of the storage bulb. Each of the storage vessels and the calibrated standard vessels was attached to the reaction vessel (RV) through a spiral (S) which was always maintained at $-78^{\circ}C$ to prevent mercury vapours from entering the reaction system.

The reaction vessel (RV) was a cylindrical quartz tube, 15 cm. long and 5 cm. in diameter, having plane parallel faces. The volume of the reaction vessel, including the dead space was calculated as 302.0 ml. Attached to the reaction vessel was a small cold finger V_6, which was used for freezing the reaction mixtures and for mixing the gases before they were photolysed. The connecting tubing from the reaction vessel to the cold finger, spiral gauge and to the attached stopcocks were all capillary and hence the dead space was only about 2% of the total volume. The outlet side of the reaction vessel was attached to the analytical system, which consisted of two titration traps (T_1) and (T_2) followed by a pump down solid N_2 trap (T_3) which in turn was attached to a Töpler pump (P_3) and a gas burette. Each volume in the gas burette was calibrated accurately by weighing with mercury or water. The end of the gas burette was closed by a three-way stopcock, one connecting the main manifold and the second connecting a CuO furnace as shown in Figure 5. The CuO furnace was used to oxidise H_2 to H_2O and hence to separate H_2 from N_2. The CuO temperature was maintained at 310°C.

Optical System

The reaction vessel (RV) was enclosed in a well insulated box, one side of which could be removed. The

temperature of the box could be controlled to any desired temperature either by heating or cooling. However, for low temperatures, namely, at 6° and -20°C, only the reaction vessel was cooled (see P. 117). The temperature of the reaction vessel could be controlled to better than ± 0.5°C, except at -20°C. The box had a window of 5 x 5 cm. where a Corning glass filter, colour specification no. 9-53, was used which cuts off light below 3000 Å and for wavelength 2537 Å a Vycor glass was used as a filter. Since the most intense lines above 3000 Å are 3130 Å and 3660 Å, which are of equal intensity, in all our experimental work the wavelength will be quoted as 3130 Å. The absorption of HI at 3660 Å is small (see Figure 7) but together with the 3130 Å wavelength sufficient photolysis could be obtained in a reasonable time.

The lamp was a medium pressure Hg arc, Hanovia S-500, which was attached to a transformer. An ammeter was placed in series with the lamp. Since the intensity of the lamp depends on the amperage and voltage, these two variables were always kept constant. However, once the lamp started to age, the intensity fell; this was indicated by a fluctuation of the voltage. When the output of a lamp became irreproducible it was replaced. The whole assembly is schematically shown in Figure 6. The lamp was enclosed

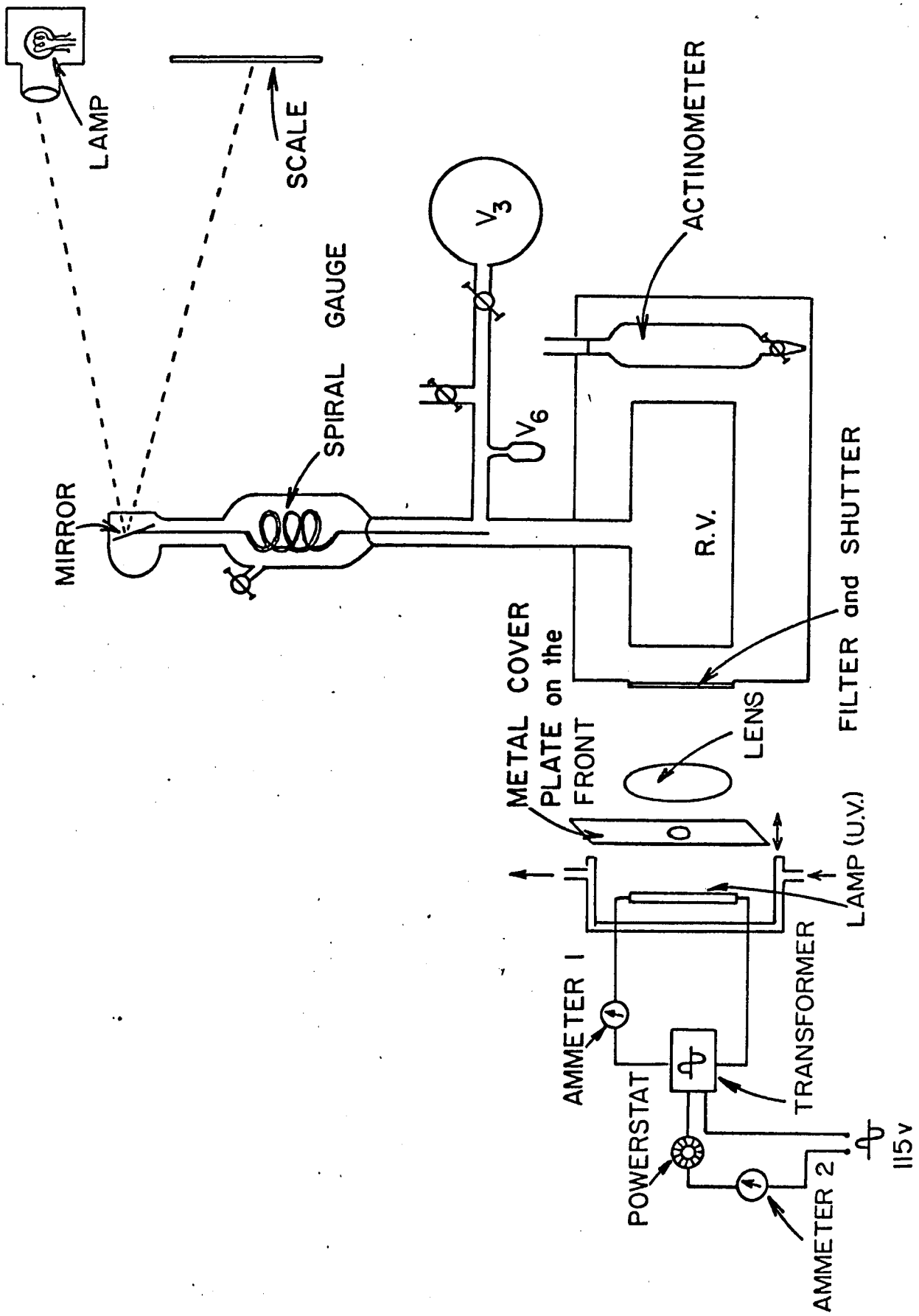

Figure 6. Optical System

in a water cooled metal box which had a light-exit hole of 1.5 cm. diameter. A quartz lens of 7.5 cm. diameter and of 10 cm. focal length was placed between the filter and the lamp, so that the light falling on the reaction vessel was almost parallel and the total volume of the cell was illuminated.

An actinometer cell of 6cm. diameter and of 3 cm. depth was placed as shown in Figure 6. The position of the actinometer was adjusted such that all the light passing through the reaction vessel passed through the actinometer solution. In any experiment the volume of the actinometer solution was always kept constant. Corrections due to reflection and absorption losses at the windows of the reaction vessel were shown to be negligible. The amount of oxalate decomposed with the reaction vessel in the path of the actinometer was 99% of that without the vessel.

Attached to the reaction vessel was a quartz spiral gauge. In order to damp out oscillations the spiral gauge, one side of which was evacuated, was immersed in silicone oil. The position of the mirror on the spiral gauge was fixed in such a way that on evacuating both sides, the reading was on zero of the scale which was kept at a distance of 1 metre from the mirror. The deflection on the scale could be calibrated, so that the pressure in the reaction vessel was

obtained directly from the deflection reading. The spiral gauge was utilised when doing runs with inert gases.

Materials

Hydrogen Iodide:- Hydrogen iodide was prepared by adding reagent grade 57% hydriodic acid (Fischer Scientific Co. U.S.A.) to phosphorous pentoxide. The liberated gas was passed through a column filled with P_2O_5 and glass wool in alternate layers. The gas was then condensed in a trap cooled by liquid N_2. The condensed HI was pumped on for about 5 minutes to remove any H_2 and then after several trap to trap distillations (-78°C to -196°C), the gas was stored in bulb V_1. Before use the hydrogen iodide was again redistilled and any non-condensible gas at -196°C removed by pumping. When freshly prepared it is a pure white solid, and yellowish white in the liquid state. HI decomposes very slowly and so before each experiment the HI was degassed and samples were taken at -78°C to avoid contamination by iodine.

Nitric Oxide:- Nitric oxide gas was obtained from Matheson and Co. The gas from the cylinder was passed through a column of silica gel (U) immersed in dry ice - acetone mixture at -78°C to remove moisture and NO_2. The gas thus obtained was then condensed in liquid nitrogen and the non-condensible gas impurity, (N_2), was pumped out for about 10

minutes. Then it was further purified by subliming the NO from a trap immersed in liquid O_2 to a trap immersed in liquid N_2. This procedure, though tedious, is very effective. The NO so obtained has a bluish white colour when solid and pale blue when liquid. For any experiment, the NO was always pumped on for about a minute or so while immersed in liquid N_2 and always taken out for a run using n - propanol - liquid N_2 mixture ($-127^{o}C$). Mass spectrometric analysis showed no N_2O as impurity.

Nitrogen, hydrogen and carbon monoxide used were all pure research grade from Matheson Co. of Canada obtained in 1 liter pyrex flasks with break-seals. These bulbs were attached to the reaction vessel at V_3.

For volumetric determination of iodine and hydrogen iodide, the following reagents were used: potassium iodide, potassium iodate and sodium thiosulfate. The potassium iodide was shown to be iodate free. All the above three reagents were Fischer certified reagent chemicals. For the volumetric determination of oxalate, potassium permanganate was used; it was standardised against $Na_2C_2O_4$ according to the procedure given in Vogel (97).

Procedure

In a typical run, a known amount of HI was taken

in the standard vessel V_4 at a known pressure. From this the initial concentration of HI was calculated from the perfect gas law. The amount of HI corresponding to a certain initial pressure was also checked by titration. In every experiment the lamp was allowed to warm up for at least half an hour before the reactants were photolysed. This ensures stability of the lamp. The hydrogen iodide was then condensed in the side arm, V_6, of the reaction vessel. The stopcock attached to the reaction vessel was closed and HI was allowed to expand into the reaction vessel and the pressure was noted from the spiral gauge. When no other gas was added, it was photolysed for a measured time, after having been allowed to come to thermal equilibrium. The time allowed for this was usually 10 to 15 minutes. When NO or other gas was added hydrogen iodide was recondensed in the finger, and a known amount of NO was also condensed in the cold finger. In order to ensure complete mixing of HI and NO and hence eliminate any errors due to variation in reactant composition, the two gases were condensed and evaporated several times before photolysing. Once it had attained the reaction temperature, it was photolysed for a known interval of time (which varied from 10 minutes to 5½ hours). The reaction was allowed to proceed to no more than 7 to 10% conversion in each case. At the end of the run the light was shut off, and the reactants

and products were condensed in the titration trap (T_1) using liquid N_2. Trap (T_2) was also cooled by liquid N_2 while trap (T_3) had solid N_2 (-210°C). The non-condensible gases were removed at -210°C and were measured in the gas burette using the Töpler pump. Analysis of the non-condensible gas at room temperature, by mass spectrometry, showed H_2 to be the major product. N_2 was less than 1% at moderate NO/HI (about 10:1 ratio) and hence was neglected. However at large NO/HI ratios the N_2 content increased to about 3%. Hence at room temperature and at moderate NO/HI ratios, no attempt was made to measure N_2. After the removal of non-condensible gases, NO was separated from HI by distilling from liquid O_2 (-183°C) to solid N_2 (-210°C). This distillation was complete in about 3 hours. The amount of NO left behind was then measured by the gas burette. I_2 and HI were then separated using acetone, dry ice and liquid N_2. The stopper in the titration trap T_1 was opened and a dilute solution of potassium iodide was introduced through the side tube. The solution with combined rinsings was titrated with standard sodium thiosulfate solution using starch indicator.

Potassium iodide solution was added to the HI while it was condensed in liquid N_2 in trap T_2. After warming to room temperature it was washed several times with distilled water. To the solution with combined rinsings was added about

10 cc. of saturated potassium iodate solution (98). The iodine so liberated was titrated against standard sodium thiosulfate solution using starch indicator.

Actinometry. The uranyl oxalate actinometry was used to determine the number of quanta absorbed by the reactants. The procedure given in Farkas and Melville (99) was adopted. Pure uranyl oxalate was prepared from analar uranyl nitrate and analar oxalic acid by treating a hot solution of uranyl nitrate with excess oxalic acid. The solution was cooled, the resulting precipitate was washed, dried and recrystallised from water. A 0.005 M solution of uranyl oxalate was used in all experiments. The oxalate solution was filled accurately up to the mark in the actinometer cell, the volume of which was exactly known. After the photolysis all the solution was taken out in a clean, dry beaker. After stirring the solution well, 10 ml. of it were pipetted into a conical flask, 10 ml. of 6N H_2SO_4 were added, and titrated at 85°C with standard N/50 potassium permanganate solution. A portion of the unexposed solution was also titrated in a similar manner. Knowing the volume of the actinometer solution and the quantum yield of oxalate decomposition, the number of einsteins absorbed by the reactant can be calculated. If A_1 moles $liter^{-1}$ of oxalate are decomposed in time 't' without any reactant in

the reaction vessel, and A_2 moles liter^{-1} are decomposed in the same time with the reactant present, then the fraction of light absorbed by the reactant is proportional to

$$\frac{A_1 - A_2}{A_1}$$

The incident intensity of light I_o is proportional to A_1 or in other words, A_1 moles liter^{-1} of oxalate has been decomposed due to the absorption of certain number of einsteins given out by the lamp. Since the volume of actinometer solution was V ml. (= 88.0 ml.) and not one liter, the amount of oxalate decomposed would be

$$\frac{A_1 \times V(= 88 \text{ ml.})}{1000} \text{ moles}$$

and taking the quantum yield as 0.55 at 25°C

$$\text{no. of einsteins initially absorbed} = \frac{A_1 \times V}{1000 \times 0.55} = E_o$$

or, no. of einsteins absorbed by the reactant

$$= \frac{A_1 - A_2}{A_1} \times \frac{A_1 \times V}{1000 \times 0.55}$$

$$E_{abs} = \frac{(A_1 - A_2)\, V}{1000 \times 0.55}$$

Thus by knowing the number of moles of product formed by the analytical method and the no. of einsteins absorbed by the actinometer, the quantum yield can be calculated.

RESULTS

At 25°C

Since in the thermal reaction between HI and NO (65) there was consumption of nitric oxide, experiments were done to determine whether any nitric oxide was used up in the photochemical reaction. Table 1 shows the amount of NO added and amount of NO recovered, for varying amounts of hydrogen iodide and nitric oxide at various times. Two sets of experiments were done, one using 2537 Å radiation and the second using 3130 Å. From the table it is clear that there is virtually no consumption of nitric oxide. However it was observed that the amount of hydrogen produced goes on decreasing with increasing nitric oxide concentration. Since hydrogen production goes on decreasing, it was decided to investigate whether there was any change in the amount of light absorbed by the addition of nitric oxide. Consequently the absorption spectra of hydrogen iodide and hydrogen iodide-nitric oxide mixtures were determined using a Beckmann model DU spectrophotometer. The spectra are shown in Figure 7, from which it can be concluded that the absorbance of HI is not affected by the addition of nitric oxide. Nitric oxide itself does not absorb in this region (100). This was also confirmed from our actinometer results, wherein it was found that the number of quanta absorbed by hydrogen iodide in a

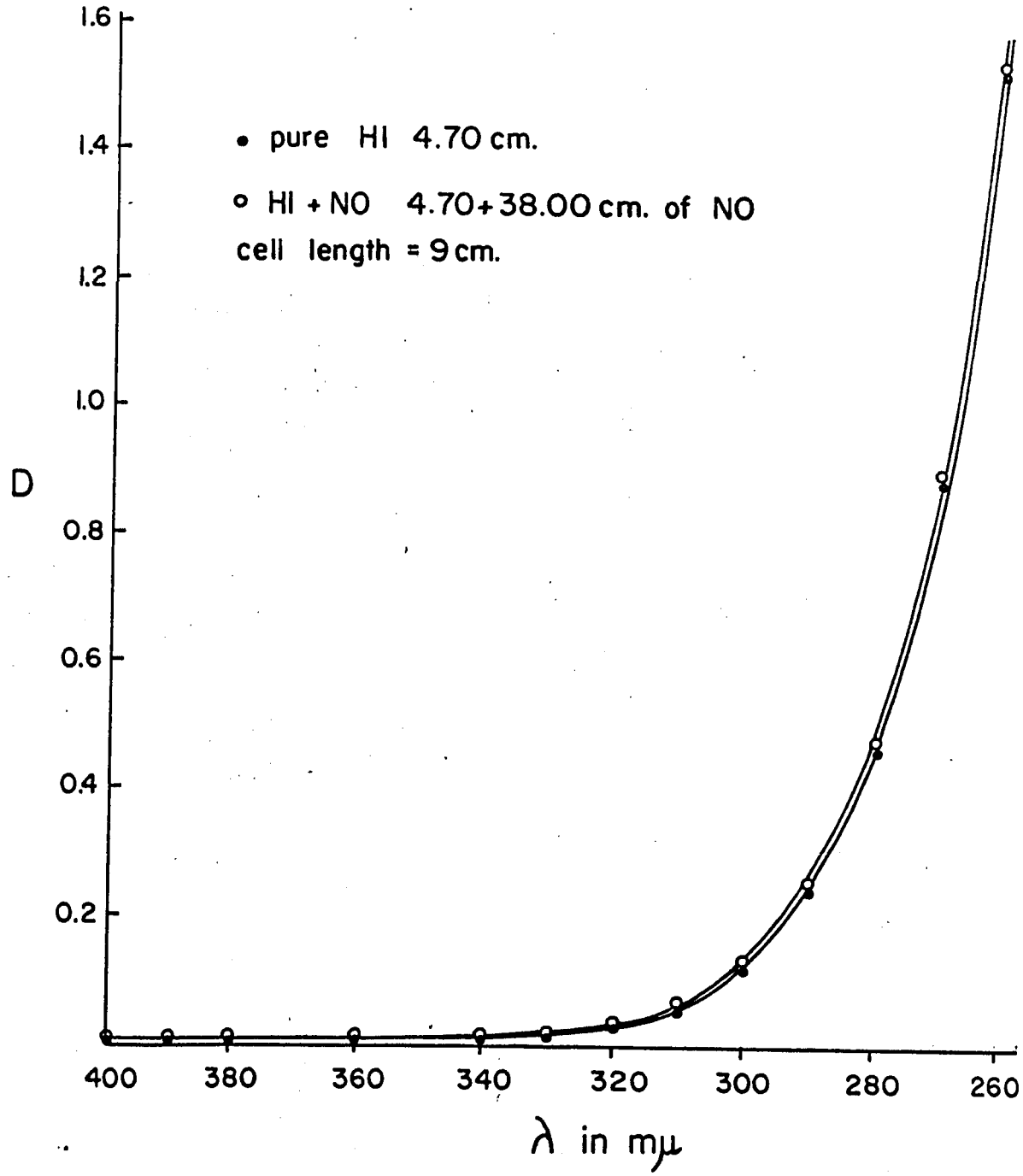

Figure 7. Plot of absorbance against wavelength for pure HI and a mixture of HI and NO at 25°C.

TABLE 1

Amount of Nitric oxide consumed in the photolysis

Temp: 25 ± 1°C

Volume of reaction vessel = 197.0 ml.

Run	Wavelength	Time in Secs.	$(HI)_o \times 10^6$ moles	$(NO)_o \times 10^6$ moles	$(H_2) \times 10^6$ moles	$(I_2) \times 10^6$ moles	$(HI)_f \times 10^6$ moles	$(NO)_f \times 10^6$ moles
A 1	2537 Å	600	115.4	-	38.7	39.0	35.0	-
2	"	"	116.5	118.8	35.4	35.6	43.9	117.4
3	"	"	108.8	235.4	29.3	31.2	42.2	234.0
4	"	"	103.0	704.9	17.3	17.3	68.0	701.5
5	"	"	99.9	532.6	21.4	21.3	55.0	529.2
B 1	3130 Å	10,800	118.1	51.5	30.7	31.0	55.8	52.0
2	"	"	112.2	244.2	25.1	25.0	60.2	243.8
3	"	"	114.4	458.7	24.0	25.1	57.9	455.8
4	"	"	111.3	764.0	22.1	22.0	64.5	761.9
5	"	19,800	39.7	742.0	6.5	7.0	24.7	734.8

$(NO)_o$ & $(HI)_o$ = initial concentrations of NO and HI

$(NO)_f$ & $(HI)_f$ = final concentrations of NO and HI

given time is constant, irrespective of the amount of nitric oxide added.

Figure 8 shows a typical time course plot at a constant NO/HI ratio. The rate of hydrogen production goes on decreasing and reaches a limiting value, once the saturated vapour pressure of I_2 is reached.

The amount of hydrogen formed in each run, divided by the number of micro einsteins absorbed by a constant amount of HI, gives the quantum yield ϕ_{H_2}. This is shown in Table 2, where for a set of nitric oxide concentrations, keeping HI and time constant, ϕ_{H_2} values were calculated. The quantum yield goes on decreasing from a value of unity in pure HI, and reaches a limiting value after which further addition of nitric oxide causes no change in ϕ_{H_2} values. It was also found that the limiting quantum yield is dependent on HI concentrations. This is shown in Figure 9. The same type of behaviour was also observed by using 2537 Å radiation. Figure 10 shows a typical plot for one concentration of hydrogen iodide. The addition of iodine causes a lowering of the limiting quantum yield. This is not very marked at 25°C, while as it is very marked at 45°C where the saturated vapour pressure of I_2 in this system is/about 22 μ moles (see P.91) equivalent to

As more and more experiments were performed, a thin layer of some white substance was deposited on the front

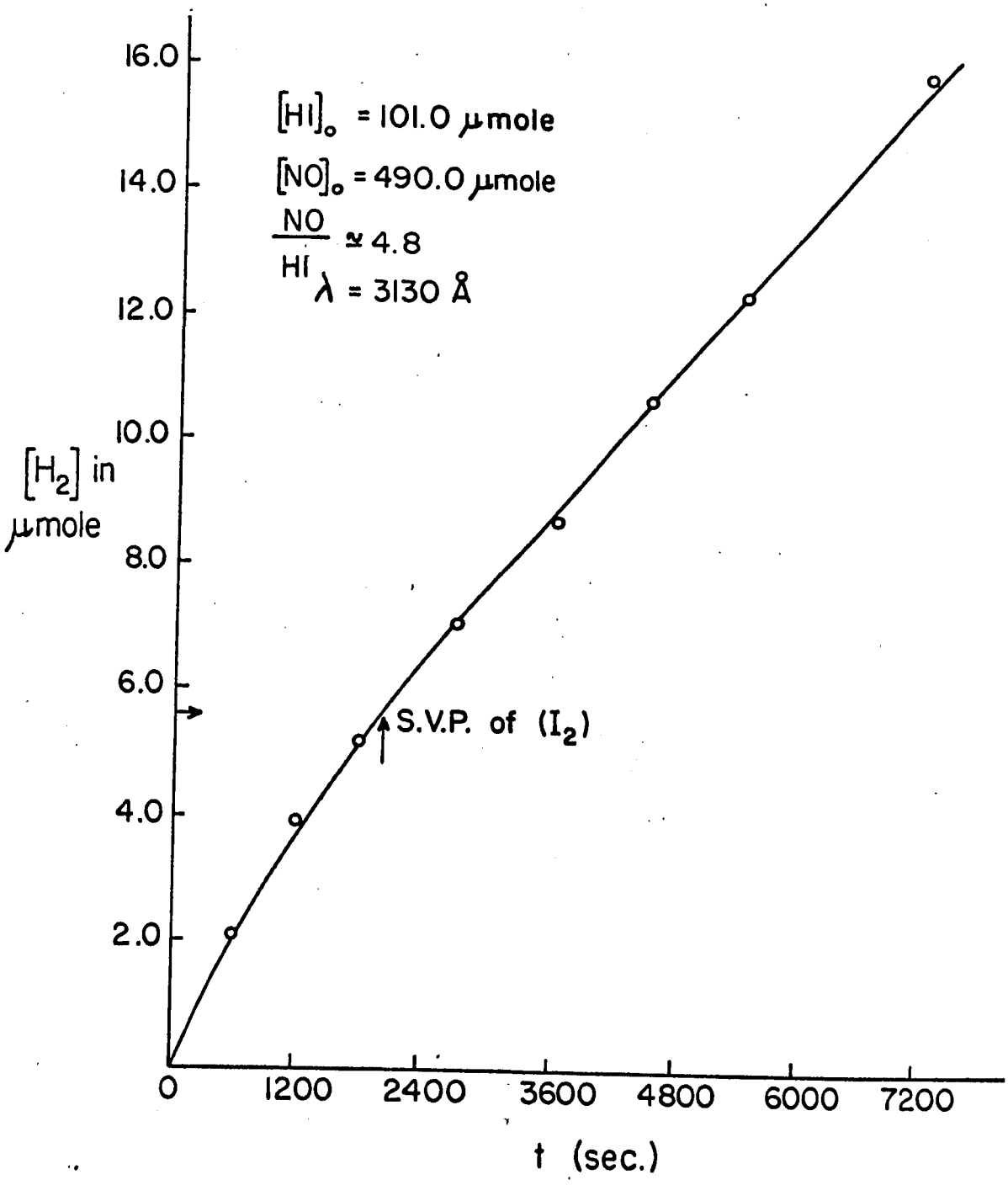

Figure 8. Time course plot for the hydrogen production at 25°C.

TABLE 2

ϕ_{H_2} values at various $\frac{NO}{HI}$ ratios and at various HI concentrations

Temp: 25°C

Vol. of the vessel = 302.0 ml.

λ = 3130 Å

Time: 4500 sec.

Run	$(HI)_o \times 10^6$ moles	$(NO)_o \times 10^6$ moles	$\frac{NO}{HI}$	$E_{abs} \times 10^6$ einstein	$(H_2) \times 10^6$ moles	$(I_2) \times 10^6$ moles	ϕ_{H_2} moles einstein^{-1}
1	427.0	-	-	24.99	25.00	25.00	1.000
2	427.3	128.2	0.30	24.96	19.60	19.70	0.785
3	429.3	858.6	2.00	25.82	17.30	17.20	0.670
4	426.0	1704.0	4.00	25.08	15.30	15.30	0.610
5	427.3	2683.4	6.28	24.57	14.50	14.60	0.590
6	438.9	4476.8	10.20	25.53	14.30	14.40	0.560
7	443.0	7575.3	17.10	25.00	13.65	16.60	0.546
8	460.0	9098.8	19.80	25.70	14.30	18.20	0.556
9	428.0	8602.8	20.10	24.50	13.40	17.30	0.546
10	428.0	9287.6	21.70	25.05	13.40	17.40	0.535

Table 2 (continued)

Temp: 25°C

λ = 3130 Å

Vol. of the vessel = 302.0 ml.

Time: 4500 sec.

Run	$(HI)_o \times 10^6$ moles	$(NO)_o \times 10^6$ moles	$\frac{NO}{HI}$	$E_{abs} \times 10^6$ einstein	$(H_2) \times 10^6$ moles	$(I_2) \times 10^6$ moles	ϕ_{H_2} moles einstein^{-1}
1	821.9	-	-	36.00	35.95	36.00	0.990
2	821.9	1150.5	1.40	36.02	27.70	27.80	0.770
3	819.2	1925.5	2.35	37.21	26.60	27.00	0.715
4	816.6	3291.6	4.03	37.38	25.23	26.00	0.675
5	810.8	5000.0	6.17	37.02	24.20	24.30	0.654
6	819.2	7271.6	8.88	37.19	23.80	24.10	0.640
7	816.6	8983.0	11.00	37.20	23.62	24.50	0.635
8	810.8	10540.4	13.00	38.05	24.20	25.30	0.636

Table 2 (continued)

Temp: 25°C

λ = 3130 Å

Vol. of the vessel = 302.0 ml.

Time: 4500 sec.

Run	$(HI)_o \times 10^6$ moles	$(NO)_o \times 10^6$ moles	$\frac{NO}{HI}$	$E_{abs} \times 10^6$ einstein	$(H_2) \times 10^6$ moles	$(I_2) \times 10^6$ moles	ϕ_{H_2} moles einstein^{-1}
1	1090.0	-	-	44.09	44.10	44.10	1.000
2	1094.3	563.0	0.51	44.44	40.00	40.25	0.900
3	1094.4	1313.1	1.20	44.37	35.50	35.60	0.800
4	1094.4	2533.8	2.32	44.12	33.09	33.10	0.750
5	1089.3	4146.7	3.81	43.90	31.74	31.80	0.723
6	1106.3	6747.0	6.10	44.32	31.25	31.30	0.705
7	1090.0	7913.4	7.26	44.28	31.00	32.00	0.700
8	1106.5	9519.0	8.60	43.29	30.39	34.30	0.702

Table 2 (continued)

Temp: 25°C

Vol. of the vessel = 302.0 ml.

λ = 3130 Å

Time: 4500 sec.

Run	$(HI)_o \times 10^6$ moles	$(NO)_o \times 10^6$ moles	$\frac{NO}{HI}$	$I_{abs} \times 10^6$ einstein	$(H_2) \times 10^6$ moles	$(I_2) \times 10^6$ moles	ϕ_{H_2} moles einstein^{-1}
1	1368.5	-	-	38.72	39.25	39.3	1.014
2	1368.5	1368.5	1.00	40.60	34.30	34.4	0.845
3	1368.5	2805.4	2.05	40.05	31.84	32.1	0.795
4	1393.2	4307.2	3.09	41.00	31.98	32.0	0.780
5	1351.2	5404.8	4.00	41.00	31.57	31.6	0.770
6	1351.2	6291.8	4.66	41.50	31.80	31.9	0.765
7	1372.9	8337.1	6.07	41.45	31.31	32.0	0.755
8	1393.2	11145.6	8.00	41.50	31.12	32.0	0.750

Table 2 (continued)

Temp: 25°C

λ = 3130 Å

Vol. of the vessel = 302.0 ml.

Time: 4500 sec.

Run	$(HI)_o \times 10^6$ moles	$(NO)_o \times 10^6$ moles	$\frac{NO}{HI}$	$E_{abs} \times 10^6$ einstein	$(H_2) \times 10^6$ moles	$(I_2) \times 10^6$ moles	ϕ_{H_2} moles einstein^{-1}
1	1613.0	-	-	48.58	48.70	48.70	1.000
2	1627.7	1638.8	1.00	48.08	41.60	41.70	0.865
3	1627.7	3255.4	2.00	48.58	39.84	39.90	0.820
4	1613.2	4839.6	3.00	49.01	39.60	39.70	0.808
5	1636.9	6547.6	4.00	49.30	39.15	39.25	0.794
6	1613.2	7693.3	4.77	49.65	39.17	39.40	0.790
7	1636.9	9068.4	5.54	49.99	38.69	39.00	0.774
8	1636.9	11458.3	7.00	50.01	39.06	40.00	0.781

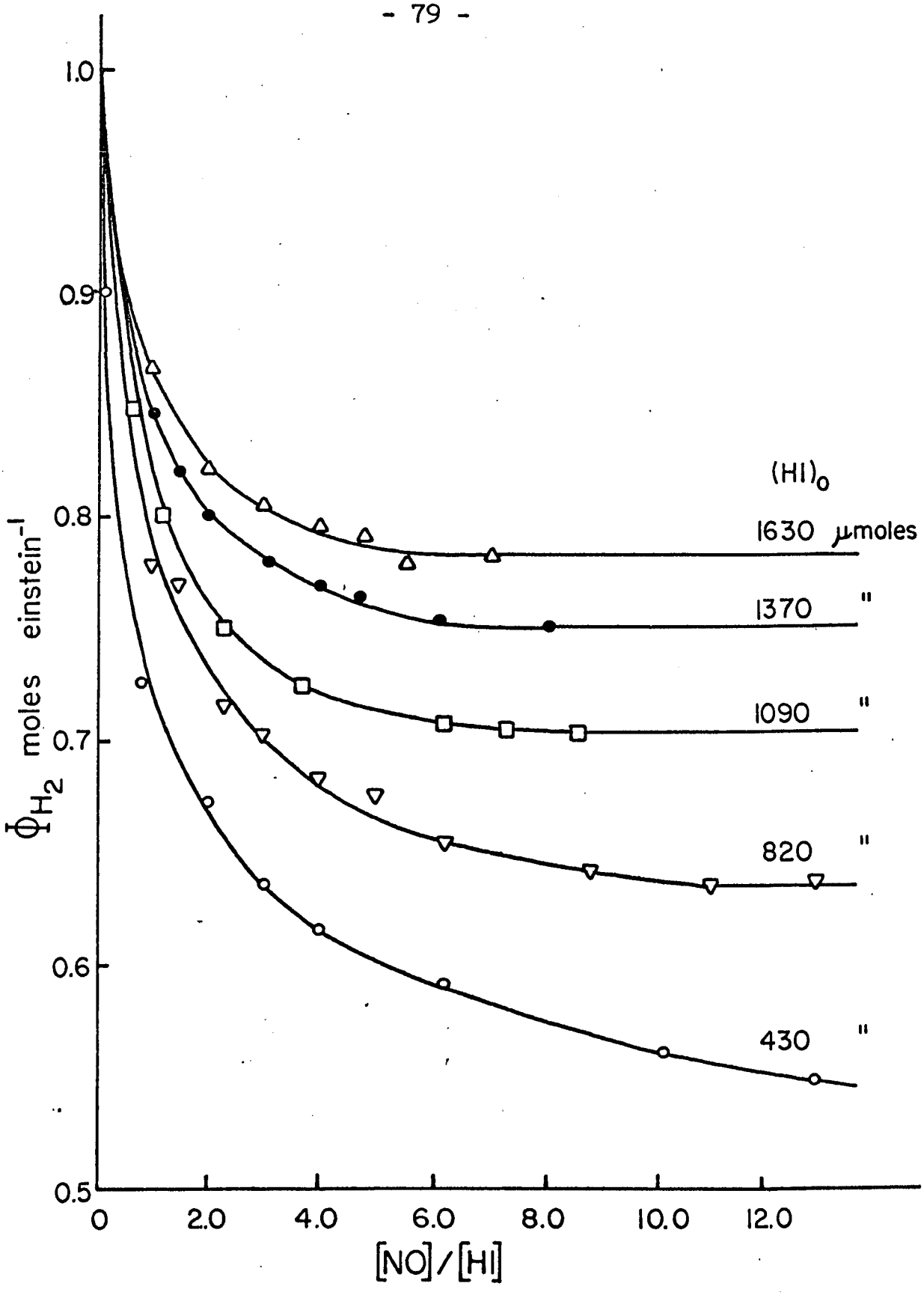

Figure 9. Variation of ϕ_{H_2} as a function of NO/HI at 25°C.

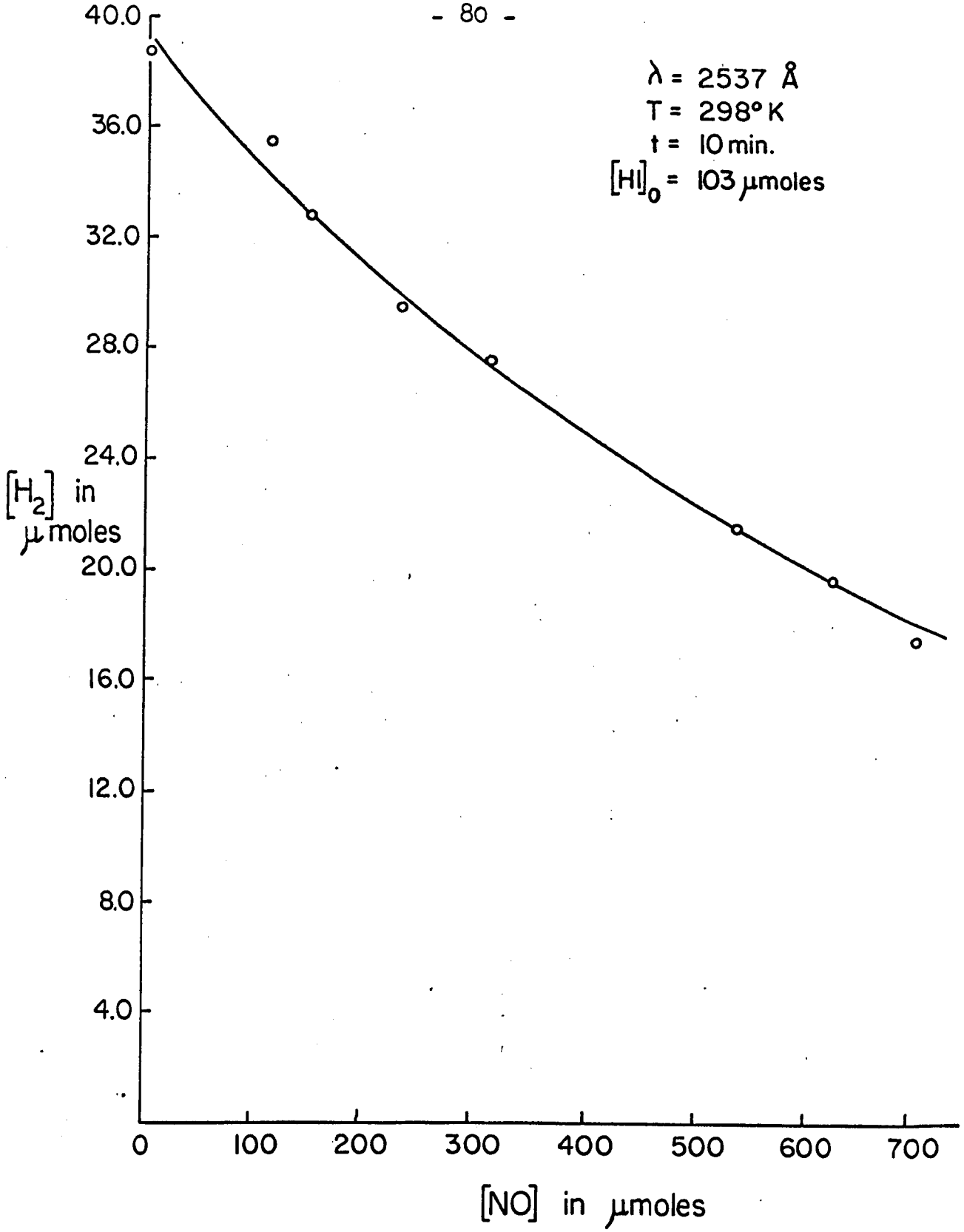

Figure 10. Plot of H_2 production at various nitric oxide concentrations using wavelength 2537 Å.

window of the reaction vessel. To avoid the decrease in intensity due to this deposit, the reaction vessel was always flamed before doing a run in order to sublime this substance to the cooler part of the system, away from the light path. After several runs the reaction vessel was cut off and the white deposit was analysed qualitatively and quantitatively. By qualitative analysis, it was found to be ammonium iodide. Quantitatively it was found that the amount of ammonium iodide in a blank thermal run at 25°C was less than 0.1 μmole, while from two photochemical runs, using the same pressures of reactants, 0.6 μmole of NH_4I were produced. The absorption spectrum of this compound was taken with a Perkin - Elmer 202 U-V. visible spectrophotometer; the spectrum is shown in Figure 11, which shows a maximum round 225 mμ. Since there was no published spectrum available for the pure compound, the absorption spectrum of pure NH_4I (Eastman - Kodak Co.) of concentration 6.89×10^{-5} molar solution, was also measured, which is shown in Figure 12. It has a maximum around 225 mμ with $\epsilon = 1.23 \times 10^4$.

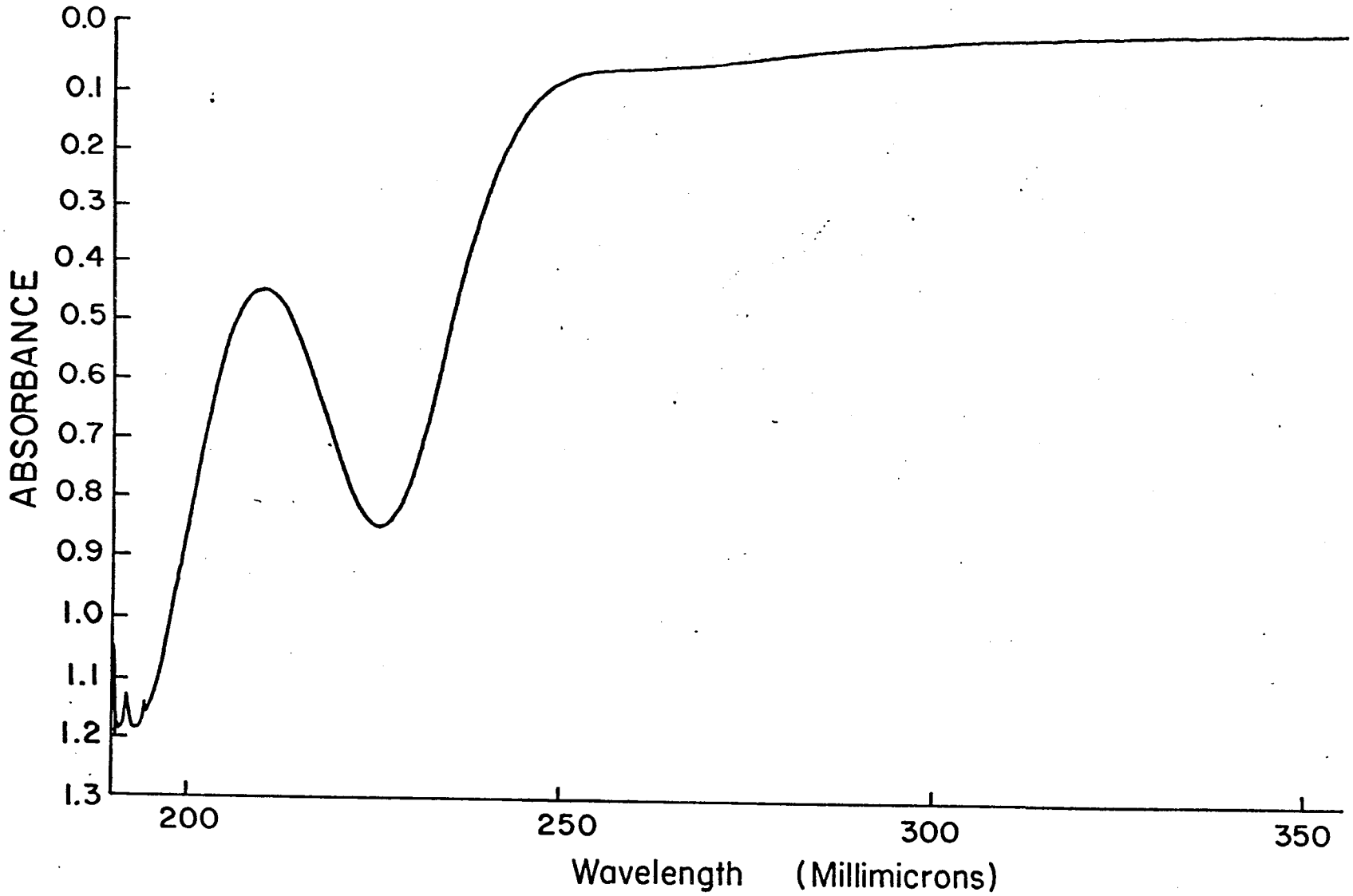

Figure 11. The ultra-violet spectrum of an aqueous solution of white deposit produced during the reaction of HI and NO.

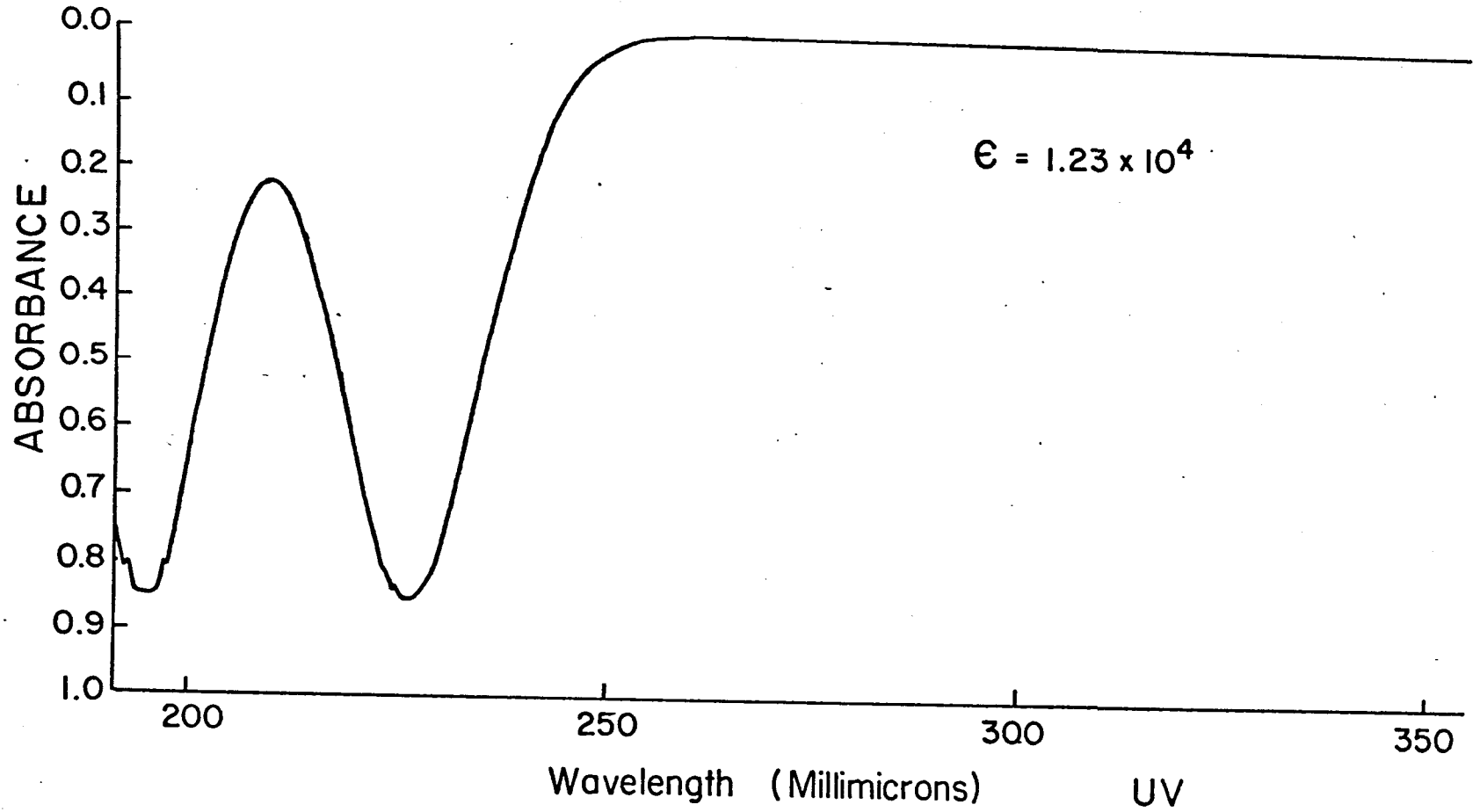

Figure 12. The ultra-violet spectrum of an aqueous solution of pure NH_4I concentration : 6.89×10^{-5} molar. cell path : one cm.

At 45°C

For the experiments conducted at 45°C the box was heated internally by a 300 w. heater; the hot air was circulated by means of a small fan. The temperature of the box could be controlled within ± 0.5°C by adjusting the heater output, and the speed of the fan. The actinometer solution was also at 45°C.

Since the quantum yield of uranyl oxalate is not known at 45°C, it was determined experimentally by doing a blank photolysis of uranyl oxalate at 25°C and 45°C, and taking the quantum yield at 25°C as 0.55. By this procedure the quantum yield at 45°C was obtained as 0.56. This value was used in all calculations pertaining to 45°C results. The analytical procedure was exactly similar to the 25°C runs.

Results

At this temperature the saturated vapour pressure of I_2 is considerably higher than that at 25°C. Therefore an appreciable photolysis time is required for this pressure to be attained. Hence all the experiments were conducted at a constant NO/HI ratio but for varying times and varying HI concentrations. Figure 13 shows the time course plot for different HI concentrations but at a constant NO/HI = 3.9. This graph is similar to the one obtained at 25°C except that

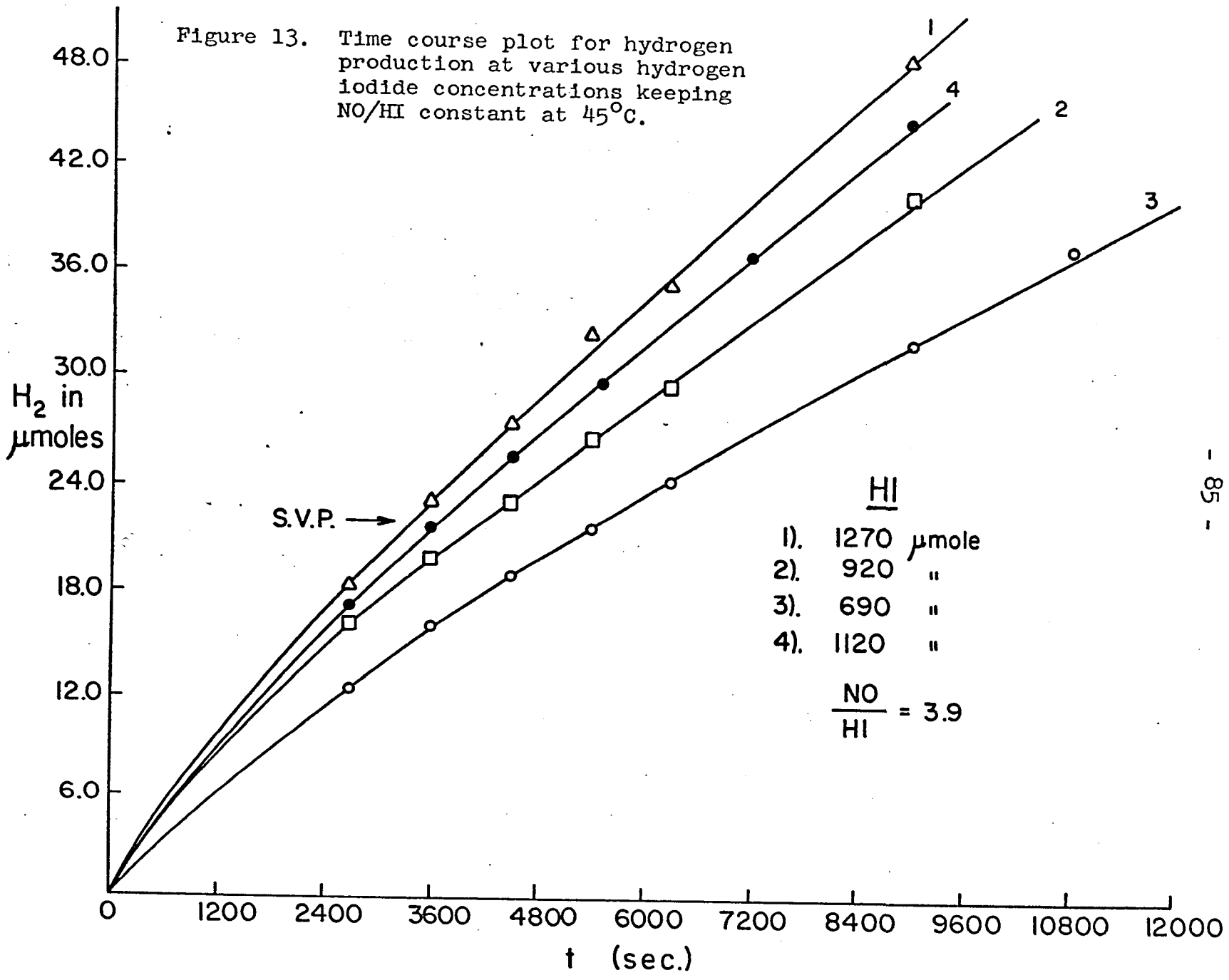

Figure 13. Time course plot for hydrogen production at various hydrogen iodide concentrations keeping NO/HI constant at 45°C.

the rate becomes constant after a longer time.

In all these experiments the amount of iodine formed is always higher than the amount of hydrogen. This is probably due to the formation of ammonium iodide, which produces extra iodine; the amount of NH_4I is considerably larger than at 25°C. It was found to be about 35 μmoles in ten runs. Table 3 shows the amount of hydrogen and iodine produced at different times and Table 4 shows the effect of added iodine on the quantum yield. From the table it is clear that the quantum yield of H_2 production goes on decreasing with the addition of I_2. The same effect is observed by increasing the time of photolysis, where iodine is building up its saturated vapour pressure.

TABLE 3

Amount of H_2 and I_2 produced at various times and at various HI concentrations

Temp: 45°C

λ = 3130 Å

Vol. of the vessel = 302.0 ml.

NO/HI = 3.92

Run	$(HI)_o \times 10^6$ moles	$(NO)_o \times 10^6$ moles	Time in sec.	$E_{abs} \times 10^6$ einstein	$(H_2) \times 10^6$ moles	$(I_2) \times 10^6$ moles	ϕ_{H_2}
1	692.5	-	9,000	42.44	41.19	41.20	0.970
2	690.0	2596.2	2,700	16.15	12.50	13.00	0.774
3	696.8	2653.8	3,600	21.52	16.00	17.60	0.743
4	692.3	2604.6	4,500	26.91	19.30	22.60	0.717
5	690.3	2596.2	5,400	32.28	21.70	23.00	0.672
6	691.8	2595.6	6,300	37.67	24.20	28.60	0.642
7	685.5	2683.0	9,000	55.73	31.90	33.00	0.572
8	687.7	2692.1	10,800	66.87	37.40	39.80	0.559

Table 3 (continued)

Temp: 45°C

λ = 3130 Å

Vol. of the vessel = 302.0 ml.

NO/HI = 3.92

Run	$(HI)_o \times 10^6$ moles	$(NO)_o \times 10^6$ moles	Time in sec.	$E_{abs} \times 10^6$ einstein	$(H_2) \times 10^6$ moles	$(I_2) \times 10^6$ moles	ϕ_{H_2}
1	927.0	-	4,500	26.79	25.80	25.70	0.963
2	918.0	3609.5	2,700	18.46	16.30	22.20	0.883
3	926.8	3644.2	3,600	24.60	20.00	20.30	0.813
4	924.0	3632.6	4,500	30.76	23.10	23.60	0.751
5	926.8	3644.2	5,400	36.91	26.70	27.00	0.723
6	918.0	3609.5	6,300	43.06	29.50	29.60	0.685
7	916.0	3572.4	9,000	61.52	40.30	41.30	0.655

Table 3 (continued)

Temp: 45°C

λ = 3130 Å

Vol. of the vessel = 302.0 ml.

NO/HI = 3.81

Run	$(HI)_o \times 10^6$ moles	$(NO)_o \times 10^6$ moles	Time in sec.	$E_{abs} \times 10^6$ einstein	$(H_2) \times 10^6$ moles	$(I_2) \times 10^6$ moles	ϕ_{H_2}
1	1111.1	-	9,000	56.44	54.40	54.60	0.964
2	1111.1	4233.3	2,700	19.29	17.30	17.40	0.896
3	1120.5	4260.0	3,600	25.73	21.70	22.00	0.843
4	1111.1	4220.3	4,500	32.16	25.40	26.00	0.790
5	1118.8	4262.6	5,400	38.59	29.70	31.50	0.769
6	1118.8	4262.6	7,200	51.46	36.60	41.30	0.711
7	1111.1	4230.2	9,000	64.32	44.50	51.10	0.692

Table 3 (continued)

Temp: 45°C

λ = 3130 Å

Vol. of the vessel = 302.0 ml.

NO/HI = 4.0

Run	$(HI)_o \times 10^6$ moles	$(NO)_o \times 10^6$ moles	Time in sec.	$E_{abs} \times 10^6$ einstein	$(H_2) \times 10^6$ moles	$(I_2) \times 10^6$ moles	ϕ_{H_2}
1	1258.3	-	4,500	30.48	31.90	32.00	1.046
2	1266.5	5107.3	2,700	20.25	18.40	19.00	0.909
3	1266.5	5048.6	3,600	26.99	23.20	24.00	0.859
4	1272.7	5090.5	4,500	33.74	27.50	30.00	0.815
5	1262.5	5082.8	5,400	40.48	32.40	34.00	0.800
6	1262.5	5074.5	6,300	47.24	35.40	36.80	0.749
7	1272.7	5001.7	9,000	67.48	48.10	49.90	0.713

TABLE 4

Effect of added iodine on the quantum yield of H_2 production

λ = 3130 Å

Volume of the vessel = 302.0 ml.

Time: 4500 sec.

Run	Temp.	(HI) x 10^6 moles	(NO) x 10^6 moles	NO/HI	$(I_2)_o$ x 10^6 moles	(H_2) x 10^6 moles	$(I_2)_f$ x 10^6 moles	ϕ_{H_2}
A 1	25°C	1102.0	2542.2	2.30	-	34.5	34.6	0.780
2	"	1106.5	2542.2	2.30	8.5	34.2	42.5	0.750
3	"	1106.5	2542.2	2.30	17.0	34.0	50.7	0.755
B 1	45°C	694.7	2537.0	3.65	6.0	19.3	27.6	0.676
2	"	694.7	2537.0	3.65	12.7	18.9	32.7	0.661
3	"	694.7	2537.0	3.65	50.0	17.3	69.0	0.605
4	"	692.3	2604.6	3.76	-	19.3	22.6	0.717

$(I_2)_o$ = initial concentration of iodine

$(I_2)_f$ = final concentration of iodine

Discussion

The production of NH_4I by the thermal reaction of HI and NO was calculated from the rate constants given by Holmes (65). At 25°C, $k = 1.977 \times 10^{-5}$ cc. $mole^{-1}$ sec^{-1}.

at 45°C, $k = 2.012 \times 10^{-4}$ cc. $mole^{-1}$ sec^{-1}.

From these rate constants, the amount of HI reacting with NO to form NH_4I was calculated and was found to be less than 0.02 μmole of HI at 25°C. Hence the thermal reaction can be neglected and will not be considered further at room temperature.

Any proposed mechanism has to explain the following experimental facts i) Hydrogen and iodine are the only main products and that there is no consumption of nitric oxide. ii) The quantum yield of hydrogen production goes on decreasing with increasing NO/HI ratio, reaching a limiting value after which further addition of NO causes no reduction in ϕ_{H_2}. iii) Addition of I_2 causes reduction in quantum yield. iv) The quantum yield is a function of both HI concentration and I_2 concentration.

Since the light used was polychromatic, the initial act of absorption by HI would be to produce H· and I· atoms. These may be represented by two different processes:

1 (a) $HI + h\nu\,(3130\ \text{Å}) \longrightarrow H^{\cdot} + I^{\cdot}(^2P_{3/2})$ Ia

$\longrightarrow H^{\cdot} + I^{\cdot}(^2P_{\frac{1}{2}})$

(b) $HI + h\upsilon\,(3660\ \mathring{A}) \longrightarrow H\cdot + I\cdot(^2P_{3/2})$

When a normal iodine atom ($^2P_{3/2}$) is produced, then the hydrogen atoms produced in process (a) will be about 20 k.cal. hot and in process (b) the hydrogen atoms will be about 6 k.cal. hot. On the other hand, if excited iodine atoms are produced ($^2P_{\frac{1}{2}}$) then the hydrogen atoms will be normal H atoms. From the absorption spectra (Figure 7), it is seen that the absorbance at 3130 $\mathring{A}$ is approximately about 8 times stronger than at 3660 $\mathring{A}$. So it is possible that some of the hydrogen atoms are hot and some are thermal. The hydrogen atoms so produced can react either with HI or I_2

[2] $H + HI \longrightarrow H_2 + I$

[3] $H + I_2 \longrightarrow HI + I$

Since the iodine concentration, in the gas phase, is very small at room temperature and since the ratio of k_3/k_2 is only 13.0 [Sullivan (64)], then reaction [3] cannot contribute much to the lowering of the quantum yield. Reaction [1] followed by [2] would give a quantum yield of hydrogen production of unity. If nitric oxide is to reduce the quantum yield, it may do so by temporarily stabilising the H atoms as HNO

[4] $H + NO + M \longrightarrow HNO + M$

The latter then undergoes competitive reaction with HI and I_2

according to steps [5] and [6]

[5] $HNO + HI \longrightarrow H_2 + NOI \longrightarrow H_2 + NO + I$

[6] $HNO + I_2 \longrightarrow HI + NOI \longrightarrow HI + NO + I$

Steps [5] and [6] are consistent with experimental observations. Quantum yield, ϕ_{H_2}, for a given NO/HI ratio, should increase with increase in HI concentration and should decrease with increase in I_2 concentration. This is evident from Figure 9 and Table 4. The absence of any other product indicates that NO is acting solely as an intermediate. There is another possible reaction for the reduction of quantum yield

[6"] $HNO + NOI \longrightarrow HI + 2NO$

The concentration of NOI in the system can be calculated from the equilibrium constant for the system,

$$NO + I \rightleftharpoons NOI$$

given by Porter, Szabo and Townsend (101). At 25°C, the value of $K = 3.53 \times 10^4$ liter mole^{-1} and at 45°C, the value of the equilibrium constant $K = 1.22 \times 10^4$ liter mole^{-1}. These were obtained from a value of $\Delta H_{NOI} = -10.0$ k.cal. and $K_{60^oC} = 6 \times 10^3$ liter mole^{-1}, given in the above paper. Hence the concentration of NOI is

$$NOI_{25^oC} = 3.53 \times 10^4 [NO][I]$$

The highest concentration of nitric oxide used was 3.8×10^{-2} moles liter^{-1}, but the concentration of iodine atoms at this

temperature is $<< 10^{-15}$ moles liter^{-1} (102), so that the concentration of NOI will be very low. This indicates that reaction [6"] will be unimportant.

The remaining reactions in the system are those giving rise to molecular iodine.

[7]
$$\begin{cases} I^{\cdot} + I^{\cdot} + M \longrightarrow I_2 + M \\ NOI + I \longrightarrow I_2 + NO \end{cases}$$

Neglecting reaction [3], the rate equation for hydrogen production is given by

$$\frac{dH_2}{dt} = k_2[H][HI] + k_5[HNO][HI] \qquad [15]$$

Applying steady state treatment, the concentration of the intermediates are

$$[H] = I_a - k_4[H][NO][M] - k_2[H][HI] = 0$$

or
$$[H] = \frac{I_a}{k_4[NO][M] + k_2[HI]} \qquad [16]$$

$$[HNO] = k_4[H][NO][M] - k_5[HNO][HI] - k_6[HNO][I_2] = 0$$

$$[HNO] = \frac{k_4[H][NO][M]}{k_5[HI] + k_6[I_2]}$$

$$= \frac{I_a . k_4[NO][M]}{(k_4[NO][M] + k_2[HI])(k_5[HI] + k_6[I_2])} \qquad [17]$$

Substituting these values of [H] and [HNO] in the above rate equation [15]

$$\frac{dH_2}{dt} = k_2[HI]\frac{I_a}{k_4[NO][M] + k_2[HI]} + k_5[HI]\left[\frac{k_4[NO][M]}{k_5[HI] + k_6[I_2]}\left(\frac{I_a}{k_4[NO][M] + k_2[HI]}\right)\right]$$

or $$\frac{dH_2}{dt} = \frac{k_2.I_a[HI]}{k_4[NO][M] + k_2[HI]} + \frac{k_5k_4[NO][M]}{k_5[HI] + k_6[I_2]}\left[\frac{I_a[HI]}{k_4[NO][M] + k_2[HI]}\right]$$

$$= \frac{I_a}{k_2 + \frac{k_4[NO][M]}{[HI]}}\left\{k_2 + \frac{k_5k_4[NO][M]}{k_5[HI] + k_6[I_2]}\right\}$$

$$= \frac{I_a}{k_2 + \frac{k_4[NO][M]}{[HI]}}\left\{k_2 + \frac{\frac{k_4[NO][M]}{[HI]}}{1 + \frac{k_6[I_2]}{k_5[HI]}}\right\} \qquad [18]$$

or $$\frac{dH_2}{I_a.dt} = k_2 + \left\{\frac{k_4[NO][M]/[HI]}{1 + \frac{k_6[I_2]}{k_5[HI]}}\right\} \Big/ k_2 + \frac{k_4[NO][M]}{[HI]} \qquad [19]$$

Calculation showed that in the present system, the iodine concentration is constant for all but the initial 5 - 7% of the reaction time (which is the time taken for building up the saturated vapour pressure) and since the conversion is

kept very low, 7 - 8%, I_2 / HI can be assumed to be constant and independent of time. This is not unreasonable at room temperature. Hence the above differential equation [19] can be integrated as a function of time

$$\frac{\int dH_2}{\int I_a.dt} = \frac{(H_2)_f - (H_2)_i}{\int_o^t I_a.dt} \equiv \phi_{H_2} \qquad [20]$$

$$\therefore \quad \phi_{H_2} = k_2 + \left\{ \frac{\frac{k_4[NO][M]}{[HI]}}{1 + \frac{k_6[I_2]}{K_5[HI]}} \right\} \Big/ k_2 + \frac{k_4[NO][M]}{[HI]} \qquad [21]$$

This equation may be rearranged to give

$$\phi_{H_2} = \frac{k_2 + \frac{k_2 k_6[I_2]}{k_5[HI]} + \frac{k_4[NO][M]}{[HI]}}{\left(1 + \frac{k_6[I_2]}{k_5[HI]}\right)\left(k_2 + \frac{k_4[NO][M]}{[HI]}\right)}$$

$$= \frac{k_2 + \frac{k_4[NO][M]}{[HI]}}{\left(k_2 + \frac{k_4[NO][M]}{[HI]}\right)\left(1 + \frac{k_6[I_2]}{k_5[HI]}\right)} + \frac{\frac{k_2 k_6[I_2]}{k_5[HI]}}{\left(k_2 + \frac{k_4[NO][M]}{[HI]}\right)\left(1 + \frac{k_6[I_2]}{k_5[HI]}\right)}$$

$$\text{or } \phi_{H_2} = \frac{1}{1 + \frac{k_6[I_2]}{k_5[HI]}} + \left[\frac{\frac{k_2 k_6[I_2]}{k_5[HI]} \Big/ 1 + \frac{k_6[I_2]}{k_5[HI]}}{k_2 + \frac{k_4[NO][M]}{[HI]}} \right] \qquad [22]$$

$$\phi_{H_2} = \left\{ \frac{1}{1 + \frac{k_6[I_2]}{k_5[HI]}} \right\} + \left\{ \frac{\frac{k_2}{k_{4a}} \cdot \frac{k_6[I_2]}{k_5[HI]}}{\left(1 + \frac{k_6[I_2]}{k_5[HI]}\right)\left(\frac{k_2}{k_{4a}} + \frac{[NO]}{[HI]}\right)} \right\} \qquad [23]$$

where $k_{4a} = k_4[M]$

At large nitric oxide concentrations, since ϕ_{H_2} does not change any more with NO/HI ratio (Figure 9), it seems that all the H atoms mainly react with NO and not with HI. This would mean that reaction [2] is negligible and therefore the second term in the above equation is very small and may be neglected. Then

$$(\phi_{H_2})_{limiting} = \frac{1}{1 + \frac{k_6[I_2]}{k_5[HI]}} \qquad [24]$$

From the above equation [24] it is seen that $(\phi_{H_2})^{-1}$ should be a linear function of the mole ratio $[I_2]/[HI]$ with a unit intercept and slope equal to k_6/k_5. Since I_2 is the S.V.P. at 25°C, which is constant, a plot of $(\phi_{H_2})^{-1}$ as a function of $1/[HI]$ should be a straight line. This is shown in Figure 14. A table containing the values used for the plot is shown in Table 5. Since the saturated vapour pressure of I_2 at 25°C is 0.35 mm. (Ref. Figure 15) (103), which corresponds to 5.685 μmoles in 302.0 ml. (the volume of the

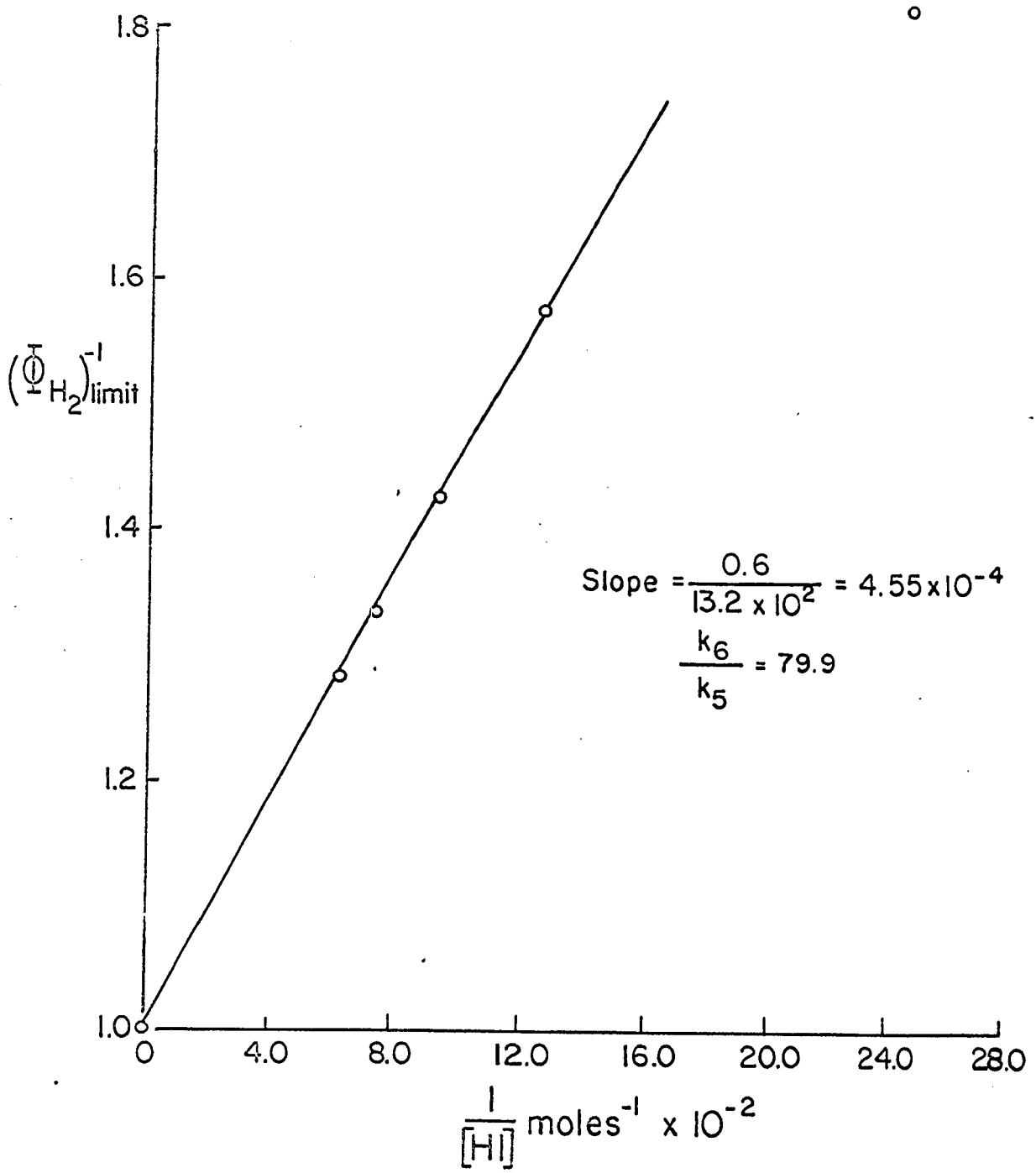

Figure 14. Plot of $(\phi_{H_2})^{-1}_{limit}$ as a function of $[HI]^{-1}$ at 25°C.

TABLE 5

Variation of limiting quantum yield at different HI concentrations.

$\lambda = 3130$ Å

Temp: 25°C

Vol. of the vessel = 302.0 ml.

Run	$(HI)_o \times 10^5$ moles	$(HI)_{av} \times 10^5$ moles	$\frac{1}{[HI]} \times 10^{-2}$	$(\phi_{H_2})_{limit}$	$(\phi_{H_2})^{-1}$
1	43.00	40.70	24.57	0.550	1.818
2	82.00	78.40	12.75	0.635	1.575
3	109.00	105.00	9.52	0.702	1.425
4	137.00	132.90	7.52	0.750	1.333
5	163.00	157.60	6.34	0.780	1.282

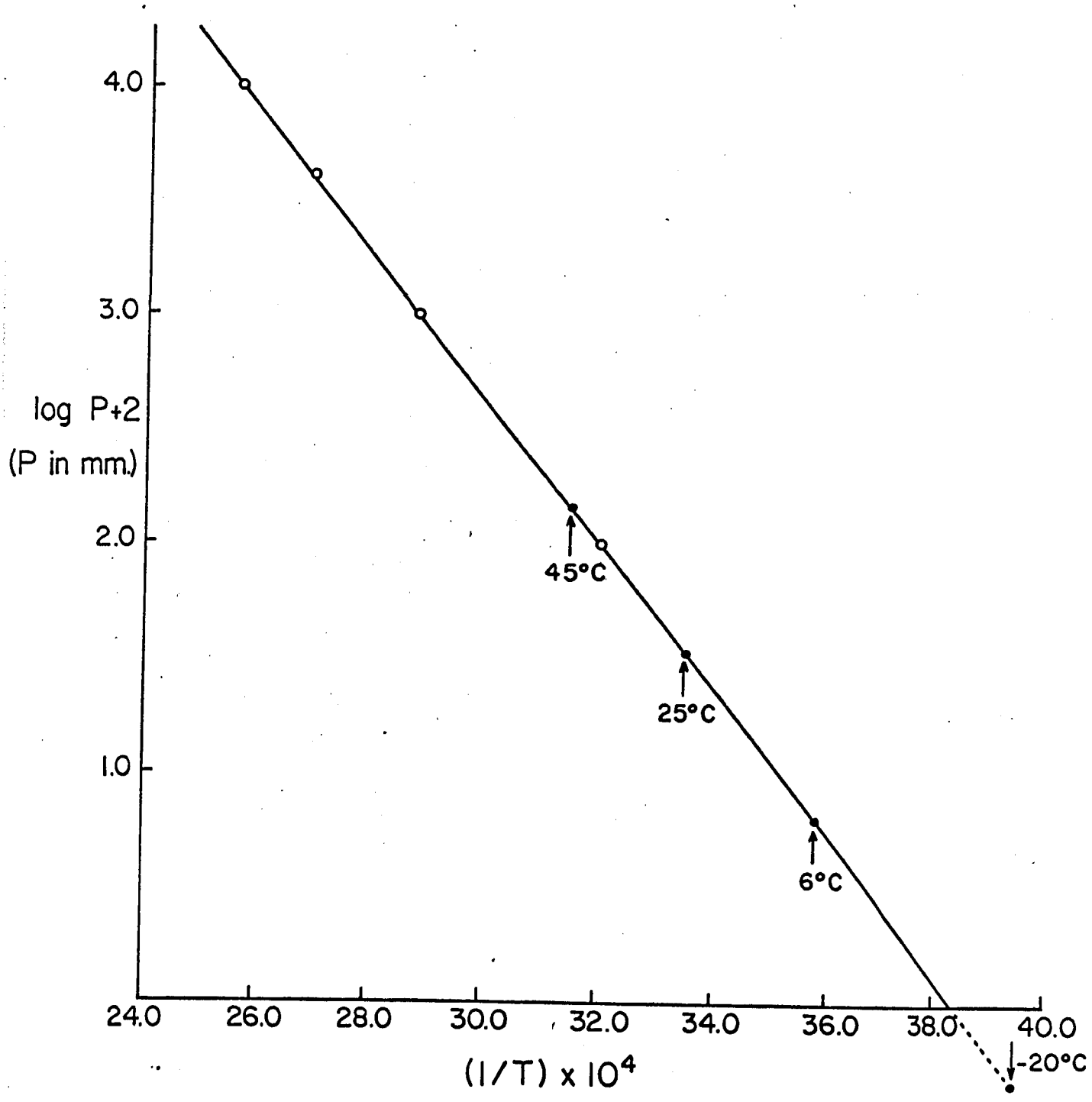

Figure 15. Logarithmic plot of saturated vapour pressure of iodine against temperature (103).

reaction vessel), the value of k_6/k_5 can be calculated as 79.9, from the slope and iodine concentration. The last point on the graph which corresponds to low hydrogen iodide pressure is not on the line, most probably because while deriving the equation [20] it was assumed that I_2 / HI is constant and is independent of time, which is not true at low HI concentrations.

At low NO/HI ratios, where there is competition for the hydrogen atoms between HI and NO, reactions [2] and [4], the full equation [23] can be used. The use of this equation was made in deriving the rate constant ratio $k_2/k_4[M]$. Substituting the values of k_6/k_5 obtained from Figure 14 and taking the values of ϕ_{H_2} corresponding to the ratio of NO/HI from Figure 9 in the descending portion of the curves, the values of $k_2/k_4[M]$ were calculated. This is shown in Table 6. When this ratio is plotted against the total pressure, Figure 16, it is seen clearly that it is pressure dependent, reaching a limiting value at very high pressures. Since there is no reason to suppose that k_2 should be pressure dependent, it is clear that $k_4[M]$, the apparent second order rate constant of reaction [4], increases with pressure. This pressure dependence implies that reaction [4] occurs in the following steps:

TABLE 6

Values of $k_2/k_4[M]$ at various [M] values

Temp: 25°C

λ = 3130 Å

Vol. of the vessel = 302.0 ml.

Time: 4500 sec.

No.	$(HI)_o \times 10^5$ moles	$(NO)_o \times 10^5$ moles	NO/HI	ϕ_{H_2} moles einstein^{-1}	$k_2/k_4[M]$	$[M] \times 10^6$ moles cc^{-1}	$1/[M] \times 10^{-5}$ cc. mole^{-1}
A1	82.0	205.0	2.5	0.705	0.608	9.503	1.052
2	82.0	246.0	3.0	0.692	0.573	10.860	0.921
3	82.0	328.0	4.0	0.675	0.514	13.576	0.737
B1	109.0	109.0	1.0	0.825	0.726	7.218	1.385
2	109.0	163.5	1.5	0.790	0.657	9.023	1.108
3	109.0	218.0	2.0	0.763	0.548	10.828	0.924
C1	137.0	137.0	1.0	0.845	0.643	9.073	1.102
2	137.0	274.0	2.0	0.795	0.485	13.609	0.735
3	137.0	342.5	2.5	0.785	0.462	15.877	0.630
D1	163.0	326.0	2.0	0.818	0.458	16.192	0.617
2	163.0	407.5	2.5	0.807	0.398	18.891	0.529
3	163.0	652.0	4.0	0.794	0.343	26.986	0.370

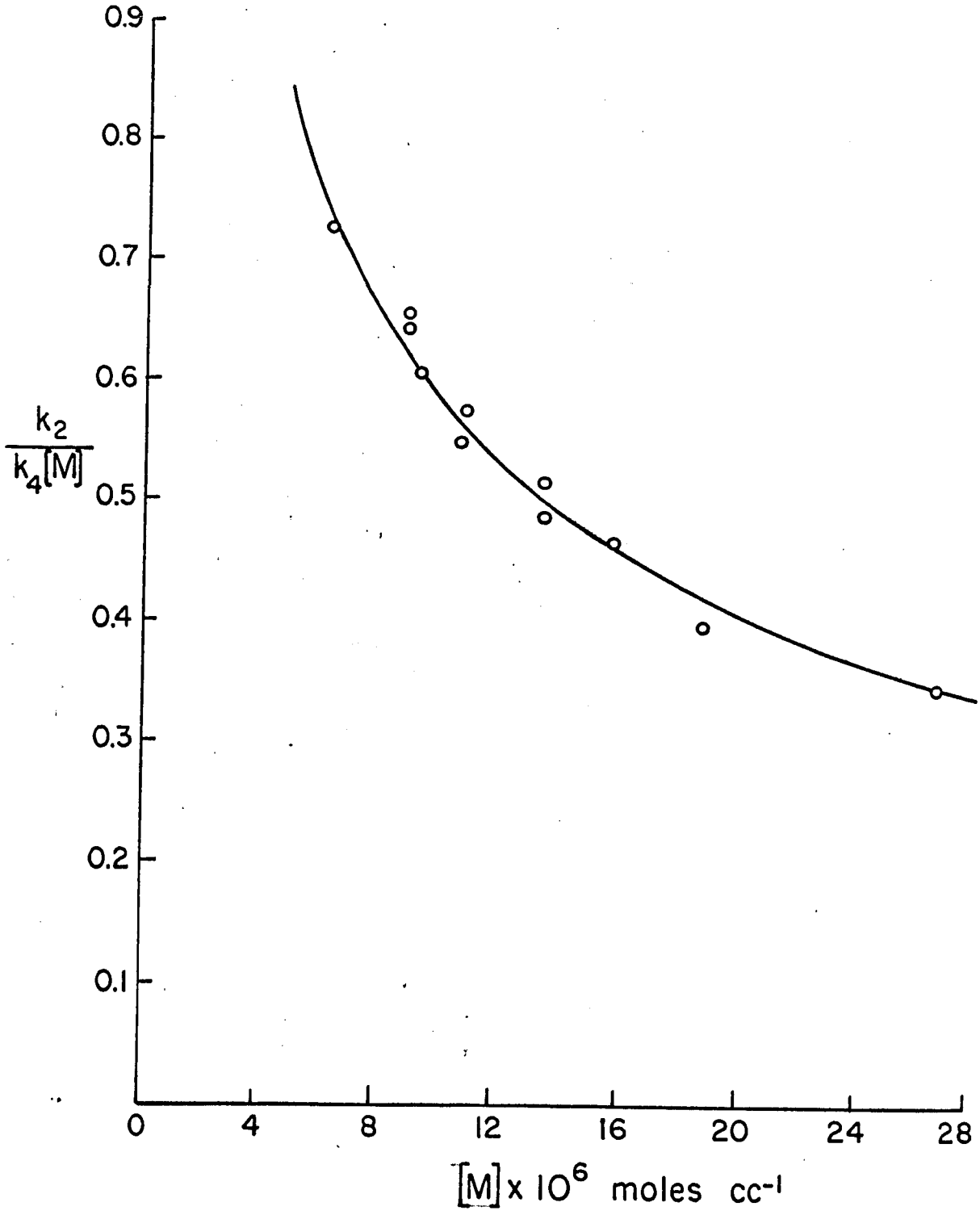

Figure 16. Plot of $k_2/k_4[M]$ for various [M] values at 25°C.

$$H + NO \underset{b}{\overset{a}{\rightleftharpoons}} HNO^*$$

$$HNO^* + M \xrightarrow{c} HNO + M$$

From this, the rate of formation of HNO can be written as

$$\frac{d[HNO]}{dt} = \frac{k_a k_c [H][NO][M]}{k_b + k_c [M]} \qquad [25]$$

If this is compared with equation [4] (page 93)

$$\frac{d[HNO]}{dt} = k_4 [H][NO][M] \qquad [26]$$

so that

$$k_4[M] = \frac{k_a k_c [M]}{k_b + k_c [M]} \quad \text{or} \quad \frac{k_2}{k_4[M]} = \frac{k_2[k_b + k_c[M]]}{k_a k_c [M]}$$

$$\frac{k_2}{k_4[M]} = \frac{k_2 k_b}{k_a k_c [M]} + \frac{k_2 k_c [M]}{k_a k_c [M]} = \frac{k_2 k_b}{k_a kc} \cdot \frac{1}{[M]} + \frac{k_2}{k_a} \qquad [27]$$

Therefore $k_2/k_4[M]$ should be a linear function of $1/[M]$, the intercept giving the value k_2/k_a and the slope k_2k_b/k_ak_c. From Figure 17, $k_2/k_a = 0.203$ and $k_2k_b/k_ak_c = 3.857 \times 10^{-6}$ moles cc^{-1} are obtained. In the absence of any contrary evidence it has been assumed that HI and NO are equally efficient as third bodies. From the above two values the ratio k_c/k_b is obtained as

$$\frac{k_2}{k_a} \times \frac{k_a k_c}{K_2 k_b} = \frac{k_c}{k_b} = \frac{0.203}{3.857 \times 10^{-6}} = 5.26 \times 10^4 \text{ cc mole}^{-1}$$

Since $k_c \leq 10^{14}$ cc. $mole^{-1}$ sec^{-1}, which would correspond to

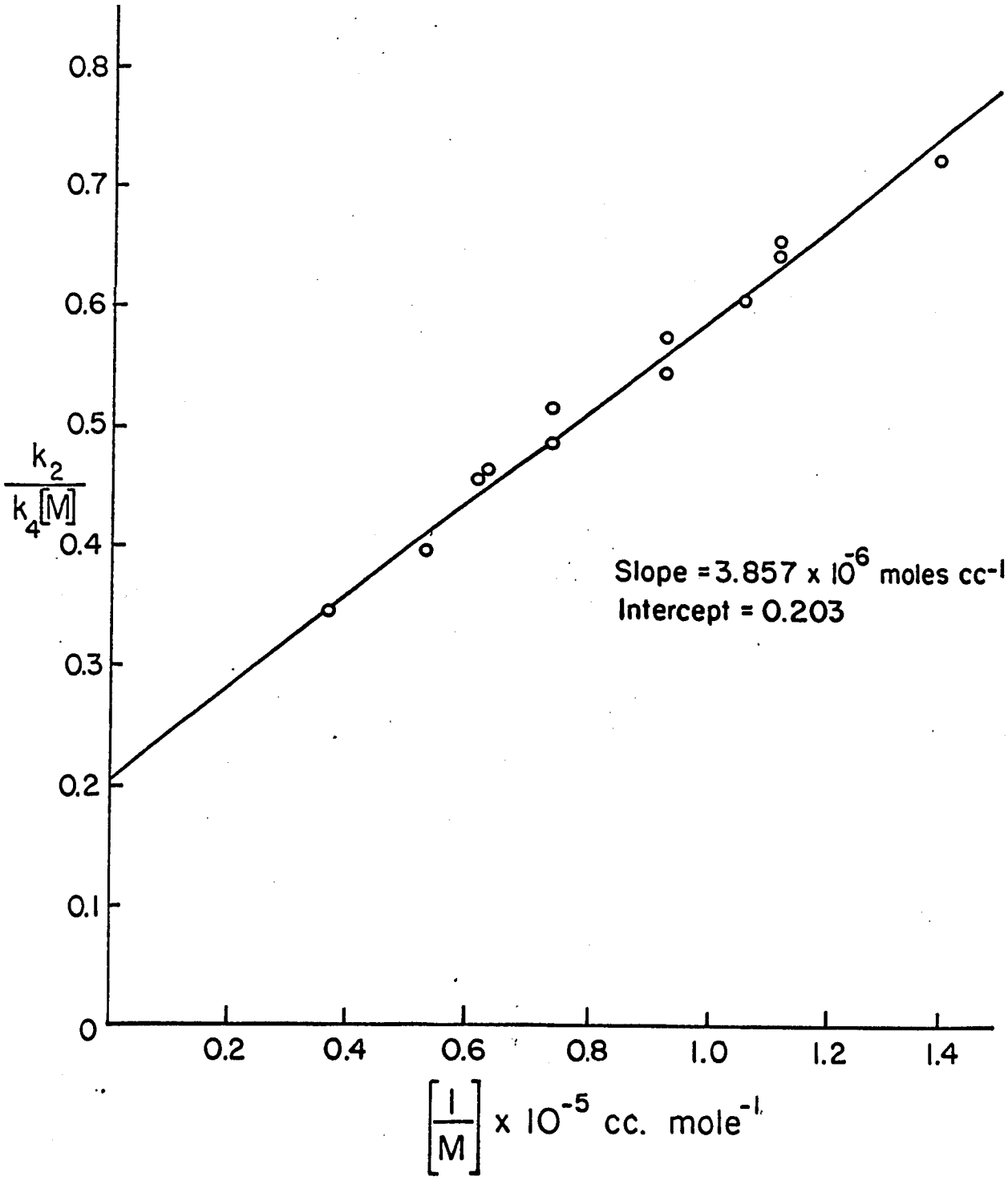

Figure 17. Plot of $k_2/k_4[M]$ as a function of $1/[M]$ at 25°C.

energy transfer reaction c occuring at every collision, $k_b \leq 2 \times 10^9$ sec^{-1} and the mean life time of HNO* complex is $\geq 5 \times 10^{-10}$ sec. Christie (104), while studying the photolysis of CH_3I in the presence of NO, found by a similar procedure the mean life time of CH_3NO^* as $\geq 10^{-8}$ sec. This has a higher life time than HNO*, which is understandable in view of the fact that CH_3NO has more degrees of freedom for the distribution of energy than HNO. It compares well with the life time of $HO_2^* = 4 \times 10^{-9}$ sec. (105). Hoare and Walsh (106) have considered several termolecular reactions and postulated how approximately, the pressure at which the change in order could be calculated. As stated above, the third order rate constant is $k_a k_c / k_b$ and the second order rate constant is k_a; and the order of magnitude of the pressure at which the overall, termolecular reaction changes from third to second order is given by

$$k_b = k_c [M] \qquad [28]$$

In the present system, $k_c / k_b \simeq 5 \times 10^4$ cc. mole^{-1} = 1/[M]. Therefore [M] $\simeq$ 0.5 atm. The change from third order to second order for the reaction [4] will occur only when the total pressure of hydrogen iodide and nitric oxide is greater than 0.5 atmospheres at 25°C.

The value of $k_{4.m}/k_2$ (where $k_{4.m}$ is the third order rate constant given by $k_a k_c/k_b$) = 2.592×10^5 cc. $mole^{-1}$, obtained from the above calculation, may be compared with the value given by Sullivan (63) and Clyne and Thrush (76). Clyne and Thrush obtained $k_{4.m}$ for M = H_2 at 25°C, a value 1.48×10^{16} cc^2 $mole^{-2}$ sec^{-1} and from equation [13] k_2, at 25°C, can be calculated as 1.22×10^{13} cc. $mole^{-1}$ sec^{-1} giving $k_{4.m}/k_2 = 1.21 \times 10^3$ cc. $mole^{-1}$. On comparing the two values, it is seen that the calculated value obtained from the results of Sullivan and Clyne and Thrush is 200 times smaller than our value. One of the reasons for this discrepancy may be that $k_{4.m}$ for $H + NO + M \longrightarrow HNO + M$, when M = H_2 may not be the same when M = NO or HI. Since no values for M = NO or HI have been reported, the values cannot be compared. However, it seems quite probable that NO is an efficient third body for the recombination of H and NO and hence $k_{4.m} > 10^{16}$ is possible. Hoare and Walsh (106) explained the great efficiency of a third body by supposing the reactions to occur as

$$H + NO = HNO^*$$

$$HNO^* = H + NO$$

$$HNO^* + NO = HNO + NO$$

Hoffman and Bernstein (107), while studying isotope effects

in mercury photosensitized reaction of H_2 and NO, observed an N^{15} enrichment in the N_2 produced. This they postulated as due to equilibrium isotope exchange reaction

$$N^*O + HNO \rightleftharpoons HN^*O + NO$$

This experimental evidence gives an added proof that NO must be an efficient third body for recombination of H and NO. At present there is no experimental evidence to show that HI is also equally efficient in this system. Another factor that will remove this discrepency is that E_2 has an activation energy greater than 0.5 k.cal., and a value of about E_2 = 3.0 k.cal. will bring both the values in agreement. However, E_2 = 3.0 is probably unreasonably large, [Benson (108) in his book has suggested a value of E_2 = 2.0 k.cal. as reasonable] but a combination of both effects will minimise the discrepancy.

The ratio of rate constants $k_{H + HI}/k_{H + NO}$ as given by the intercept in Figure 17 is 0.203. Since

$$k_{(H + I_2)} = 13\ k_{(H + HI)}$$

as determined by Sullivan (64), the ratio

$$\frac{k_{(H + I_2)}}{k_{(H + NO)}} = 13 \times 0.2 = 2.6$$

The ratio of rate constants for analogous reactions were

given by Christie (109) as

$$\frac{k_{(\text{isopropyl} + I_2)}}{k_{(\text{isopropyl} + NO)}} = 22 \qquad \frac{k_{(\text{propyl} + I_2)}}{k_{(\text{propyl} + NO)}} = 11$$

$$\frac{k_{(\text{ethyl} + I_2)}}{k_{(\text{ethyl} + NO)}} = 7 \qquad \frac{k_{(\text{methyl} + I_2)}}{k_{(\text{methyl} + NO)}} = 6$$

and from the present work $\frac{k_{(H + I_2)}}{k_{(H + NO)}} = 2.6$

This may be summarised as

$$R_{C_3H_7} > R_{C_2H_5} > R_{CH_3} > R_H$$

where R stands for the ratio of rate constants as described above. The values of $k_2/k_4[M]$ calculated and shown in Table 6 are sensitive to the ϕ_{H_2} values used. This is particularly so for the high HI concentrations, where the error in reading ϕ_{H_2} (Figure 9) can lead to a probable error of slope and intercept (Figure 17) of $\pm$ 5 and $\pm$ 20% respectively.

45°C

The experimental results shown in Figure 13 indicate that the rate of hydrogen production becomes constant once the saturated vapour pressure of iodine is reached. Since the iodine concentration is comparatively high, at this temperature, reaction [3] cannot be neglected. Application of steady state treatment including reaction [3] yields

$$\frac{dH_2}{I_a.dt} = \frac{1 + \frac{k_6[I_2]}{k_5[HI]} + \frac{k_4[M]}{k_2} \cdot \frac{[NO]}{[HI]}}{\left(1 + \frac{k_4[M]}{k_2}.\frac{[NO]}{[HI]} + \frac{k_3[I_2]}{k_2[HI]}\right)\left(1 + \frac{k_6[I_2]}{k_5[HI]}\right)} \qquad [29]$$

The I_2 / HI ratio is no longer independent of time and hence this equation cannot be integrated. The differential equation [29] was used to calculate k_6/k_5. The use of this equation requires a knowledge of k_3/k_2 and $k_4[M]/k_2$ at this temperature. Due to uncertainties in these values and the 'I_a' value, k_6/k_5 obtained by the use of the above equation is not accurate. The values so calculated are shown in Table 7. The rate of hydrogen production has been calculated from the linear portion of the graph (figure 13) and the number of quanta absorbed, 'I_a', from the actinometer readings. The saturated vapour pressure of I_2 was taken as 1.445 mm.

TABLE 7

Calculation of k_6/k_5 at 45°C

Vol. of the vessel = 302.0 ml.

$\lambda = 3130$ Å $\qquad [I_2] = 21.99 \times 10^{-6}$ moles

Run	$(HI)_o \times 10^6$ moles	$(NO)_o \times 10^6$ moles	$\frac{NO}{HI}$	$[M] \times 10^6$ moles cc^{-1}	$\frac{1}{[M]}$	$\frac{k_2}{k_4[M]}$	$\frac{[I_2]}{[HI]}$	$\frac{dH_2}{dt} \times 10^9$ moles sec^{-1}	$I_a \times 10^9$ einstein sec^{-1}	$\frac{dH_2}{I_a.dt}$	$\frac{k_6}{k_5}$
1	692.0	2710.0	3.92	11.265	0.888	0.545	0.0339	2.857	5.979	0.478	38.36
2	927.0	3643.1	3.93	15.133	0.661	0.460	0.0249	3.750	6.836	0.548	37.70
3	1120.0	4267.2	3.81	17.838	0.560	0.420	0.0204	4.186	7.147	0.586	38.97
4	1270.0	5080.0	4.00	21.026	0.476	0.387	0.0179	4.661	7.499	0.621	37.50

(Figure 15), which in terms of concentration was 21.99 x 10^{-6} moles in the reaction vessel. The value of k_3/k_2, being temperature independent (64), was taken as 13.0. Since the values for $k_4[M]/k_2$ are not available at this temperature, calculations were done using the values for the above ratio from 25°C results. Corresponding to a certain value of [M], $k_4[M]/k_2$ was obtained from Figure 17. This assumes that $k_4[M]/k_2$ is temperature independent. From these values, the ratio k_6/k_5 was calculated and is shown in the last column of Table 7. The values obtained for four different pressures seem to be quite consistent. The average value may be obtained as 38.1. Taking this value and the value of 79.9 at 25°C, the activation energy difference, $E_5 - E_6$, can be calculated as 6.9 k.cal. $mole^{-1}$. This must be an upper limit, because it can be shown that if E_4 is negative, as was observed by Clyne and Thrush, and if E_2 is small but positive, then at 45°C, the ratio $k_4[M]/k_2$ will be smaller than at 25°C. If this is so, then the ratio k_6/k_5 increases and the activation energy difference will be less than that calculated above.

The quantum yield of uranyl oxalate, which was used in these calculations, was taken as 0.56. Leighton and Forbes (42) have stated that the temperature coefficient for this actinometer was 1.03 for 10°C at 20°C in the temperature

range 9° to 25°C. If this can be extrapolated to 45°C, then taking $\phi_{25°C} = 0.55$, the value of $\phi_{45°C}$ comes as 0.58. Recently, Volmann and Seed (110), while studying the photochemistry of uranyl oxalate at 30°C and 50°C, have calculated the ratio of moles of CO formed to moles of oxalate decomposed as 0.52 at 30°C and 0.49 at 50°C, using a wavelength 2537 Å, and they did not give any quantum yield values. Thus there is some disagreement as to the temperature coefficient for this actinometer. This adds another uncertainty in the 'I_a' values used. The last factor that creates uncertainty in the 45°C runs is the formation of NH_4I. It may be that the simple mechanism given at 25°C is not applicable at 45°C and that the reaction

$$HNO + HI \longrightarrow NH_2IO \longrightarrow NH_4I$$

may have to be included. If there are two reactions between HNO and HI, one producing H_2 and NOI, and the second producing NH_4I, the rate constant ratio k_6/k_5 calculated at 45°C is not a ratio of simple rate constants but k_5 is a sum of two rate constants, one for H_2 production and one for NH_4I production. Thus it may be concluded that if all these corrections can be made on the value of k_6/k_5 obtained by the above procedure, it will lead to a correct estimate of the above rate ratio.

There is an alternative explanation for the behaviour we have observed, namely the reduction in quantum yield of hydrogen production with increasing NO/HI ratios. This is the hot atom effect. From the kinetic considerations and the rate equation alone, it is difficult to judge which explanation is right, because both yield the same type of rate equation. However, the 'hot atom' effect can be rejected on the following grounds: (1) A hot atom effect would predict a quantum yield reduction which is independent of I_2/HI. This is not found in the present system (Refer to Figure 9). (2) The formation of ammonium iodide (Figure 11) clearly indicates the presence of HNO. This is also confirmed from the low temperature work, where N_2 is one of the products and this can arise only from the reaction between HNO and NO (77)(78). (3) The effect of added inert gas, like H_2 and N_2, on HI photolysis is shown in Table 8, from which it is clear that the hot atom effect is negligible when wavelength 3130 Å is used. Experiments with added H_2 and He at higher temperatures also showed the same effect, namely, a very small hot atom effect (see appendix).

Thus, it may be concluded that the proposed mechanism satisfactorily explains the experimental observations of the photolysis of hydrogen iodide in the presence of nitric oxide.

TABLE 8

Effect of added inert gas on quantum yield

Vol. of the vessel = 302.0 ml.

λ = 3130 Å T = 25°C

Run	Added inert gas M	$(HI)_o \times 10^5$ moles	$\frac{[M]}{[HI]}$	Time sec.	$(I_2) \times 10^6$ moles	ϕ_{I_2} moles einstein^{-1}
A1	Nitrogen	46.94	2.23	5,000	19.03	0.991
2	"	46.94	5.68	"	18.90	0.985
3	"	48.63	8.22	3,600	14.00	0.990
4	"	53.80	7.50	"	17.50	0.990
5	"	53.80	5.80	"	17.50	0.990
B1	Hydrogen	48.63	2.00	5,000	19.00	0.955
2	"	48.35	3.86	"	18.62	0.936
3	"	46.94	6.00	"	18.00	0.937
4	"	46.94	9.00	"	17.32	0.902

CHAPTER IV

Reactions at 6° and -20°C

At higher temperatures it was observed that the addition of nitric oxide reduces the rate of hydrogen production in the photolysis of hydrogen iodide. However, at lower temperatures not only does nitric oxide inhibit the photolysis but it also reacts with HNO to form N_2 as a new product. The reaction of HNO leading to the nitrogen production was therefore studied in detail at these lower temperatures.

Experimental

The general set up of the apparatus was essentially the same as described in the previous chapter. A new type of reaction vessel was constructed, so that only the vessel was cooled to the desired temperature.

The reaction cell assembly, with the thermostat is schematically shown in Figure 18. It was a cylindrical quartz vessel, 10 cm. long and 5 cm. diameter. The total volume was calculated as 314.0 ml. The vessel was enclosed in an annular jacket, through which cooling liquid could be circulated, and the temperature read by means of a

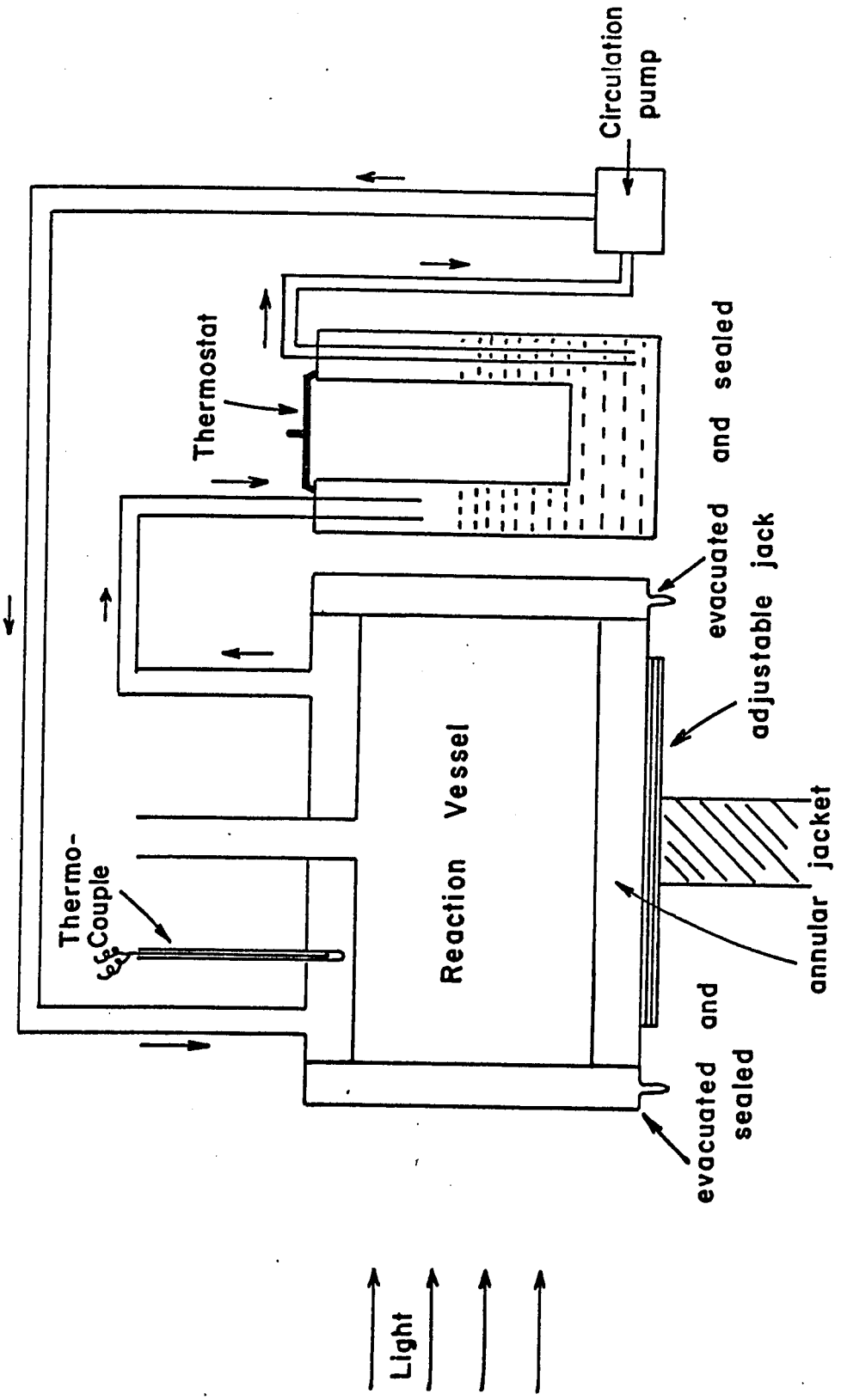

Figure 18. Low temperature assembly.

thermocouple. The windows were enclosed by vacuum jackets (see Figure 18). This prevented condensation of water vapour on the windows. The whole assembly was surrounded by a close fitting styrofoam box. Dry nitrogen was blown onto the windows to further ensure that no moisture was condensed thereon.

A temperature of 6°C was attained by means of circulating "anti-freeze" through the reaction vessel jacket. The "anti-freeze" was cooled in a 'Lo-temp' bath (Wilkens - Anderson Co., U. S. A.). It was circulated by means of an electrically driven pump. The tubing from the pump to the reaction vessel and back to the thermostat, was well insulated to minimise heat losses. The copper - constantan thermocouple, which was used to read the temperature in the reaction vessel, was calibrated against the boiling point of water and the melting point of ice. The temperature varied within $\pm$ 0.5°C during a run.

To attain -20°C the above method was unsuitable, because the "anti-freeze" solution became too viscous to be conveniently pumped when cooled to about -35°C. Hence another procedure was adopted to attain -20°C in the reaction vessel. Ethanol was cooled in a dewar flask, by the insertion of a metal can containing dry ice. This cold ethanol was then circulated. By adjusting the amount of dry

ice in the can and the speed of circulation, a temperature of -20°C could be attained. However, the temperature control was difficult and it varied by about ± 1°C during any run.

Procedure: Preliminary experiments showed that in the photolysis of HI in the presence of NO at 6°C, the amounts of hydrogen and iodine were never the same. Hence, attempts were made to find other products. A mass spectrometric analysis of the total non-condensible gas from a run in which NO/HI = 10, showed 17% N_2 and 83% H_2. Therefore, at these low temperatures H_2 and N_2 were separated and measured individually.

In any run, a known mixture of HI and NO was photolysed for a certain length of time. After photolysis, the products were condensed in traps T_1 and T_2 (Figure 5). Solid N_2 was used as a coolant in trap T_3. This prevented any carry over of nitric oxide from traps T_1 and T_2. As described earlier, non-condensible gases were taken out at -210°C and measured in the gas burette. This gives the total amount of H_2 and N_2. All the gas was then displaced into the CuO furnace, which was maintained at 310°C, by raising the mercury in the gas burette up to the three way stopcock (Figure 5). Trap T_4 was cooled by liquid nitrogen, to condense the H_2O formed by the oxidation of hydrogen by CuO.

After about 45 minutes the residual gas was recirculated into the gas burette and its pressure was measured. The process of combustion and recirculation was repeated until the gas burette reading showed no change. This required about 2 or 3 repetitions. When the pressure was constant, the value was noted; this gives the amount of N_2 present in the mixture. The difference gives the amount of H_2.

After the removal of H_2 and N_2, the nitric oxide was separated from the hydrogen iodide by distilling the mixture in trap T_1 at liquid oxygen temperature, to trap T_3, at solid nitrogen temperature. Blank experiments showed that it takes about 3 hours for complete separation (vapour pressure of NO at $-185^{\circ}C$ is 1 mm.). After separation of NO at liquid oxygen temperature, distillation at $-161^{\circ}C$ (isopentane slush) yielded some gas, which was collected and measured in the gas burette. It was in the range 0.5 to 1.0 μ mole and identification by mass spectrometric analysis showed it to be nitric oxide and not nitrous oxide.

Every batch of nitric oxide was always tested for its purity, by mass spectrometric analysis for its N_2O content, and for its N_2 content by doing a blank photolysis run on nitric oxide alone and determining the amount of non-condensible gas as described above. The N_2 content was always less than 0.001% mole.

For doing runs at different initial intensities, a neutral density filter (transmitting 40% of incident light) was used. The intensity was further reduced by using a suitably blackened wire gauze. This, in conjunction with the neutral density filter, reduced the initial intensity of the lamp by about 90%.

Results

Figure 19 shows that at 6°C the rate of hydrogen and nitrogen production is constant and is independent of time. Figure 20 shows hydrogen production at different times in the photolysis of a constant amount of hydrogen iodide, containing various amounts of nitric oxide. As the nitric oxide concentration is increased the amount of hydrogen produced goes on decreasing, as was found at higher temperatures, but the reduction is small in comparison with room temperature results.

For 750 μmoles of HI at 6°C, the rate of hydrogen production is 5.67×10^{-9} moles sec^{-1} (from Figure 20). In experiments containing the same amounts of hydrogen iodide and with NO/HI = 5.5, the rate of hydrogen production was 4.51×10^{-9} moles sec^{-1}. This reduction is much smaller than that observed at room temperature (compare Figure 9). The reason for this effect is that the iodine concentration in

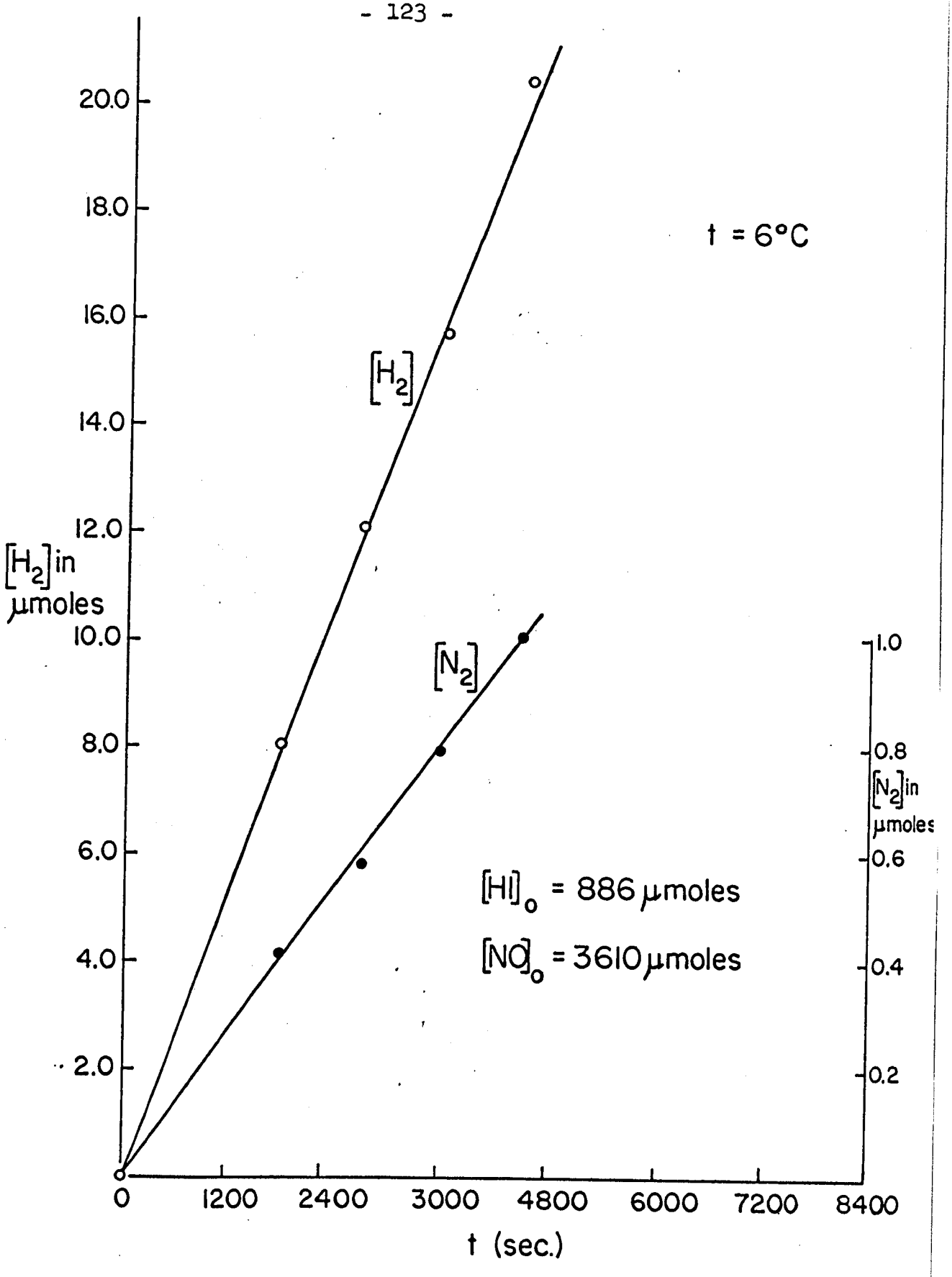

Figure 19. Time course plot for H_2 and N_2 production at 6°C.

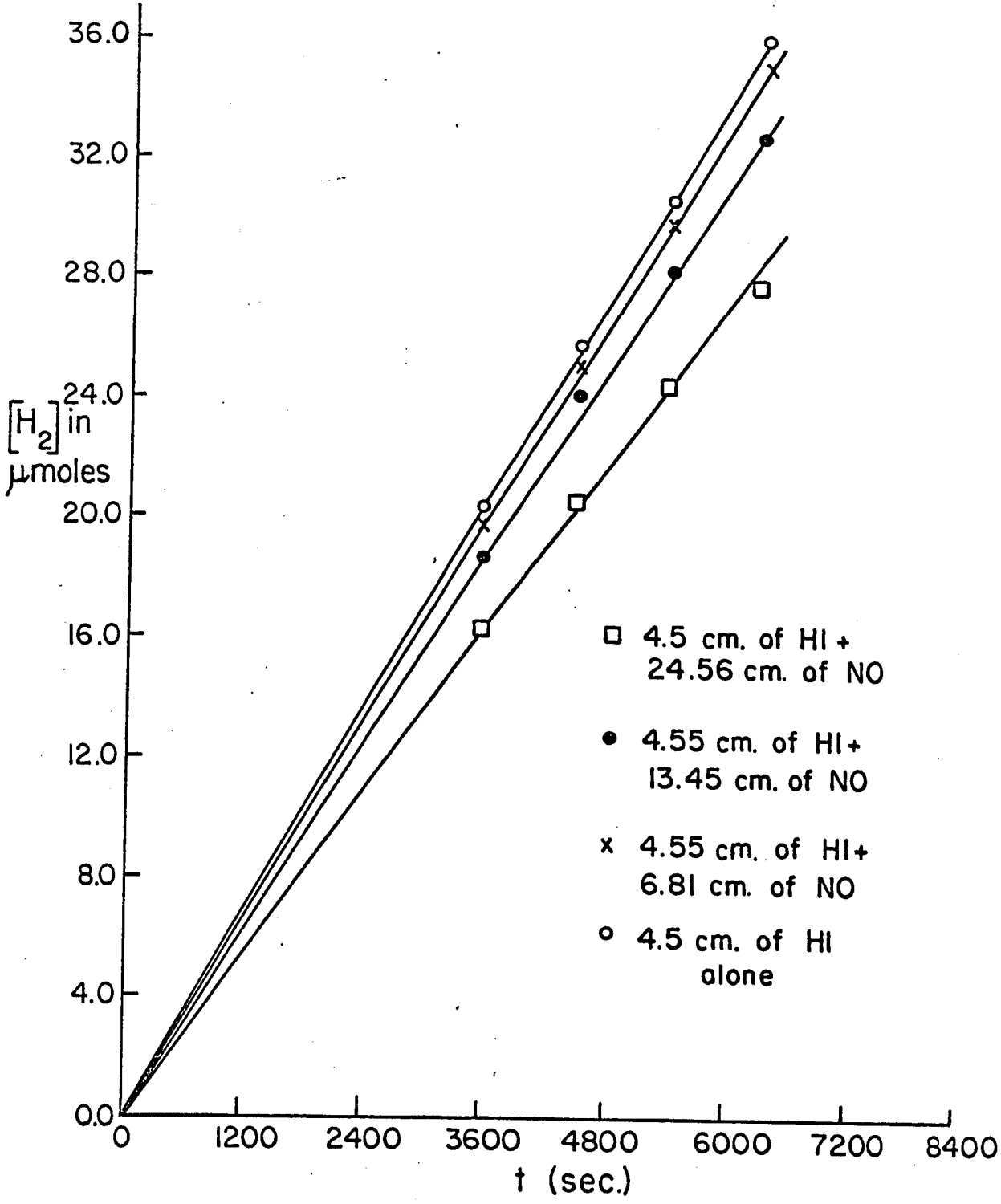

Figure 20. Time course plot for H_2 production at various NO/HI ratios at 6°C.

the gas phase at 6°C (S. V. P. = 0.063 mm.) is much less than at 25°C (S. V. P. = 0.35 mm.). This gives an added proof to our mechanism put forward in the last chapter i.e. I_2 is involved in the quantum yield reducing reaction and not NOI. At lower temperatures it is expected that the steady state concentration of NOI would be greater than at 25°C (101).

It was found in all experiments at 6°C and -20°C that the products obeyed a mass balance equation

$$H_2 + 2N_2 \equiv I_2 \qquad [30]$$

This is shown in Tables 9 and 10, where H_2, N_2 and I_2 produced at various NO and HI concentrations are presented.

At -20°C the behaviour is the same as at 6°C. Figure 21 shows that the H_2 and N_2 production are linear with time.

TABLE 9

Table showing mass balance between H_2, N_2 and I_2

Temp: 6°C $\lambda = 3130$ Å Time: 4500 sec.

Vol. of the vessel = 314.0 ml. $I_o = 29.49 \times 10^{-9}$ einsteins sec^{-1}

Run	$(HI)_o \times 10^6$ moles	$(NO)_o \times 10^6$ moles	$\frac{NO}{HI}$	$(H_2) \times 10^6$ moles	$(N_2) \times 10^6$ moles	$H_2 + 2N_2$ µmoles	$(I_2) \times 10^6$ moles
1	891.8	-	-	24.45	-	-	24.5
2	895.1	1925.5	2.15	23.02	0.38	23.8	23.6
3	889.0	2964.3	3.31	21.17	0.73	22.6	22.7
4	895.1	3910.2	4.37	20.38	1.09	22.6	22.8
5	895.2	4796.9	5.39	17.05	1.39	19.8	19.9
6	895.2	5286.8	5.90	17.32	1.54	20.4	20.4
7	662.9	2119.8	3.20	17.40	0.38	18.2	18.2
8	-	2567.1	-	-	0.03	-	-
9	662.9	2379.8	3.59	17.10	0.57	18.2	18.3
10	662.9	2786.9	4.20	16.46	0.66	17.8	17.7
11	662.9	3526.6	5.32	15.70	0.94	17.6	17.7
12	672.0	3749.0	5.66	15.28	1.09	17.5	17.5
13	662.9	-	-	19.37	-	-	19.5
					Average =	19.85	19.88

Table 9 (continued)

Temp: 6°C λ = 3130 Å Time: 4500 sec.

Vol. of the vessel = 314.0 ml. $I_o = 45.78 \times 10^{-9}$ einsteins sec^{-1}

Run	$(HI)_o \times 10^6$ moles	$(NO)_o \times 10^6$ moles	$\frac{NO}{HI}$	$(H_2) \times 10^6$ moles	$(N_2) \times 10^6$ moles	$H_2 + 2N_2$ μmoles	$(I_2) \times 10^6$ moles
1	466.0	-	-	23.80	-	-	23.7
2	464.6	2017.1	4.34	20.31	0.79	21.90	21.9
3	462.9	2775.2	5.99	17.77	1.23	20.20	20.3
4	462.9	4423.9	9.56	13.44	2.36	18.10	18.1
5	467.9	3651.8	7.83	16.25	1.75	19.70	19.8
6	466.4	4156.0	8.91	13.85	2.15	18.10	18.1
					Average =	19.60	19.64

$H_2 + 2N_2 \equiv I_2$

TABLE 10

Table showing mass balance between H_2, N_2 and I_2

Temp: -20°C λ = 3130 Å Time: 4500 sec.

Vol. of the vessel = 314.0 ml. $I_o = 2.848 \times 10^{-8}$ einsteins sec^{-1}

Run	$(HI)_o \times 10^6$ moles	$(NO)_o \times 10^6$ moles	NO/HI	$(H_2) \times 10^6$ moles	$(N_2) \times 10^6$ moles	$H_2 + 2N_2$ µmoles	$(I_2) \times 10^6$ moles
1	734.8	1799.0	2.45	18.50	0.30	19.1	19.2
2	734.8	2586.0	3.52	16.50	0.62	17.7	17.9
3	734.8	3581.0	4.87	15.80	1.39	18.6	18.5
4	724.8	4318.0	5.96	13.20	1.89	17.0	17.1
5	734.8	5295.0	7.21	13.49	2.33	18.2	18.2
6	732.5	6832.0	9.29	9.48	3.20	16.0	16.3
7	730.8	8420.0	11.46	7.26	4.06	15.4	15.5
8	740.5	10603.0	14.32	4.94	4.35	14.6	14.6
					Average =	17.07	17.16

$H_2 + 2N_2 \equiv I_2$

Table 10 (continued)

Temp: -20°C ± 1°C λ = 3130 Å Time: 5400 sec.

Vol. of the vessel = 314.0 ml. $I_o = 2.287 \times 10^{-8}$ einsteins sec^{-1}

Run	$(HI)_o \times 10^6$ moles	$(NO)_o \times 10^6$ moles	NO/HI	$(H_2) \times 10^6$ moles	$(N_2) \times 10^6$ moles	$H_2 + 2N_2$ µmoles	$(I_2) \times 10^6$ moles
1	484.0	-	-	15.60	-	-	15.5
2	502.5	2153.4	4.28	13.65	0.65	15.0	15.1
3	485.6	2282.0	4.70	13.00	0.65	14.3	14.3
4	494.0	2964.0	6.00	12.63	1.08	14.8	15.0
5	485.6	4256.0	8.76	9.83	1.81	13.5	13.6
6	485.6	6113.7	12.59	6.84	3.06	12.9	12.9
7	485.6	7449.0	15.34	6.16	4.29	14.7	14.3
8	490.7	9127.0	18.60	3.97	4.73	13.4	13.5
9	-	1756.0	-	-	0.03	-	-
10	502.5	10462.0	20.82	2.89	5.73	14.4	14.5
					Average	14.12	14.15

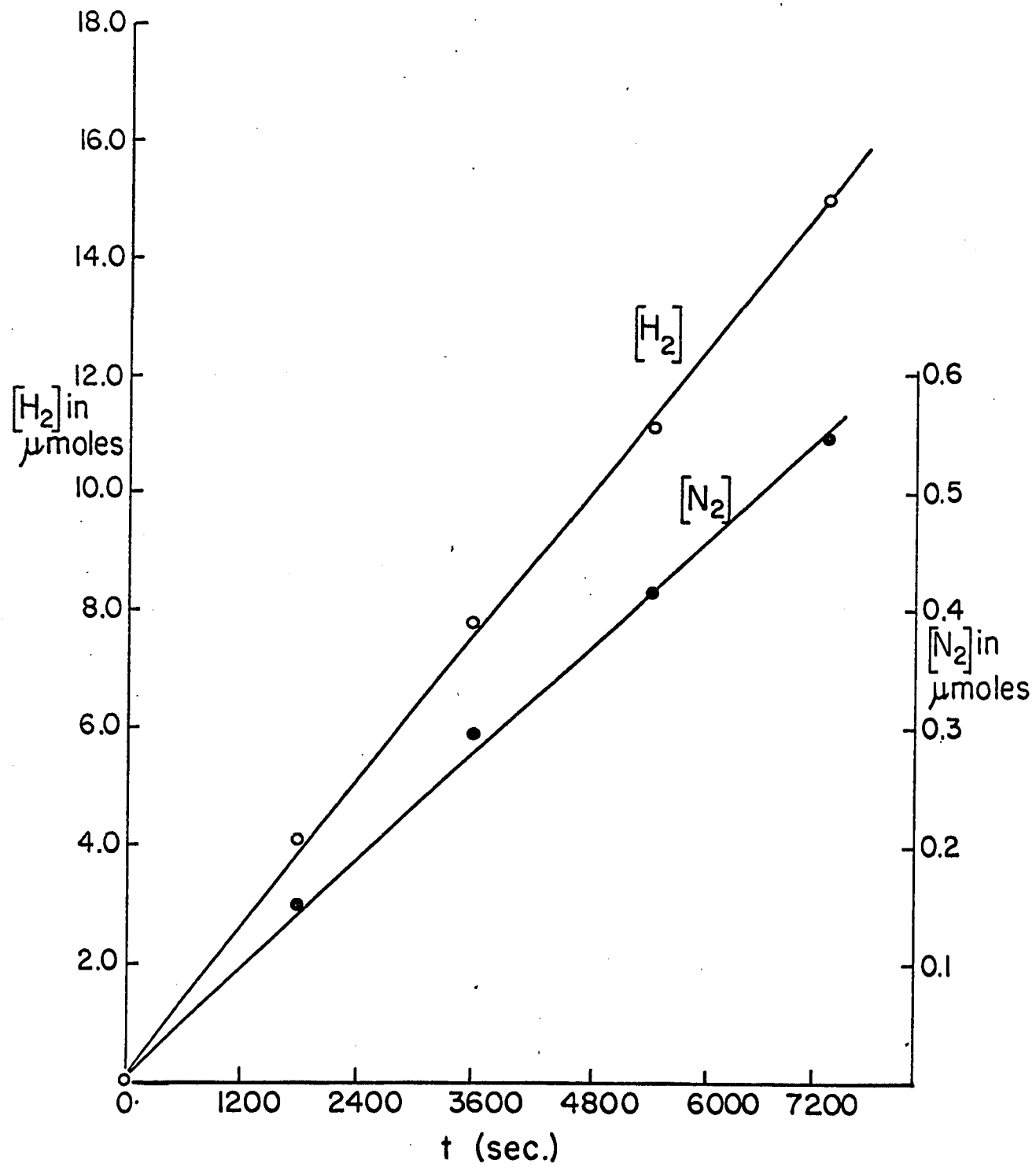

Figure 21. Time course plot for H_2 and N_2 production at $-20^{\circ}C$.

Discussion

At these lower temperatures the addition of nitric oxide to the photolysis of hydrogen iodide again reduces the rate of hydrogen production, but nitrogen is now an important product. The amount of nitrogen increases with increase in nitric oxide concentration. Great care was taken to see that N_2 was not an impurity in NO. Both the time effect and intensity effect justify this conclusion.

As far as the inhibition is concerned, reactions [5] and [6] are still valid, namely

[5] $HNO + HI \longrightarrow H_2 + NOI \longrightarrow H_2 + NO + I$

[6] $HNO + I_2 \longrightarrow HI + NOI \longrightarrow HI + NO + I$

However, since the I_2 concentration in the gas phase is only about 1.1 μmoles, reaction [6] will contribute much less to the overall mechanism.

The nitrogen producing reaction can be postulated to be

[13] $HNO + 2NO \longrightarrow N_2 + HNO_3$

as suggested by Strausz and Gunning (77). In the present system if HNO_3 is formed, as suggested above, it cannot be isolated because it reacts very rapidly with HI to give H_2O, I_2 and NO. This may proceed as

$$HNO_3 + 3HI = 2H_2O + NO + 3/2I_2$$

It can be seen from the above reactions [5] and [13] that if HNO were to react with HI only, then for every two moles of HNO reacting with HI, two moles of H_2 and two moles of I_2 would be obtained. However, if one mole of HNO reacts with HI and one mole with NO, then two moles of HNO would give rise to one mole of H_2, one mole of N_2 and three moles of I_2 because of the reactions of HNO_3 with HI (thermal reaction). This implies that in the present system, the mass balance

$$H_2 + 2N_2 \equiv I_2$$

should be obeyed. Tables 9 and 10 clearly show that the above stoicheiometry is well obeyed in the present system. Hence it is concluded that HNO_3 is one of the products of photolysis.

Two different mechanisms have been proposed for the N_2 production. Arden and Phillips (111) suggested that the reaction occurs as

$$[13'] \quad \left.\begin{array}{l} HNO + 2NO \underset{b}{\overset{a}{\rightleftharpoons}} HN(NO)O.NO \\ HN(NO)O.NO \xrightarrow{c} H\cdot + N_2 + .NO_3 \end{array}\right\} \Delta H \simeq 0 \text{ k.cal. mole}^{-1}$$

while Strausz and Gunning (77) suggested

$$[13] \quad \begin{array}{l} HNO + NO \underset{b}{\overset{a}{\rightleftharpoons}} HNO.NO \\ HNO.NO + NO \xrightarrow{c} HNO_3 + N_2 \end{array}$$

Since nitroso compounds reacting with nitric oxide (80) to produce N_2, proceeds with a negative activation energy, it is

possible that the HNO + NO reaction may also go by steps as postulated above, instead of a one step reaction.

In the photolysis of formaldehyde in the presence of nitric oxide, Strausz and Gunning (77) found that the apparent third order rate constant for N_2 production falls above 50 mm. of Hg of NO pressure and reaches half its value at about 84 mm. This suggests that reaction 13 occurs in steps.

A distinguishing feature between the two mechanisms is that the former involves H atoms as chain carriers and hence the N_2 producing reaction should be a chain reaction, while as the latter suggests a non-chain mechanism for N_2 production. Christie, Gillbert and Voisey (79) while studying the photolysis of methyl nitrite in the presence of nitric oxide could not detect any NO_2 in the products. However, using a more sensitive detecting system, they observed a small amount of NO_2 from which it was concluded that the quantum yield of NO_2 production, estimated approximately from comparison with the results for alkyl iodide photolysis, was not greater than 0.05. It has been suggested by several workers (112) that HNO is an intermediate in the photolysis of methyl nitrite. Thus from Christie's result it can be concluded that one molecule of NO_2 is formed from one nitroxyl molecule. In contrast, Christie's (79) results, on the

photolysis of RI in the presence of NO, show that one molecule of nitroso alkane can lead to the decomposition of several hundred nitric oxide molecules. Thus, the RNO + NO reaction is a chain reaction, whereas HNO + NO reaction is a non-chain reaction. In the present work, the quantum yield of nitrogen production is less than one ($\phi^{N_2}_{60^oC} = 0.06$ and $\phi^{N_2}_{-20^oC} = 0.09$), which indicates a non-chain reaction. This rules out the possibility of mechanism [13'].

Reaction [13'] indicates that two molecules of NO are involved in the complex formation with HNO and so N_2 production should be second order in NO. Reaction [13] indicates that the rate of nitrogen production can be second order at low pressures when [13c] is the rate determining step, and if [13a] is the rate determining step, which can occur at high pressures, the rate will be proportional to the first power of nitric oxide concentration.

Taking these into consideration, it was decided to determine the order of reaction with respect to nitric oxide, by following the rate of nitrogen production as a function of nitric oxide pressure, keeping intensity constant. The results are shown in Figure 22 and Figure 23 for two different initial intensities, where log R_{N_2} is plotted against log P_{NO}. It is indeed second order at lower pressures, slowly changing to first order at higher pressures.

Figure 22. Double logarithmic plot for N_2 production at one initial intensity of 2.949×10^{-8} einsteins sec^{-1}, at 6°C.

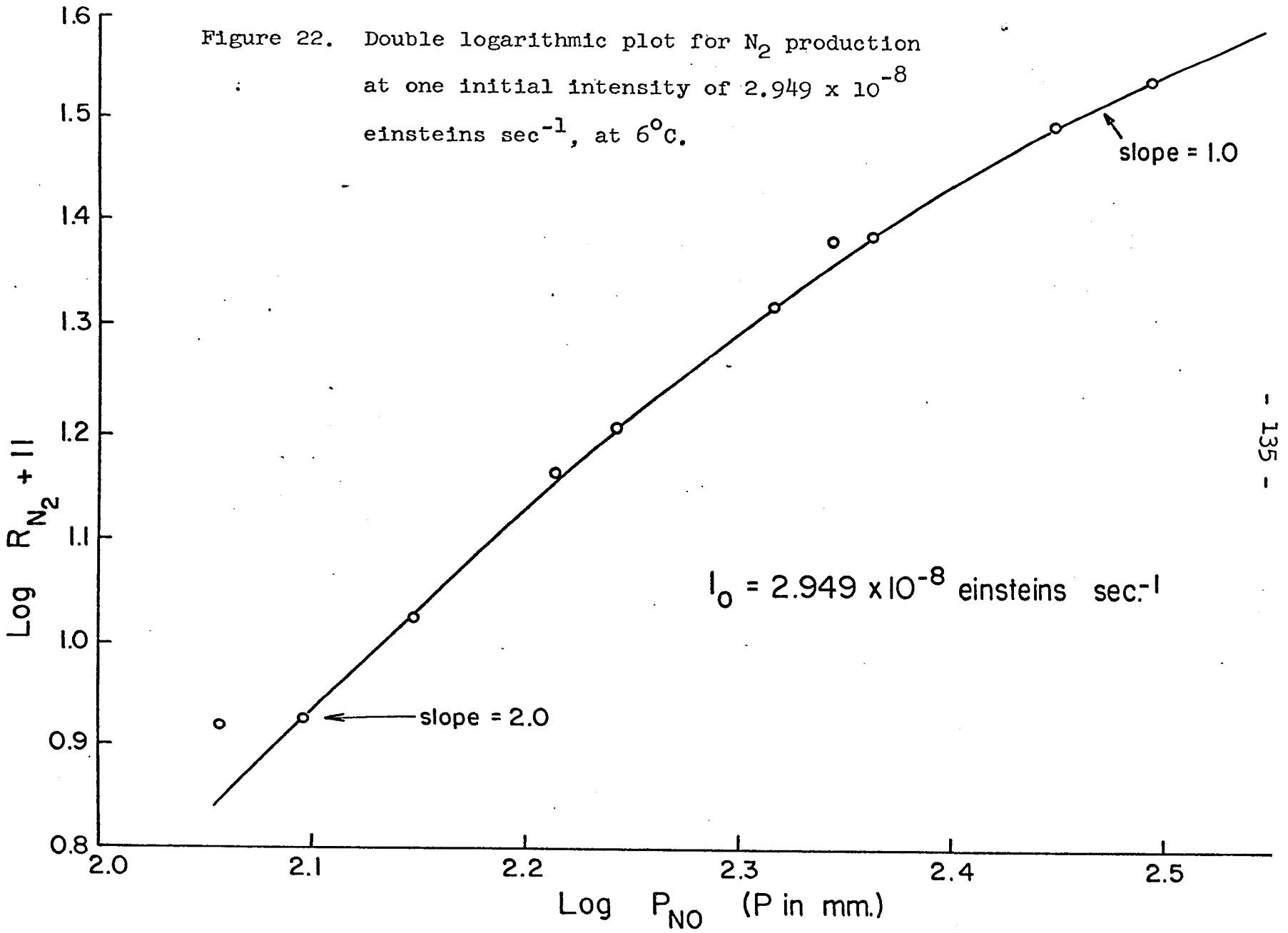

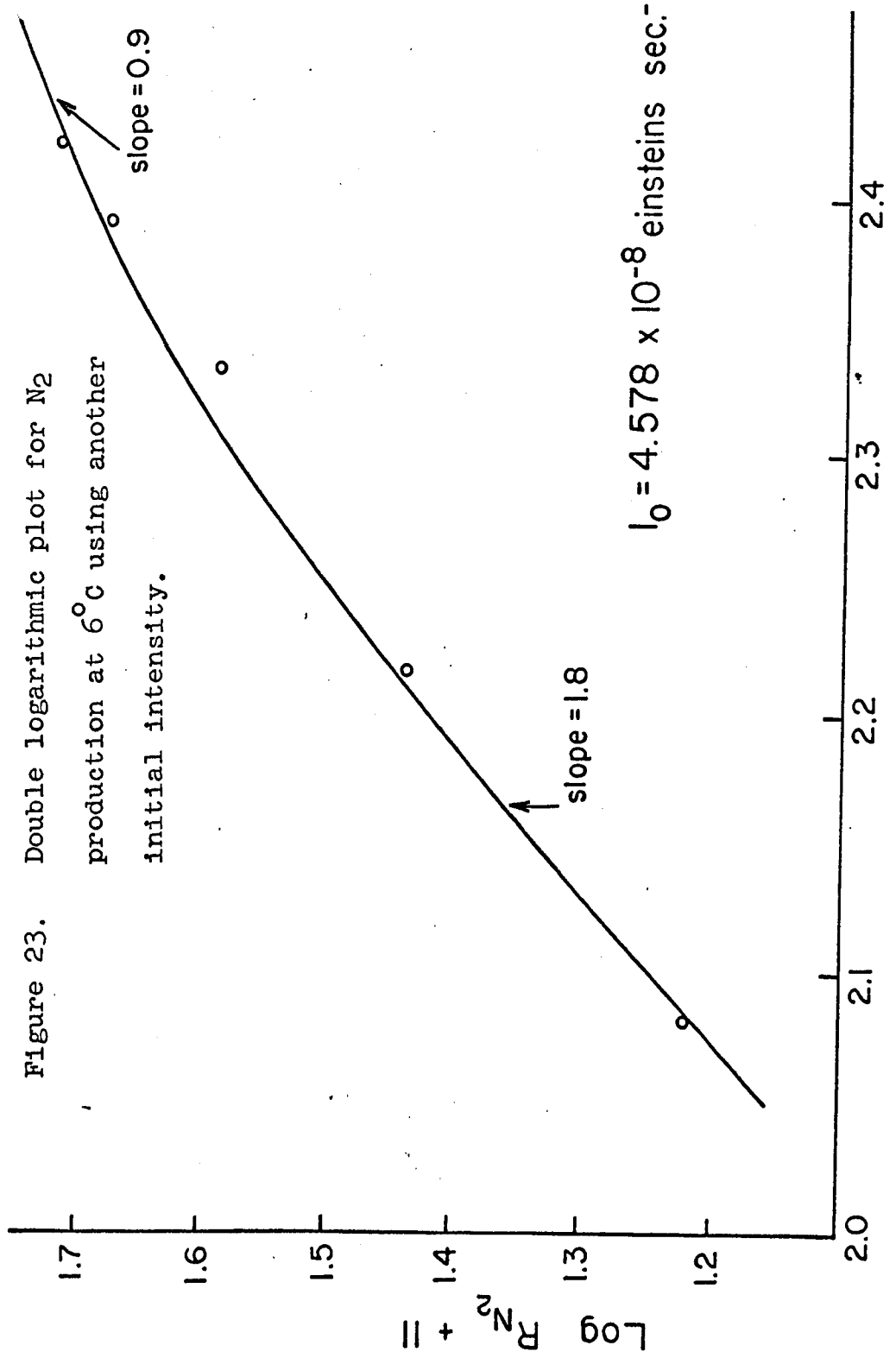

Figure 23. Double logarithmic plot for N_2 production at 6°C using another initial intensity.

At -20°C the same behaviour was observed and this is shown in Figure 24. The change in the order of the reaction for N_2 production agrees well with the observations of Strausz and Gunning; Christie (79) finds that in the nitroso alkane reactions, N_2 production is first order in RNO and second order in NO. From their experimental results it can be seen that they worked over a small pressure range and hence could not have detected any change in order. Another reason may be that RNO + NO reaction, being a chain reaction, is kinetically different from the non-chain HNO + NO reaction.

Reaction [13] shows that N_2 production should be dependent on the first power of HNO concentration which, as can be seen from equation [17], is proportional to the first power of I_a, the intensity of light absorbed in einsteins sec^{-1}. Keeping HI and NO concentrations and time constant, the rate of nitrogen production was determined at different initial light intensities. This is shown in Tables 11 and 12 for 6°C and -20°C, and it can be seen from the last column that I_o/R_{N_2} is constant. From this it may be concluded that nitrogen production is due to the reaction between HNO and NO. This can be represented as

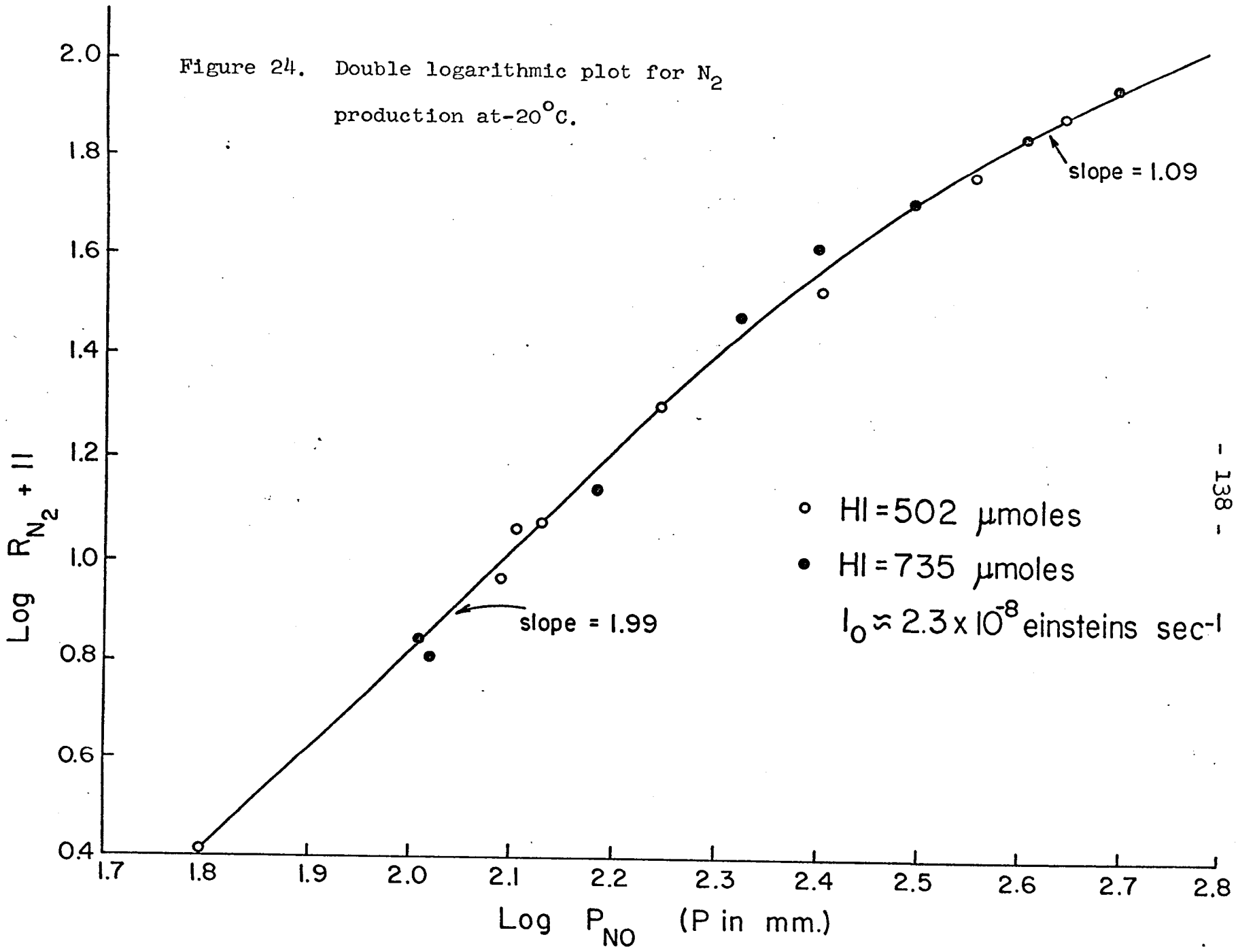

Figure 24. Double logarithmic plot for N_2 production at -20°C.

TABLE 11

Rate of nitrogen production as a function of light intensity

Temp: 6°C Vol. of the vessel = 314.0 ml.

Run	$(HI)_o \times 10^5$ moles	$(NO)_o \times 10^5$ moles	$I_o \times 10^9$ einstein sec^{-1}	$R_{N_2} \times 10^9$ moles sec^{-1}	R_{H_2}/R_{N_2}	I_o/R_{N_2}
A1	46.46	201.7	45.78	0.175	25.71	262
2	46.63	201.7	29.49	0.111	25.60	265
3	46.63	201.7	8.93	0.035	23.44	255
B1	46.29	277.3	45.78	0.273	14.45	168
2	46.29	277.3	29.49	0.168	15.00	175
3	46.46	278.6	8.93	0.053	14.75	168

TABLE 12

Rate of nitrogen production at different light intensities

Temp: $-20^{o} \pm 1^{o}C$ Vol. of the vessel = 314.0 ml.

Run	$(HI)_o \times 10^5$ moles	$(NO)_o \times 10^5$ moles	$I_o \times 10^9$ einstein sec^{-1}	$R_{N_2} \times 10^9$ moles sec^{-1}	R_{H_2}/R_{N_2}	I_o/R_{N_2}
A1	50.99	205.63	21.75	0.104	28.10	209
2	51.52	207.77	12.01	0.058	27.14	207
3	51.35	207.08	3.03	0.015	26.60	202
B1	91.96	310.16	21.75	0.231	19.20	94
2	91.40	312.39	12.01	0.114	20.50	105
3	92.60	311.89	3.03	0.033	19.80	92

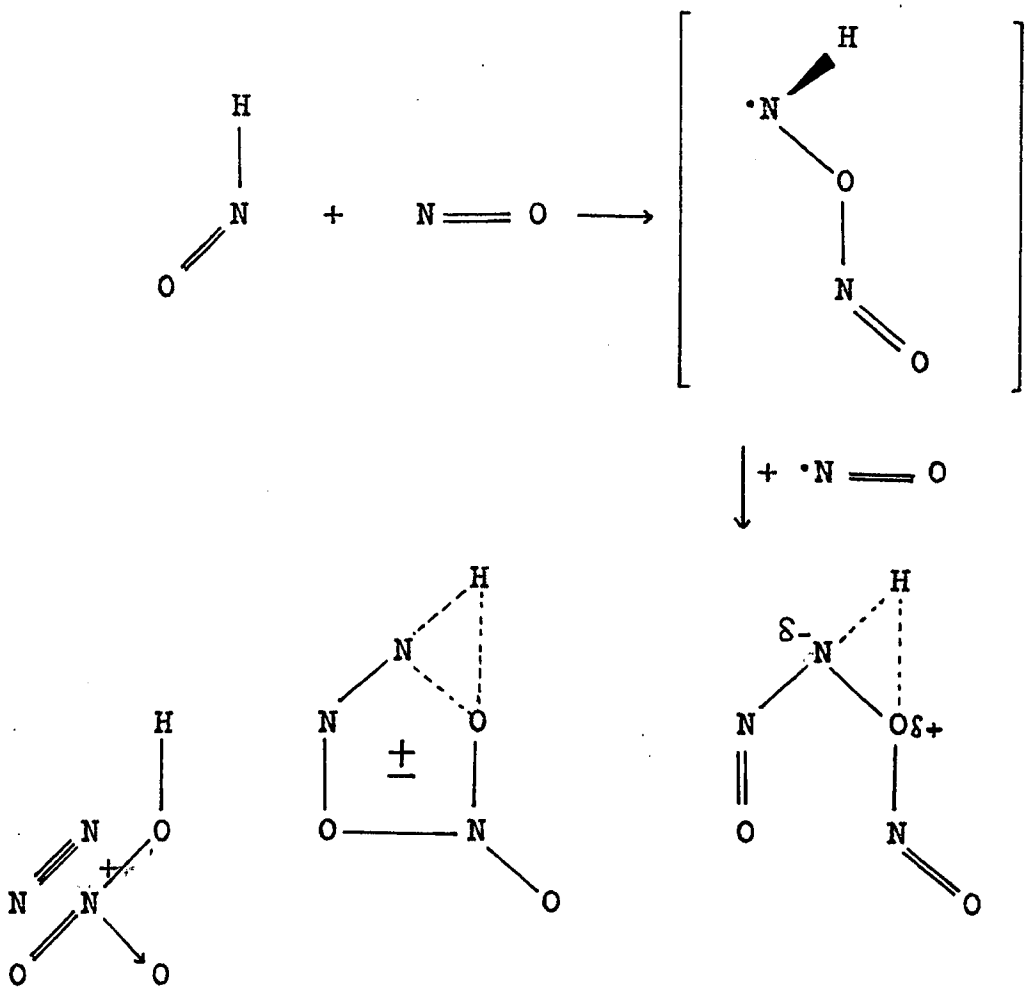

We could not detect any N_2O in the system. N_2O has been postulated by various workers (72)(77)(78) as arising from dimerization of HNO, followed by decomposition to N_2O and H_2O.

[8] $$HNO + HNO \rightleftharpoons (HNO)_2$$

[9] $$(HNO)_2 + M \longrightarrow N_2O + H_2O + M$$

Christie, Frost and Voisey (80) have studied the

equilibrium for the dimerization of RNO.

[4'] $$2RNO \rightleftharpoons (RNO)_2$$

At 25°C they measured the equilibrium constant K_4' and it decreased in the sequence Pr > Et > Me > i-Pr and the rate of dimerization decreased in the sequence Pr > i-Pr > Et > Me. This was in the photolysis of alkyl iodides in the presence of nitric oxide. If the iodides obey the above sequence, then the rate of HNO dimerization may be negligibly small and hence production of N_2O will be of minor importance.

The N_2 production in these systems could well explain the observance of N_2 in the mercury photosensitized reaction of H_2 and NO, studied by Taylor and Tanford (72). They also did not observe any N_2O in their system. The observation made by Srinivasan (78), that in the photolysis of ^{15}N - ammonia in the presence of nitric oxide, not only was $^{14}N^{15}N$ obtained but also $^{14}N_2$. This could be explained by the following sequence.

$$^{15}NH_3 + h\nu \longrightarrow {}^{15}NH_2 + H$$

$$H + {}^{14}NO \longrightarrow H{}^{14}NO$$

$$^{15}NH_2 + {}^{14}NO \longrightarrow {}^{15}N{}^{14}N + H_2O$$

$$H{}^{14}NO + 2{}^{14}NO \longrightarrow {}^{14}N_2 + HNO_3$$

If the hydrogen producing reactions [2] and [5] are compared, it is obvious that at high nitric oxide

concentrations, all the hydrogen atoms will react with nitric oxide to form HNO, rather than react with hydrogen iodide and hence at NO/HI ratios greater than four, it can be assumed that reaction [5] is the only hydrogen producing reaction. This is also borne out by our experimental observations, as will be discussed below.

On comparing reactions [13] and [5], we can write

$$\frac{R_{H_2}}{R_{N_2}} = \frac{k_5[HNO][HI]}{k_{13}[HNO][NO]^2} = \frac{k_5}{k_{13}} \cdot \frac{[HI]}{[NO]^2} \qquad [31]$$

where R_{H_2} and R_{N_2} denote rate of hydrogen and nitrogen production respectively. This equation is of limited applicability, in the sense that at low NO concentration, this will not be valid, because the numerator should contain another term, $k_2[H][HI]$, and the simple linear relation between R_{H_2}/R_{N_2} and $[HI]/[NO]^2$ will not hold. On the other hand, at very high NO pressures, where the HNO + NO reaction has become first order in NO, it should deviate from linearity. However, the graph (Figure 25) plotted as R_{H_2}/R_{N_2} against $[HI]/[NO]^2$ (for 6°C results) does not show any deviation.

Figure 26 shows the typical R_{H_2}/R_{N_2} plots against $[HI]/[NO]^2$ at -20°C. From the figure it is clear that within a certain range, it is linear. The line passes through the origin and the slope gives k_5/k_{13}. The slopes calculated at

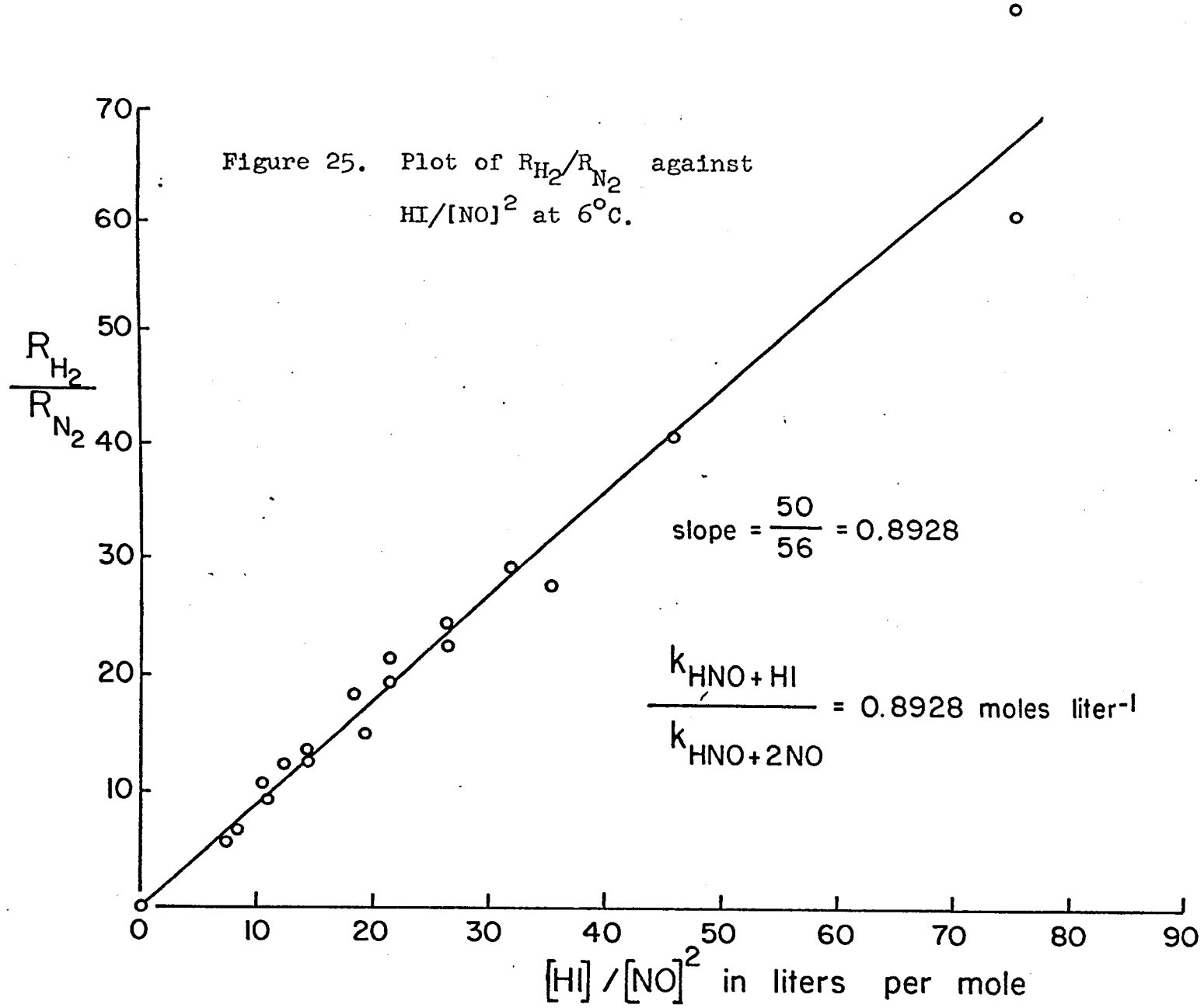

Figure 25. Plot of R_{H_2}/R_{N_2} against $HI/[NO]^2$ at 6°C.

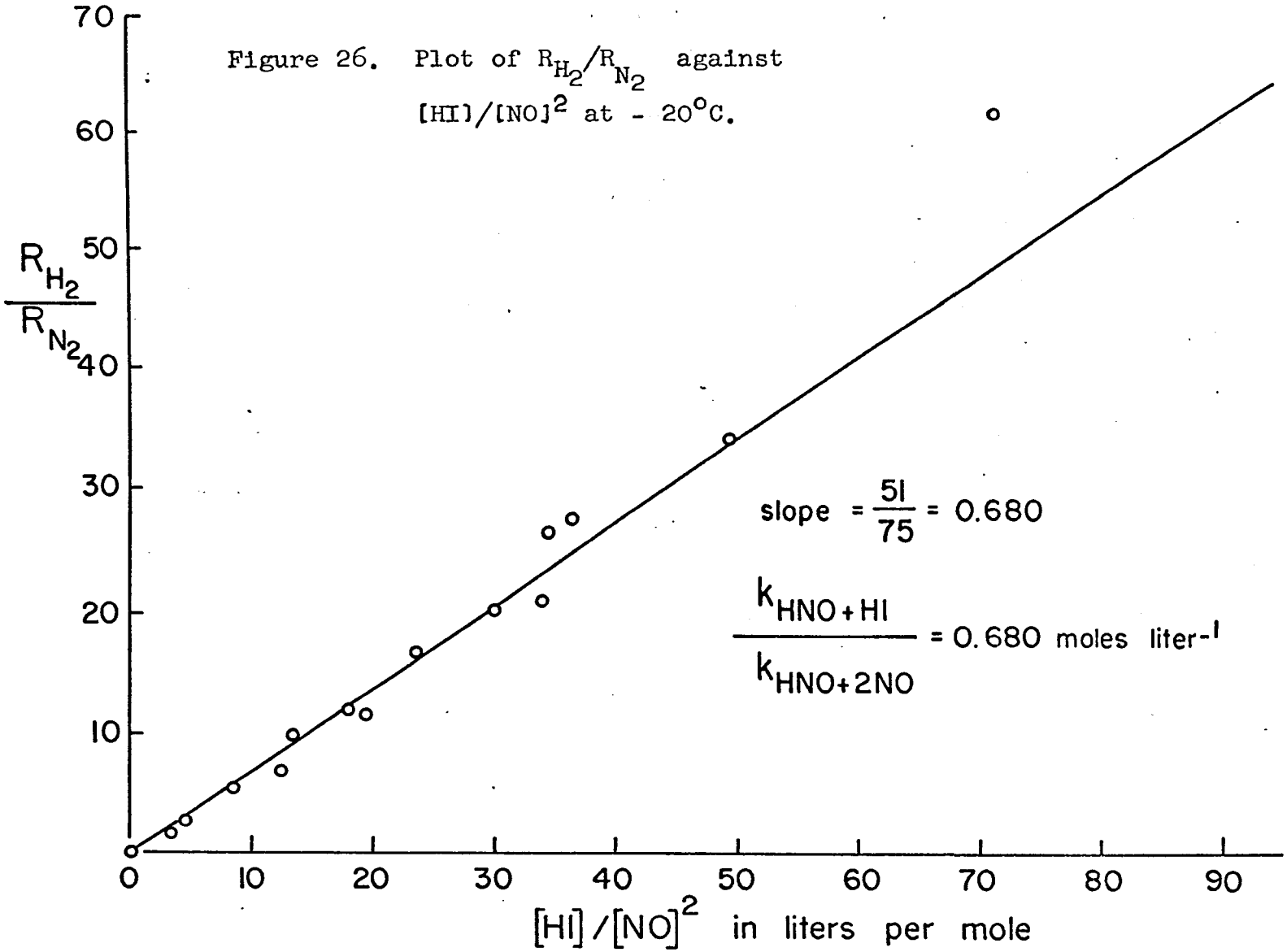

Figure 26. Plot of R_{H_2}/R_{N_2} against $[HI]/[NO]^2$ at - 20°C.

two temperatures are 0.893 moles liter^{-1} at 6°C and 0.680 moles liter^{-1} at -20°C. It was also found that the amount of N_2 produced was slightly higher at -20°C than at 6°C, for the same amount of HI and NO. This indicates that the rate of nitrogen production increases with decrease in temperature.

This increase in rate with decrease in temperature implies that reaction [13] has either a negative activation energy (as was observed in similar reactions

[2'] $\quad RNO + 2NO = R\cdot + N_2 + \cdot NO_3$

by Christie and co-workers (80)) or it may have a zero activation energy (similar to the nitric oxide - oxygen reaction) and the increase in rate is just due to the decrease in temperature. In the case of the nitric oxide - oxygen reaction, Gershinowitz and Eyring (113) have shown, by the application of transition state theory, that the rate is inversely proportional to T^3. This means that the rate will increase with the decrease in temperature, even though it has a zero activation energy.

Since nitrogen was produced at lower temperatures, then the question arises whether it is a product at higher temperatures. As stated earlier, we could not detect any N_2 at moderate NO/ HI ratios. However, at large NO/HI ratios, greater than 10, the mass balance of H_2 and I_2 were never the

same , indicating that some N_2 might be produced also (see Table 2). As an approximation, we calculated the amount of N_2 produced in some experiments at very high NO/HI ratios, using the $2N_2 + H_2 \equiv I_2$ mass balance equation. From the results, Figure 27 was plotted. A straight line was obtained with a slope = 1.53 moles liter^{-1} at 25°C.

These three values at 25°, 6° and -20°C are shown as an Arrhenius plot (Figure 28) for k_5/k_{13}. The three points are not co-linear. The curvature of the plot indicates clearly that N_2 production at higher temperatures will be smaller than that obtained by extrapolating the 6° and -20°C results. This type of curvature in the Arrhenius plot was also observed by Strausz and Gunning (114) when they plotted ln ϕ_{N_2} as a function of $(T)^{-1}$, in the nitroso alkane reactions. A genuine curvature in the plot would indicate that the mechanism is complex.

An alternative explanation is that the points are scattered and the activation energy difference, $E_5 - E_{13}$, can be obtained by drawing the best line through these points. This 'best straight line' through the three points (Figure 28) gives $E_5 - E_{13} = 2.7$ k.cal. mole^{-1}. Since it is not possible to calculate the individual activation energies, only a comparison can be made with other alkyl iodide

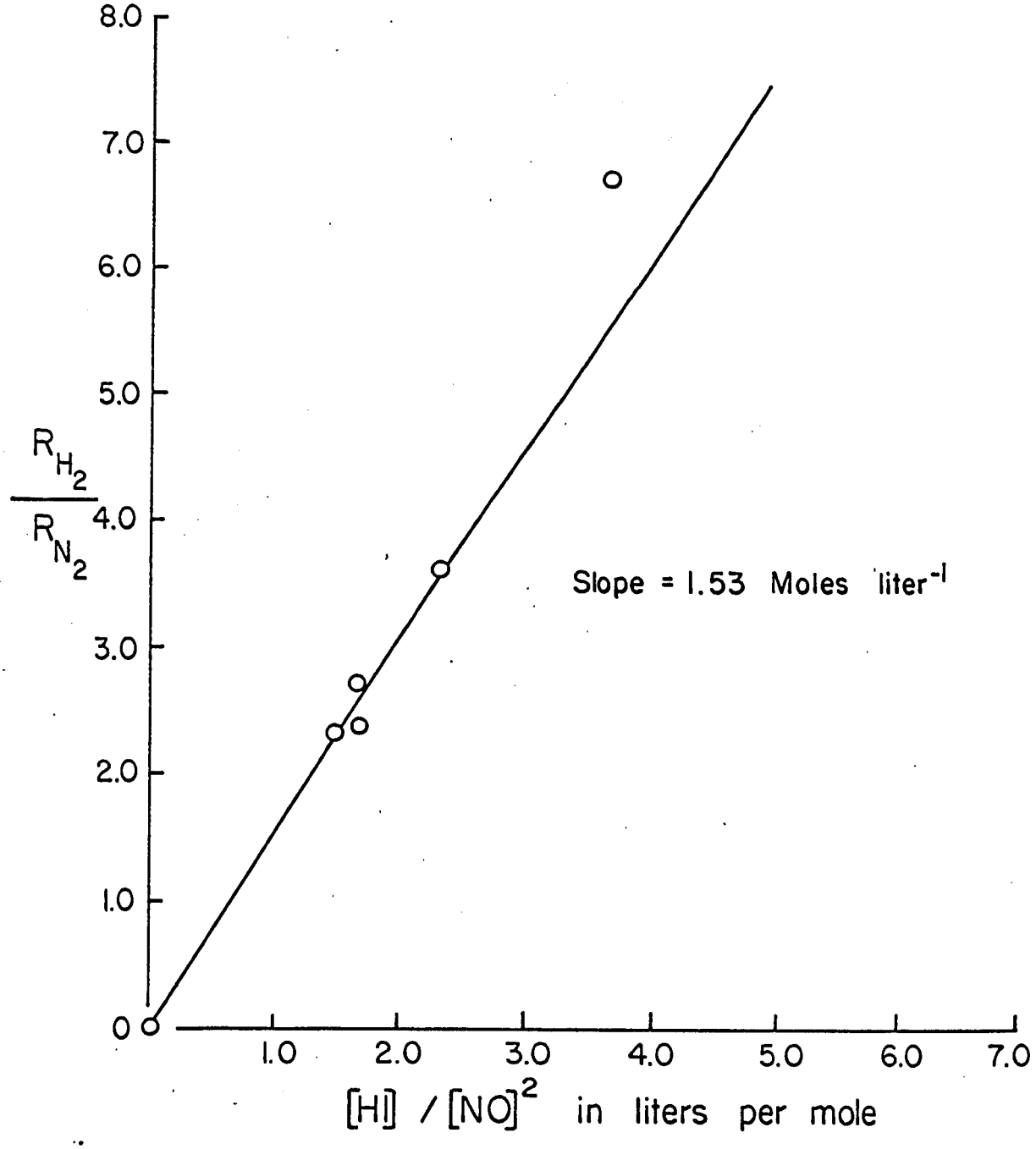

Figure 27. Plot of R_{H_2}/R_{N_2} against HI / NO ^{2} at 25°C.

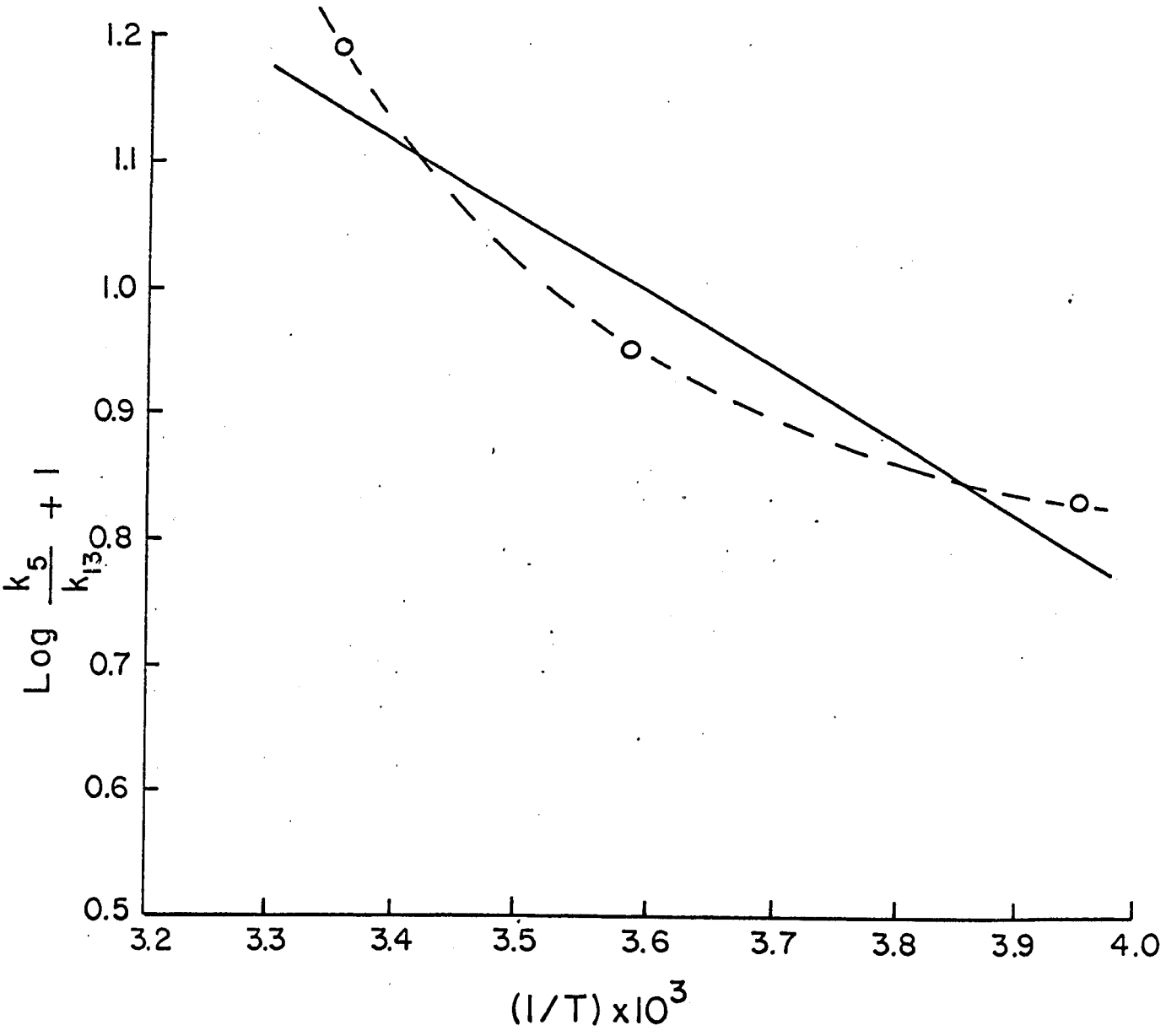

Figure 28. Arrhenius plot for the rate ratio k_5/k_{13}.

photolytic reactions. All our previous results, when compared with Christie's results, indicate that the HI + NO system behaves in the same way as RI + NO (see Pages 110 and 142).

Christie and co-workers (80) determined the activation energy for reaction [2'] and they found that it increases in the order

$$E_{t\text{-}Bu} < E_{i\text{-}Pr} < E_{Pr} < E_{Et} < E_{Me}$$

all having negative activation energies ranging from -7.5 k.cal. mole^{-1} for t-butyl to -1.8 k.cal. mole^{-1} for methyl. The fact that nitrogen production increases with decrease in temperature and to correlate our results with the above sequence, it seems probable that E_{13} has either a negative activation energy of about 0.5 k.cal. mole^{-1} or zero activation energy. This will give rise to $E_5 \simeq 2.7$ to 3.0 k.cal. mole^{-1}. Since the difference in endothermicities of reactions [5] and [6] is about 2.5 k.cal. mole^{-1}, it may be conjectured that E_5 = 3.0 k.cal. and E_6 = 0.5 k.cal. The endothermicity difference is calculated on the basis D(NO–I) is 10 k.cal. mole^{-1} (101) which again seems to be only approximate.

[5] $\underset{48.0}{HNO} + \underset{70.5}{HI} \longrightarrow \underset{103.0}{H_2} + \underset{10.0}{NOI}$ +5.5 k.cal.

[6] $\underset{48.0}{HNO} + \underset{35.5}{I_2} \longrightarrow \underset{70.5}{HI} + \underset{10.0}{NOI}$ +3.0 k.cal.

$\therefore \quad \Delta H_5 - \Delta H_6 = \Delta(\Delta H) \backsimeq 2.5$ k.cal. [32]

Hence it may be concluded that reactions [5], [6] and [13] have activation energies 3.0, 0.5 and -0.5 k.cal. $mole^{-1}$ respectively.

APPENDIX

In view of the difference between the work of Hamill, Williams and Ogg (30) and Sullivan (64) on the values of the rate constant ratios k_3/k_2 and activation energy difference $E_3 - E_2$, as already discussed on Pages 44-5, we decided to repeat the work of Hamill and Williams and to reinvestigate the effect of various inert gases on the photolysis of HI, using wavelength 2537 Å. In our calculations at 45°C, the value of 13.0 given by Sullivan (64) was used to obtain k_6/k_5 (see P. 113). To justify this value, the present work was done, using inert gases such as He and H_2 at 70° and 110°C. A few experiments were also conducted to see whether there is any effect of CO on HI photolysis. An inhibitory effect due to transitory formation of HCO (by analogy with HNO) might lead to a determination of D(H-CO), a quantity which is still uncertain.

As a continuation of the low temperature work, the effect of carbon monoxide on the photolysis of HI, using wavelength 3130 Å, was studied. The experimental set up was the same as described in Chapter 4. The quantum yield of I_2 was calculated by using pure HI as an internal actinometer. The results are shown in Table 13. It appears from the results that at 6°C there was very little effect, while at -20°C, a definite reduction of quantum yield was found. This may be due to the formation

of HCO, which then reacts with HI and I_2 as does HNO.

The photolysis of hydrogen iodide using a wavelength 2537 $\mathring{A}$ will produce H atoms which may be hot to the extent of 42 k.cal. or 20 k.cal. depending on whether a normal or excited iodine atom is produced (Page 43). To study the 'hot atom' effect, the photolysis was carried out in the presence of added inert gases such as H_2 and He at 70° and 110°C.

The experimental procedure was the same used in Chapter 3, except that HI photolysis, by itself, was used as an internal actinometer to calculate $I_{abs} \times t$ in equation 12 .

$$I_{abs} \times t - (I_2)_f = R\left[\frac{(HI)_i}{4} \ln\frac{(HI)_i}{(HI)_i - 2(I_2)_f} - \frac{(I_2)_f}{2}\right] \qquad [12]$$

By the use of this equation, the values for $R = k_3/k_2$ were calculated and this was plotted as a function of M / HI , where 'M' is the inert gas added. The results are shown in Figure 29. It was found that R was independent of I_2/HI but was only dependent on M/HI at low M values. This was similar to the observation by Schwarz, Williams and Hamill (30). The above workers studied the photolysis of HI in the presence of H_2, He and Ar and obtained $R = k_3/k_2$, at infinite inert gas pressures, the values 13.5 at 114°C, 9.0 at 154°C and 4.7 at 198°C, yielding an activation energy difference, $E_2 - E_3$, = 4.5 k.cal. $mole^{-1}$.

The present results at 70°C and 110°C show R = 8.6 and 7.9

respectively, at infinite inert gas pressure, yielding an activation energy difference, $E_2 - E_3 = 0.6$ k.cal. mole^{-1}. These results agree fairly well with the findings of Sullivan (64) that $E_2 - E_3$ is very small. Our values of k_3/k_2 are in disagreement with the results of Sullivan in that an extrapolation of our k_3/k_2 to 666°K, using $E_2 - E_3 = 0.6$, would give values lower by a factor of two than his values.

TABLE 13

Effect of added carbon monoxide

$\lambda = 3130$ Å Vol. of the vessel = 314.0 ml.

$I_o = 3.105 \times 10^{-8}$ einsteins sec^{-1}

Temp.	$(HI)_o \times 10^5$ moles	$\frac{CO}{HI}$	Time in sec.	$(HI)_f \times 10^5$ moles	$(I_2) \times 10^6$ moles	ϕ_{I_2}
6°C	75.15	-	5,400	69.10	24.9	1.00
	74.92	3.30	"	70.00	23.3	0.94
	75.94	6.07	"	71.25	23.2	0.93
-20°C	36.20	-	6,200	32.89	17.6	1.00
	37.79	7.27	"	34.30	17.1	0.97
	36.93	10.70	"	34.00	16.6	0.94
	36.06	12.32	"	33.09	14.9	0.85

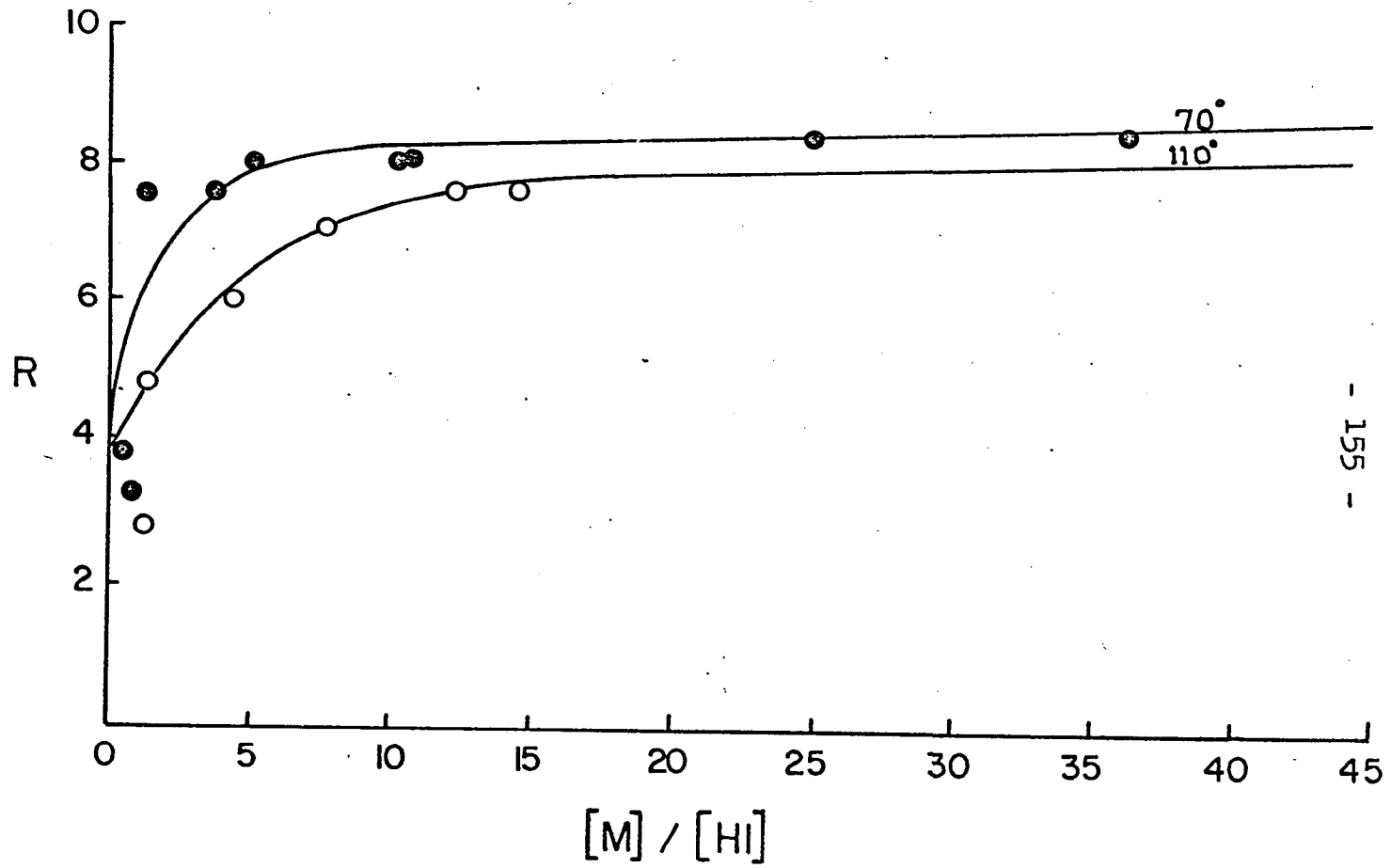

Figure 29. Plot of R, the inhibition constant, as a function of M/HI at 70° and 110°C, using λ = 2537 Å.

CLAIMS TO ORIGINAL RESEARCH

1) The photolysis of hydrogen iodide in the presence of nitric oxide was studied for the first time at 45°C, 25°C, 6°C and -20°C.

a) The addition of nitric oxide at 45° and 25°C inhibits the photolysis of hydrogen iodide, thereby reducing the quantum yield of hydrogen production. Mechanisms were proposed involving HNO as a reactive intermediate. Rate equations were derived from which the rate constant ratios for the reactions $HNO + I_2 \longrightarrow HI + NOI$ and $HNO + HI \longrightarrow H_2 + NOI$ were calculated. From the pressure dependence of the rate constant for the reaction $HNO^* + NO + M \longrightarrow HNO + M$, the life time of HNO* was calculated and also the pressure at which there is change in order for this reaction was obtained.

b) At 6° and -20°C, the reaction of HNO with NO, to produce N_2 and HNO_3, was studied in detail. Mechanisms were proposed which satisfactorily explained the experimental results.

c) From temperature and pressure effects at the above four temperatures, activation energies were calculated for $HNO + HI \longrightarrow H_2 + NOI$, $HNO + I_2 \longrightarrow HI + NOI$ and $HNO + 2NO \longrightarrow N_2 + HNO_3$

d) Similarities and dissimilarities between RNO + NO (where R = alkyl) and HNO + NO reactions are discussed.

2) The effect of added gases on photolysis of HI was examined to study the hot atom effect.

a) The addition of non-reactive gases like H_2, N_2 and He was studied at 25°, 70° and 110°C, and the rate constant ratio for the reactions $H + I_2 \longrightarrow HI + I$ and $H + HI \longrightarrow H_2 + I$ was calculated at higher temperatures. This was studied using both 2537 and 3130 Å radiation.

b) The addition of carbon monoxide to the photolysis at 6° and -20°C was studied. The reduction in quantum yield of iodine production at -20°C may be possibly due to HCO reacting with HI and I_2.

REFERENCES

1 J. Stark, Physik. Z. 9, 889, 894 (1908). A. Einstein, Ann. Physik. 37, 832; 38, 881 (1912).

2 M. Bodenstein, Z. Physik. Chem. (Leipzig) 85, 329 (1913).

3 A. N. Terenin, Phys. Rev. 36, 147 (1930); A. N. Terenin and B. Popev, Z. Phys. 75, 338 (1932).

4 K. Watanabe, F. F. Marmo and E. C. Y. Inn, Phys. Rev. 91, 1155 (1953).

5 R. A. Back and D. C. Walker, J. Chem. Phys. 37, 2348 (1962).

6 W. C. Price, R. Bralsford, P. V. Harris and R. G. Ridley - Proceedings of the Conference on Molecular Spectroscopy - Ed. E. Thoronton and H. W. Thompson, Pergamon Press, London, 1959 P. 54.

7 H. Okabe and J. R. McNesby, J. Chem. Phys. 34, 668 (1961) and subsequent papers.

8 E. W. R. Steacie, Atomic and Free Radical Reactions, Reinhold Publishing Co., New York, 1954, P. 411.

9 W. A. Noyes Jr., G. Porter and J. G. Jolley, Chem. Rev. 56, 49 (1956).

10 R. Srinivasan, J. Am. Chem. Soc. 81, 1546 (1959).

11 J. C. Anderson and C. B. Reese, Proc. Chem. Soc. 217 (1960).

12 H. Kobsa, J. Org. Chem. 27, 2293 (1962).

13 J. Franck, Trans. Faraday Soc. 21, 536 (1925); E. U. Condon and P. M. Morse, Quantum Mechanics, McGraw Hill, New York, 1929, P. 164.

14 K. J. Laidler, The Chemical Kinetics of Excited States, Clarendon Press, Oxford, 1955, P. 43.

15 E. Wigner, Nachr. Götting, Ges., 375 (1927).

16 W. A. Noyes Jr., and I. Unger, Pure Appl. Chem. 9, 461 (1964)

17 C. F. Goodeve and A. W. C. Taylor, Proc. Roy. Soc. (London) A 154, 181 (1936).

18 A. C. G. Mitchell and M. W. Zemansky, Resonance Radiation and Excited Atoms, Cambridge, 1934, Ch. 4.

19 H. E. Gunning and O. P. Strausz in Advances in Photochemistry, Vol. 1, Ed. W. A. Noyes Jr., G. S. Hammond and J. N. Pitts, Interscience, 1963.

20 O. Stern and M. Volmer, Physik. Z. 20, 183 (1919); for a discussion of a more complex system see B. deB. Darwent, J. Chem. Phys. 20, 1673 (1952).

21 V. N. Kondrat'ev, Chemical Kinetics of Gas Reactions, Pergamon Press, London, 1964, P. 433.

22 R. B. Cundall and D. G. Milne, J. Am. Chem. Soc. 83, 3902 (1961).

23 H. Spooner, Radiation Res. Suppl. 1, 558 (1959).

24 C. L. Braun, S. Kato and S. Lipsky, J. Chem. Phys. 39, 1645 (1963).

25 R. E. Kellog and R. G. Bennett, J. Chem. Phys. 41, 3042 (1964).

26 H. Ishikawa and W. A. Noyes Jr., J. Chem. Phys. 37, 583 (1962).

27 M. Kasha, Discussions Faraday Soc. 9, 14 (1950) and subsequent reviews.

28 R. S. Mulliken, J. Chem. Phys. 7, 14 (1939); R. S. Mulliken and C. A. Rieke, Rep. Progr. Phys. 8, 231 (1941).

29 G. Herzberg, Molecular Spectra and Molecular Structure, 1 Spectra of Diatomic Molecules, D. Van Nostrand, New York, 1950.

30 H. A. Schwarz, R. R. Williams and W. H. Hamill, J. Am. Chem. Soc. 74, 6007 (1952).

31 R. M. Martin and J. E. Willard, J. Chem. Phys. 40, 2999 (1964).

32 J. C. Polanyi, J. Chem. Phys. 31, 1338 (1959); J. K. Cashion and J. C. Polanyi, J. Chem. Phys. 35, 600 (1961); N. Basco and R. G. W. Norrish, Can. J. Chem. 38, 1769 (1960).

33 F. P. Lossing, D. G. H. Marsden and J. B. Farmer, Can. J. Chem. 34, 701 (1956).

34 Y. Tanaka, A. S. Jursa and F. J. Leblanc, J. Opt. Soc. Am. 48, 304 (1958).

35 F. S. Feates, B. Knight and E. W. T. Richards, Spectrochim. Acta. 18, 485 (1962).

36 F. J. Comes and E. W. Schlag, Z. Physik. Chem. (Frankfurt), 21, 212 (1959).

37 H. Okabe, J. Opt. Soc. Am. 54, 478 (1964).

38 "Glass color filters" - Corning Glass Works, Optical Sales Dept., Corning, New York.

39 E. J. Bowen, J. Chem. Soc. 76 (1935) and Chemical Aspects of Light, 2nd. Edn., Clarendon, Oxford, 1946, P. 276.

40 P. A. Leighton and G. S. Forbes, J. Am. Chem. Soc. 51, 3549 (1929); L. J. Heidt and F. Daniels, J. Am. Chem. Soc. 54, 2384 (1932); E. K. Rideal and J. S. Mitchell, Proc. Roy. Soc. (London) A' 159, 206 (1937).

41 J. Strong, Procedure in Experimental Physics, Prentice Hall, New York, 1939, Ch. 8.

42 W. G. Leighton and G. S. Forbes, J. Am. Chem. Soc. 52, 3139 (1930); G. S. Forbes and L. J. Heidt, J. Am. Chem. Soc. 56, 2363 (1934).

43 C. A. Parker, Proc. Roy. Soc. (London) A 220, 104 (1953).

44 H. Melville and B. G. Gowenlock, Experimental Methods in Gas Reactions, 2nd. Edn., Macmillon and Co., London, 1964.

45 W. A, Noyes Jr. and P. A. Leighton, The Photochemistry of Gases, Reinhold, New York, 1941, P. 82.

46 C. M. Masson, V. Boekelheide and W. A. Noyes Jr., in "Catalytic, Photochemical, Electrolytical Reactions", Technique of Organic Chemistry, Vol. 2, 2nd. Edn.,

A. Weissberger Ed., Interscience Publishers, New York, 1956, P. 294.

47 L. P. Zill, Arch. Biochem. Biophys. 59, 473 (1955).

48 K. Porter and D. H. Volman, J. Am. Chem. Soc., 84, 2011 (1962).

49 K. Porter and D. H. Volman, Anal. Chem. 34, 748, (1962).

50 C. G. Hatchard and C. A. Parker, Proc. Roy. Soc. (London) A 235, 518 (1956).

51 J. Lee and H. H. Seliger, J. Chem. Phys. 40, 519 (1964).

52 D. S. Herr and W. A. Noyes Jr., J. Am. Chem. Soc. 62, 2052 (1940).

53 D. S. Weir, J. Am. Chem. Soc. 83, 2629 (1961).

54 A. G. Leiga and H. A. Taylor, J. Chem. Phys. 41, 1247 (1964).

55 M. Zelikoff and L. M. Aschenbrand, J. Chem. Phys. 22, 1685 (1954).

56 G. K. Rollefson and J. E. Booher, J. Am. Chem. Soc. 53, 1728 (1931).

57 J. Romand, Ann. Phys. (Paris) 4, 527 (1948).

58 R. S. Mulliken, Phys. Rev. 51, 310 (1937).

59 E. Warburg, Sitzer. Preuss. Akad. Wiss. 26, 300 (1918).

60 M. Bodenstein and F. Lieneweg, Z. Physik. Chem. (Leipzig) 119, 123 (1926).

61 R. R. Williams Jr. and R. A. Ogg Jr., J. Chem. Phys. 15, 691 (1947).

62 R. A. Ogg Jr. and R. R. Williams Jr., J. Chem. Phys. 13, 586 (1945).

63 J. H. Sullivan, J. Chem. Phys. 30, 1292 (1959).

64 J. H. Sullivan, J. Chem. Phys. 36, 1925 (1962).

65 J. L. Holmes, Proc. Chem. Soc. 75 (1962).

66 M. J. Y. Clement and D. A. Ramsay, Can. J. Phys. 39, 205 (1961).

67 E. Hirschlaff and R. G. W. Norrish, J. Chem. Soc. 1580 (1936) L. J. Hillenbrand and M. L. Kilpatrik, J. Chem. Phys. 21, 525 (1953); H. W. Thompson and C. H. Purkis, Trans. Faraday Soc. 32, 1466 (1936); J. B. Levy, J. Am. Chem. Soc. 78, 1780 (1956).

68 F. W. Dalby, Can. J. Phys. 36, 1336 (1958).

69 J. K. Cashion and J. C. Polanyi, J. Chem. Phys. 30, 317 (1959).

70 H. W. Brown and G. C. Pimentel, J. Chem. Phys. 29, 883 (1958).

71 J. L. Bancroft, J. M. Hollas and D. A. Ramsay, Can. J. Phys. 40, 322 (1962).

72 H. A. Taylor and C. Tanford, J. Chem. Phys. 12, 47 (1944).

73 H. W. Melville, Proc. Roy. Soc. (London) A 146, 737 (1934); J. K. Dixon, J. Am. Chem. Soc. 56, 101 (1934).

74 P. Harteck, Ber. 66, 423 (1933).

75 H. M. Smallwood, J. Am. Chem. Soc. 51, 1985 (1929).

76 M. A. A. Clyne and B. A. Thrush, Trans. Faraday Soc. 57, 1305 (1961); Discussions Faraday Soc. 33, 139 (1962).

77 O. P. Strausz and H. E. Gunning, Trans. Faraday Soc. 60, 347 (1964).

78 R. Srinivasan, J. Phys. Chem. 64, 679 (1960).

79 M. I. Christie, G. Gillbert and M. A. Voisey, J. Chem. Soc. 3147 (1964).

80 M. I. Christie, J. S. Frost and M. A. Voisey, Trans. Faraday Soc. 61, 674 (1965).

81 M. I. Christie, J. M. Collins and M. A. Voisey, Trans. Faraday Soc. 61, 462 (1965).

82 B. G. Gowenlock and J. Trotman, J. Chem. Soc. 4190 (1955).

83 L. Batt and B. G. Gowenlock, Trans. Faraday Soc. 56, 682 (1960).

84 E. A. Arden and L. Phillips, J. Chem. Soc. 5118 (1964).

85 K. J. Laidler, N. H. Sagert and B. W. Wojciechowski, Proc. Roy. Soc. (London) A 270, 254 (1962).

86 R. G. W. Norrish and G. L. Pratt, Nature 197, 143 (1963).

87 L. A. K. Staveley and C. N. Hinshelwood, Proc. Roy. Soc. (London) A 154, 335 (1936); J. Chem. Soc. 1568 (1937).

88 F. O. Rice and O. L. Polly, J. Chem. Phys. 6, 273 (1938).

89 F. J. Stubbs and C. N. Hinshelwood, Discussions Faraday Soc. 10, 129 (1951); C. N. Hinshelwood, Chem. Soc. (London) Spec. Publ. No. 9, 49 (1957).

90 F. O. Rice and R. E. Varnerin, J. Am. Chem. Soc. 76, 324 (1954); R. E. Varnerin and J. S. Dooling, J. Am. Chem. Soc. 78, 2042 (1956).

91 F. J. Stubbs and C. N. Hinshelwood, Proc. Roy. Soc. (London) A 200, 458 (1950).

92 B. W. Wojciechowski and K. J. Laidler, Can. J. Chem. 38, 1027 (1960).

93 K. S. Echols and R. N. Pease, J. Am. Chem. Soc. 61, 1024 (1939).

94 K. J. Laidler and B. W. Wojciechowski, Proc. Roy. Soc. (London) A 260, 103 (1961).

95 D. J. Mckenney, B. W. Wojciechowski and K. J. Laidler, Can. J. Chem. 41, 1993 (1963).

96 N. H. Sagert and K. J. Laidler, Can. J. Chem. 41, 848 (1963).

97 A. I. Vogel, A Text Book of Quantitative Inorganic Analysis, Longmans, London, 1946, P. 338, 340.

98 E. J. Schorn, Pharm. J. 134, 117 (1935); Chemists and Druggists 122, 128 (1935).

99 A. Farkas and H. W. Melville, Experimental Methods in Gas Reactions, Macmillan and Co., London, 1934, P. 255.

100 F. F. Marmo, J. Opt. Soc. Am. 43, 1186 (1953).

101 G. Porter, Z. G. Szabo and M. G. Towensend, Proc. Roy. Soc. (London) A 270, 493 (1962).

102 M. L. Perlman and G. K. Rollefson, J. Chem. Phys. 9, 362 (1941)

103 Handbook of Physics and Chemistry, 45th. Ed., Chemical Rubber Co., Ohio, 1964.

104 M. I. Christie, Proc. Roy. Soc. (London) A 249, 248 (1959).

105 R. H. Burgess and J. C. Robb, Chem. Soc. Spec. Publ. No. 9 183 (1957). (London).

106 D. E. Hoare and A. D. Walsh, Trans. Faraday Soc. 53, 1102 (1957); Chem. Soc. (London) Spl. Pub. No. 9, 17 (1957).

107 M. Z. Hoffman and R. B. Bernstein, J. Phys. Chem. 64, 1753 (1960).

108 S. W. Benson, The Foundation of Chemical Kinetics, McGraw - Hill Co., New York, 1960, P.397.

109 M. I. Christie and J. S. Frost, Trans. Faraday Soc. 61, 468 (1965).

110 D. H. Volman and J. R. Seed, J. Am. Chem. Soc. 86, 5095 (1964).

111 E. A. Arden and L. Phillips, Proc. Chem. Soc. 354 (1962).

112 J. A. Gray and D. W. G. Style, Trans. Faraday Soc. 48, 1137 (1952); P. L. Hanst and J. G. Calvert, J. Phys. Chem. 63, 2071 (1959).

113 H. G. Gershinowitz and H. Eyring, J. Am. Chem. Soc. 57, 985 (1935).

114 O. P. Strausz and H. Gunning, Can. J. Chem. 41, 1207 (1963).